

ACKNOWLEDGEMENTS

I would like to express my appreciation to:

The Director and personnel of the Department of Defense Gravity Library, St. Louis, Missouri for supplying the marine and land gravity data;

Dr. Milton B. Dobrin for suggesting the topic, reading the drafts, and for criticism and advice throughout the project;

Dr. D. C. Van Siclen for discussions concerning the deep structure of the Texas coastal plain and the offshore area;

Mr. Jack Weyand of Sidney Schafer and Associates, Houston, Texas for supplying the regional gravity maps and the magnetic profile and for interesting discussions about the Texas offshore area;

Dr. George Batten of the University of Houston Mathematics Department for programming assistance;

Dr. J. Bargainer of the University of Houston Electrical Engineering Department for use of the plotter;

Mr. Ralph Preston, Houston, Texas for interesting discussions about his masters thesis;

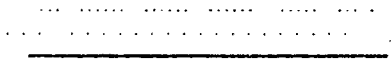
Mr. Dave Pettus, geology graduate student, for photography;

My wife, Carol, for typing the manuscript and for the inspiration to complete this project.

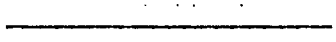
Computer facilities were provided by the University of Houston Computing Center.

Partial financial support was provided through a National Science Foundation grant, GA-29756 awarded to Dr. Alan Hales, formerly of the Department of Geosciences, University of Texas at Dallas, now Director of the Research School, Earth Sciences, Australian National University, Canberra. A grant from the University of Houston Geology Foundation was also provided. For this assistance I am extremely grateful.

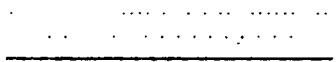
INTERPRETATION OF
REGIONAL GRAVITY ANOMALIES ON THE MARGIN OF THE NORTHWEST GULF OF MEXICO



An Abstract of a Thesis
Presented to
the Faculty of the Department of Geology
The University of Houston



In Partial Fulfillment
of the Requirements for the Degree
Master of Science



by
Michael Douglas Burnaman
August, 1974

ABSTRACT

Free-air gravity anomalies along portions of 27 shiptracks observed in 1970 during five cruises of the USNS "GEORGE B. KEITHLEY" in the area of the Texas continental shelf and part of the continental slope reveal a continuous linear maximum, bifurcating at the latitude of Baffin Bay, of as much as +32 mgals which may extend along the entire Texas continental shelf at distances of 40-75 km offshore. An oval positive anomaly of +57 mgals exists offshore Port Isabel, Texas.

A regional gravity map, prepared from the "KEITHLEY" data and land Bouguer gravity data available in the literature reveals that a positive Bouguer anomaly similar to the linear free-air maximum offshore is present southwest of Freeport, Texas, while the oval anomaly offshore Port Isabel is shown to extend onshore and is associated with sediment loading on the continental margin by the Rio Grande Delta.

A crustal section perpendicular to the coastline in the vicinity of Port O'Conner, Texas, constructed using a two-dimensional gravity model, indicates that the Freeport maximum and the linear shelf maximum may be caused by high density, probably ultramafic intrusions up to 14 km wide within the basement of oceanic crust offshore and the Paleozoic meta-sediments onshore.

Magnetic models of the intrusion using an aeromagnetic profile extending southeast from the vicinity of Galveston yield depths and widths for the intrusive similar to those indicated by the gravity model near Port O'Conner, approximately 200 km to the south. Plotting the locations of the gravity maximum along 18 of the shiptracks indicated apparent strike-slip displacement of the intrusive, perpendicular to the coast, of as much as 14 km.

Integration of the gravity and magnetic data presented in this thesis with modern examples of extensive ultramafic intrusions and a recently published model for a late Triassic opening of the Gulf of Mexico by sea-floor spreading suggests that the ultramafic intrusions along the Texas coastline may represent a "relict" site of the original rifting of that time.

Several curvilinear free-air minima are present on the south Texas continental shelf. These are thought to be caused by low density, highly pressured marine shale diapirs. Isolated Bouguer minima over the upper continental slope substantiate that the "hummocky" topography of that area is due to salt diapirism.

TABLE OF CONTENTS

	PAGE
ACKNOWLEDGEMENTS	iv
ABSTRACT	v
INTRODUCTION	1
Objective of Thesis	2
Location of study area	3
PREVIOUS GEOPHYSICAL INVESTIGATIONS	4
Gravity	4
Seismic Refraction	7
Seismic Reflection	9
Magnetic	10
GEOLOGY OF THE STUDY AREA	12
Regional Structure	12
Development of the Texas Gulf Coast Basin	13
Sediment Thicknesses	14
Shallow Structure of the South Texas Continental Shelf	14
Stratigraphy and Lithology	15
Introduction	15
Pre-Upper Jurassic	16
Upper Jurassic	16
Cretaceous	16
Cenozoic	17
DESCRIPTION OF THE MARINE GRAVITY MEASUREMENTS	19
Brief Explanation of the Gravity Meter and Raw Data Corrections	19
ACCURACY OF THE MARINE GRAVITY MEASUREMENTS	27
ANOMALY COMPUTATION	34

	PAGE
PROCEDURE USED IN PREPARING THE GRAVITY MAP	37
LOCATION, MAGNITUDE, AND EXTENT OF THE MAJOR GRAVITY ANOMALIES . .	43
QUALITATIVE ANALYSIS OF THE RIO GRANDE DELTA GRAVITY MAXIMUM . . .	55
Location and Association with other Gravity Anomalies	55
Modern Deltas and Isostasy	55
Comparison of the Gravity Effects of the Rio Grande with other Modern Deltas	56
Walcott's Hypothesis about Flexural Rigidity of the Lithosphere	58
PREPARATION OF THE CRUSTAL SECTION	61
Introduction	61
Selecting the Location	61
Validity of the Computation Method	67
Lithologic Characteristics and Geometry of the Layering	68
Selecting the Depth of Compensation and a "Standard Section"	69
Description at each Layer and its Inferred Density	70
Mantle	70
Oceanic Crust	71
Continental Crust and Paleozoic Metasediments	73
Mesozoic and Cenozoic Sediments	75
Water	77
Computing the Standard Section	77
Computing the Model	79
DISCUSSION OF THE CRUSTAL SECTION	84
Introduction	84
The Relation of the M-discontinuity and Water depth to a Continental "Edge" Effect	84
Is the Texas Continental Shelf Gravity Maximum caused by and Edge Effect?	85

	PAGE
Are the Components of the Texas Continental Shelf Gravity Maximum the Result of Basement Topography?	92
Are the Components of the Texas Continental Shelf Gravity Maximum caused by Shallow High Density Material?	94
Discussion of the High Density Intrusions associated with the Texas Continental Shelf Gravity Maximum	95
Other Features of the Crustal Section	97
ANALYSIS OF THE MAGNETIC ANOMALY SOUTHEAST OF GALVESTON, TEXAS	99
EVIDENCE FOR HORIZONTAL OFFSETS ALONG PART OF THE TEXAS CONTINENTAL SHELF GRAVITY MAXIMUM	108
Discussion of Significance of the Inferred Faults	112
TECTONIC IMPLICATIONS OF THE FREEPORT AND TEXAS CONTINENTAL SHELF GRAVITY MAXIMA	115
INTERPRETATION OF GRAVITY MINIMA ON THE SOUTH TEXAS CONTINENTAL SHELF AND UPPER CONTINENTAL SLOPE	121
Introduction	121
Computing the Bouguer Anomalies	121
Gravity Minima on the Southern Continental Shelf	126
Gravity Minima on the Southern Continental Slope	130
Other Comments on the South Texas Offshore Gravity Minima	133
SUMMARY AND CONCLUSIONS	135
The Gravity Map	135
The Crustal Section	135
The Magnetic Model	136
The Horizontal Offset of the Shelf Gravity Maxima	137
Conclusions	137
REFERENCES	139
APPENDIX 1	146
File Description Form	147
Contents of a Logical Record	148
Explanation of Tab List Heading	149

	PAGE
Gravity Station Data Card Format	151
Source Listing, Gulf Coast Continental Shelf	161
APPENDIX 2	163
Introduction	163
Explanation of File Terminology	163
List of All Programfiles, Datafiles, and Elementfiles	164
Explanation of Documentation	166
Listings of Files	166
Documentation	167
DATACOUNTER	167
DATALISTER	171
DATAPROCESOR	174
PROFILEPLOT	184
MAPPLOT	191
GRAVITYMODEL	196
APPENDIX	205
DATALISTFILE	210
TAPEWRITE	214
FILERESTORE	217
REVISEDMODEL	222
3PARTLUMP	227

LIST OF ILLUSTRATIONS

FIGURES	PAGE
1. Location of study area, sources of geophysical data, regional structural features, and the crustal section . . .	6
2. Locations of ship tracks of the "GEORGE B. KEITHLEY" showing free-air gravity anomalies	22
3. Regional gravity map of the Texas coastal plain and offshore area	42
4. Locations of the five regional gravity anomalies	45
5. Location of curvilinear free-air-minima on the south Texas continental shelf	47
6. Location of five profiles taken from the regional gravity map	51
7. Five profiles taken from the regional gravity map	53
8. Location of the crustal section	64
9. Location of gravity maxima along the Texas coastal plain and continental shelf	66
10. The crustal section computed using a two-dimensional gravity model	83
11. Free-air and Bouguer anomalies along track H16	87
12. Free-air and Bouguer anomalies along track D3	89
13. Free-air anomaly and total intensity magnetic anomaly along track D1	101
14. Free-air anomaly and total intensity magnetic anomaly along track D1 with computed magnetic anomalies for three models	106
15. Location of possible horizontal offsets along the Texas continental shelf gravity maximum	111
16. Bathymetry of part of the Texas upper continental slope showing residual Bouguer minima from tracks H12-H16 and D3-D4 and published locations of diapiric structures .	123
17. Location of computed minimum anomaly in Figure 18	129
18. Two-dimensional gravity model for a curvilinear south Texas continental shelf minimum anomaly	132

Graph	Log-log plot of mean vs. standard deviation of crossing errors	33
Plate I.	In Pocket
Plate II	In Pocket

LIST OF TABLES

	PAGE
1. Cruises of the USNS KEITHLEY contributing data to the thesis	20
2. Locations of ship tracks	23
3. Locations and magnitudes of crossing errors	28
4. Statistics of crossing errors	31
5. Layer densities used for crustal sections and isostatic computations in and adjacent to the western Gulf of Mexico	72
6. Standard sections for the south Texas coastal plain	80

INTRODUCTION

Objective of Thesis

The deep crustal structure of the Texas continental margin extending from Brownsville, Texas north to the Texas-Louisiana border has long been a subject of much speculation. Specifically, the composition of the crust under the sediments of the continental shelf and its overall thickness have not been determined due to the excessive depths (up to 15-17 kms) to the "basement" surface. These depths severely limit the resolution of seismic refraction methods since the amount of explosives necessary to produce acceptable signal-to-noise ratios over the long receiving distances that would be necessary (especially when the refraction line is shot along dip) exceeds acceptable environmental limits (Dorman et al., 1972, p. 329).

The gravity method of determining crustal structure, however, is not limited by excessive depths or environmental concerns. When there exists seismic control in the area to determine densities (empirically, at best) and the geometry of the layering it is then possible to construct crustal models whose gravitational attraction equals the observed gravity field. These models do not represent a unique solution as to the exact number, interface depths, and densities of crustal layers (Skeels, 1947) but they can produce limiting approximations which, when integrated with existing geologic data in the area, can give a reasonably accurate representation of the crustal geology and structure.

For any gravity calculations of regional crustal structure the observed gravity field should be known within an absolute accuracy of a few milligals. Greater accuracy than this is easily obtained in land gravity measurements; however, it is only within the last few years that

marine gravity measurements having the highly accurate navigation techniques required for proper data reduction have been available (Talwani, 1964). Prior to this time the only gravity measurements taken on the Texas continental shelf and slope available in the literature are found in the free-air gravity map of the Gulf of Mexico by Dehlinger and Jones, 1965. This map shows a broad maximum of over 40 mgals offshore from Port Isabel, Texas decreasing in width and magnitude somewhat to the north. The positive anomaly begins to broaden and increase in magnitude again offshore from Port O'Conner to reach a maximum of over 40 mgals in a wide area approximately 100 km southeast of Galveston, Texas. The regional extent of this gravity anomaly has led to some interpretations (Dehlinger and Jones, 1965; Shurbet, 1968) that the anomaly off of Galveston can be accounted for by the Mohorovicic discontinuity (M) rising to within 22 and 16 km of the surface at distances of 100 and 75 km offshore respectively. The positive anomaly at Brownsville, Texas has been interpreted by Preston (1970) as being caused by the mantle rising to a depth of 22.3 kms. Dehlinger and Jones and Preston all indicate that the mantle surface then descends to approximately 30 km at a distance of 300 km offshore while Shurbet (1969) shows a mantle depth of 14-15 km at a distance of 300 km offshore.

The general accuracy of the previously cited gravity map is questionable due to errors (mainly positional) discovered subsequent to the survey which were not apparent when the data were acquired. Specifically, the broad positive anomaly which encompasses most of the Texas continental shelf is more complex than shown, a factor which could severely alter any interpretation as to its geological significance.

The objectives of this thesis are:

- (1) To prepare a regional free-air gravity map of the Texas

continental shelf and slope of higher resolution and accuracy than that previously available in the literature by utilizing high quality marine surface gravity data recently released by the United States Department of Defense.

(2) To combine the marine gravity data with previous published and unpublished land gravity data to produce a regional gravity anomaly map extending from the Texas coastal plain across the continental shelf to the upper continental slope.

(3) To integrate available seismic refraction and magnetic data with the observed gravity field to obtain, by computer modeling techniques, a crustal section across the Texas coastal plain, continental shelf, and upper continental slope.

(4) To examine local gravity anomalies present on the continental shelf south of 28° N latitude to see if the diapiric structures in the South Texas onshore area described by Bruce (1972, p. 24) extend offshore.

(5) And to associate any new features suggested by the gravity map and models with the geological history of the Gulf Coast geosyncline.

Location of Study Area

The area chosen for the regional gravity map is between latitude 26° - 30° N and longitude 94° - 98° W (Fig. 1). Lack of available coverage over the continental slope made it impossible to include any data in the southeastern corner of the mapped area.

The approximate location of the crustal section is shown in Figures 1 and 8. The location of the model of the local residual minimum anomaly is shown in Figure 17.

PREVIOUS GEOPHYSICAL INVESTIGATIONS

There are numerous published and unpublished geophysical investigations in the vicinity of the Gulf Coast geosyncline (Fig. 1). The location of important gravity data, seismic refraction profiles, and a magnetic profile is shown in Figure 1. In addition to these geophysical studies in the South Texas area there are regional structural data available from reports of some seismic reflection surveys.

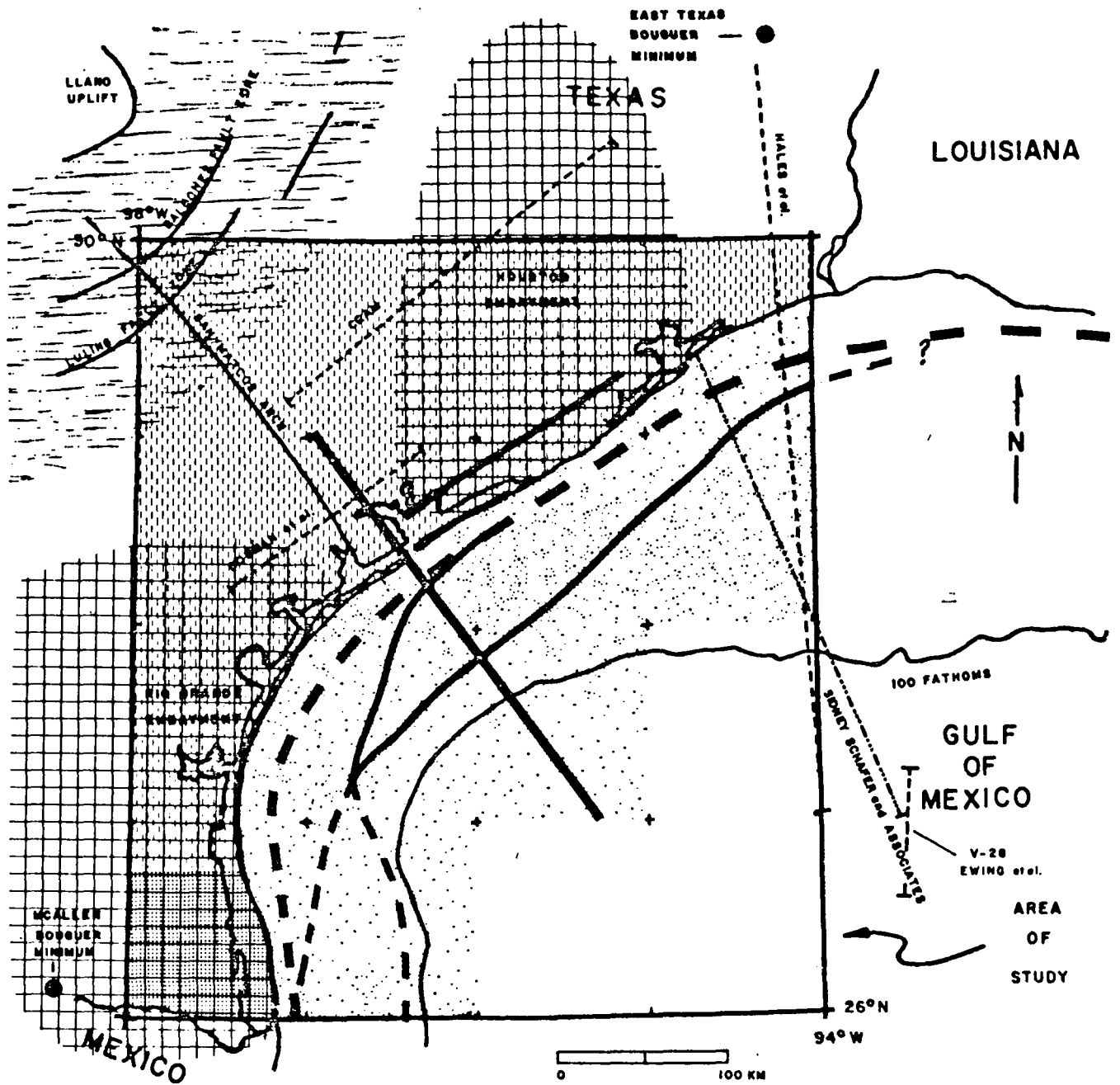
A description of these data is given below:

Gravity

A regional Bouguer anomaly gravity map of Texas and Oklahoma was compiled by Exploration Services, inc. in 1953 and was published by Logue, 1954. This map was prepared using a density of 2.67 gm/cc for the Bouguer correction and a contour interval of 5 mgals on the coastal plain. An important feature of this map (part of which is reproduced in Fig. 3 and Plate II of this thesis) is the wide relative maximum, flanked on both sides by relative minima, in the northwest corner of the map. This feature runs from the Ouachita mountains in southeastern Oklahoma southward to the area just east of the Llano region in central Texas and then swings almost due west, south of Llano at San Antonio, Texas. These anomalies have been studied by Watkins, 1961; Fish, 1971; and Keller and Cebull, 1973. The maximum has been attributed to higher density rocks of the Ouachita Structural Belt by Fish and by Keller and Cebull. Southeast of the relative maximum the gravity field becomes lower forming a minimum of less than -35 mgals in the vicinity of 27°N lat., 97°W long. (Dewitt-Victoria county line). Farther southeast at the coast the anomaly is approximately -20 mgals. Going south toward Brownsville, Texas (26°N lat.) the gravity

FIGURE 1

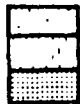
Location of the study area, location and sources of geophysical data used, location of the crustal section, and regional structural features.



|-|-|-|-| SEISMIC REFRACTION PROFILE

|-|-|-|-| MAGNETIC PROFILE

SURFACE GRAVITY COVERAGE



USNS GEORGE B. KEITHLEY (FREE-AIR)

LOGUE, 1954 (BOUGUER)

PRESTON, 1970 (BOUGUER)

— TREND OF GRAVITY MAXIMA

- - - INFERRED TREND OF GRAV. MAXIMA

— CRUSTAL SECTION

- - - AXIS OF GULF COAST GEOSYNCLINE



OUACHITA STRUCTURAL TREND EMBAYMENTS

V-28
EWING et al.

field increases to a maximum of 40 plus mgals on Padre Island east of Brownsville. This anomaly has been detailed through surveys by Preston, 1970 and Jones, 1974 (personal communication). This anomaly here termed the Rio Grande Delta Gravity Maximum (RGDGM) has been mentioned by Krivoy and Pyle, 1972, who interpret it as being caused by isostatic effects. Also available in the literature is the regional (land) Bouguer gravity map (10 mgal contour interval) of the Gulf Coast by Nettleton (1949, pp. 276-277). Along with the gravity map, Nettleton constructed a gravity profile from Roswell, New Mexico to Freeport, Texas (p. 281) and discussed the significance of the regional anomalies present on the profile. Of Major interest in Nettleton's discussion of this profile is his remark about a positive Bouguer anomaly of 10-15 mgals located just west of Freeport:

"The maximum near Freeport, which is parallel with the coast is not related to regional geology within the explored section of the sediments so far as we know" (p. 282).

Lyons (1957, p. 4) shows a regional isostatic anomaly map of the southern half of North America and the Gulf of Mexico. His data for the entire Gulf of Mexico were derived from the pendulum stations occupied by Vening Meinesz and Wright (1930). None of these pendulum stations are on the Texas continental shelf. Indicated on another map by Lyons (p. 8, Fig. 5) showing igneous activity around the Gulf of Mexico, is a symbol at the Freeport gravity maximum indicating that it is of probable igneous origin.

Seismic Refraction

In the vicinity of the inland portion of the crustal section there

are two refraction lines parallel to the strike of the geosyncline. Their locations are shown in Figure 1.

Cram, 1961, was able to identify four layers over the Mohorovicic discontinuity (M). The velocities and thicknesses of the layers are shown in Figure 10. The survey of Dorman, et al. (1972) was able to discern three horizons of sedimentary material above two layers inferred to be continental and oceanic crust overlying the presumed M surface (Figs. 1 and 10).

In the northeast corner of the study area a refraction line by Hales, et al. (1970) runs almost north-south extending from 32°N to 28°N lat. along 94°W long. (Fig. 1). They had a total of 15 receiver positions of which seven were offshore. They did not observe any mantle velocities. An interesting feature of their survey is an apparent down-faulted block of indeterminate lateral extent between 50 and 90 km offshore. The displacement of the upper horizons (less than five km deep) may be as much as two km while the surface of the oceanic crust may be dropped as much as a half km. They also constructed a gravity model along the profile using gravity data from Woolard and Joesting (1964) and Dehlinger and Jones (1965). They concluded from the gravity model that the mantle surface was 33 km deep under Galveston rising to 27 km 250 km offshore. This 27 km depth is questionable since they infer a zone in the mantle with density of 3.1 gm/cc to reconcile the refraction horizons with the observed gravity anomalies.

Offshore seismic refraction measurements consist of those by Ewing, et al. (1955), J. Ewing et al. (1960), and Antoine and Ewing (1963). Locations of two of these stations are shown in Figure 1. Station V-24 (Ewing, et al., 1955) was used as the southeast tie line of the crustal

section. Lines P-B-17 Antoine and Ewing, 1963 (not shown) and V-28 (Ewing, et al., 1955) were used primarily as indicators of minimum sediment thicknesses as they did not yield any crust or mantle velocities. At V-24 the oceanic crust is 14.1 km deep and the mantle is at 19.1 km.

Seismic Reflection

Seismic reflection data located on the South Texas continental shelf available in the literature are limited to a sparker survey by Moore and Curray (1963) along a line from Aransas Pass ($28^{\circ}50' N$ lat., $97^{\circ}4' W$ long.) southeast to $28^{\circ}15' N$ lat., $95^{\circ}30' W$ long.. Their data show several isolated groups of shallow normal faulting with development of graben systems. In one instance on the continental slope a shallow obviously diapiric intrusion is encountered. The relationship of these shallow structures to the inferred curvilinear relative minimum anomalies indicated by the colored lines on Figure 5 will be discussed in a following section. Lehner (1969) shows several reflection profiles (down to 4.0 seconds) along the area of the continental slope shown in Figure 16. These profiles show many diapiric salt features which, in some instances, rise to within 800 feet of the water bottom.

Bruce (1972) discusses seismic reflection data both on and offshore in the South Texas area. Although the exact positions of the seismic profiles are not given, the similarity of features found on all the lines allow certain general conclusions about lithology at depths down to six km to be made. These conclusions are: (1) Diapiric shale rather than salt appears to be the dominant mechanism for near surface (down to 6.5 km minimum depth) structural development in the South Texas area; (2) The dominant lithology to a depth of at least 6.5 km appears to be interbedded sands and shales with intrusive bodies of lower density, highly pressured

marine shale; and (3) These conditions prevail to the 100 fathom isobath.

Magnetics

Published magnetic data in the vicinity of the crustal section are limited to the regional total intensity magnetic anomaly map of the Gulf of Mexico compiled by Heirtzler, et al. (1966, p. 521). This map has had the regional field subtracted and is contoured with a 100 gamma interval. In the area 40-50 km south of Freeport is a broad -100 gamma closed contour which was interpreted by the authors as representing the area of greatest sediment thickness in the Gulf Coast geosyncline. Neither the Freeport gravity maximum nor the Rio Grande Delta gravity maximum are associated with a magnetic anomaly distinguishable within the 100 gamma resolution of their contours. Along the line of the crustal section the residual magnetic intensity varies from +200 gammas just inshore to less than 100 gammas approximately 50 km offshore. At a distance of 83 km offshore there is a small closed high of +200 gammas. This high is offset toward the basin 16 km from the continental shelf gravity maximum delineated in the present study.

The location of an aeromagnetic total intensity profile acquired by Sidney Schafer and Associates, Inc., Houston, Texas, in 1963 by Fairchild is shown in Figure 1. This profile was made available to the author by Mr. Jack Weyand. The flight elevation was 500 feet. A regional gradient of 10 gammas/mile has been subtracted from the total field. At the coast the field is 85 gammas increasing to 100 gammas 20 km offshore and then decreasing to -10 gammas 53 km offshore. At this point the field then increases to 180 gammas 85 km offshore and then decreases rapidly to 120 gammas at 130 km offshore. A steady increase in the field is then

noted farther offshore. This profile is 200 km northeast of the crustal section. An interesting feature of the magnetic profile is that the minimum anomaly 53 km offshore coincides within a few km of the location of the continental shelf gravity maximum outlined in this thesis.

GEOLOGY OF THE STUDY AREA

Regional Structure

The location of the crustal section includes both the northwest Gulf of Mexico and a portion of the Texas Coastal Plain as shown in Figure 1. The author's study area includes a large portion of the Gulf Coast geosyncline, an extensive depositional feature paralleling the coastline and extending from Northwestern Mexico to Alabama with its' axis of maximum deposition lying offshore (Hardin, 1962) (Fig. 1, this thesis). Total thickness of sediment in some areas of the geosyncline may be as much as 19,000 meters.

Local positive structural features present in the study area are the San Marcos arch, extending from the Llano uplift in Central Texas as a ridge into the middle Texas coast, possibly offshore and the Sabine uplift and arch centered approximately 200 km north of the Gulf along the Texas-Louisiana border and extending south to the coast. Negative structural features are the East Texas and Houston embayments north and east of the San Marcos arch and the Rio Grande embayment south and west of the San Marcos arch (Hardin, 1962, pp. 2-4). The continuity of the San Marcos arch through time has led Waters et al., (1955, p. 1849) to declare that it is the most stable structural feature on the entire Gulf Coast. Relative subsidence south of this feature has produced a thickness of more than 15 km of Cenozoic sediments alone (Hardin, 1962, p. 2).

Major zones of both up and down-to-the-coast faults such as the Luling and Balcones zones and the Mexia-Talco fault zone to the north together with the Oauchita Structural Belt, (Fig. 1) a subsurface Paleozoic fold belt, mark the northwestern rim of the Gulf of Mexico basin (Woods and

Addington, 1973, p. 93).

.....
Development of the Texas Gulf Coast Basin

The development of the western Gulf Coast geosyncline is thought to have begun in the late Paleozoic, coinciding with the Ouachita orogeny of that time (Murray, 1961, p. 89). This deformation, initiated during Pennsylvanian time, resulted in the thrusting to the northwest of the massive geosynclinal facies composed mainly of clastic and carbonate rocks (King, p. 186 in Flawn, 1961). Woods and Addington (1973, pp. 93-94) make the following statement about the development of the basin:

"The gross subsurface pattern of the Ouachita System have been mapped, using limited well data at zones of metamorphic facies from central Mississippi to the Ouachita Uplift, Southeastern Oklahoma, and across Texas to the Marathon-Solitario Uplifts. It is this structural rim which established the present configuration of the Northern Gulf basin, controlled major trends of subsequent tension faulting within the basin and provided a platform for the deposition of late Paleozoic and shallow water near-shore sediments. The width and down dip extent of the Ouachita belt is unknown. It is not unreasonable to speculate that the Northern arc of the Cretaceous reef trend that nearly encircles the Gulf basin is related to a major structural break near the south margin of the Belt."

Erosion and subsidence of the quiescent Ouachita Structural belt began in the Mesozoic, becoming more rapid in the Cenozoic. The initial subsidence was accompanied by the deposition of the Louann salt and the Werner formation as a Mesozoic transgression (King, in Flawn, 1961, p. 190). Following these deposits came the Upper Jurassic and Lower Cretaceous limestones and finally the extensive Cenozoic deltaic clastic deposits. All of these post-Paleozoic sediments have regional dip toward the Gulf

basin with the axis of maximum thickness in the area of the present coastline and offshore.

Sediment Thicknesses

The estimated thickness of post-Paleozoic sediments present under the northwestern Gulf of Mexico continental shelf, the deepest point of the western Gulf Coast geosyncline, may be as much as 16-19 km. Hardin (1962, p. 2) shows in an isopach of Cenozoic sediments just north of the Rio Grande delta that projections of regional dip from available well control will result in sediment thicknesses of 50,000 feet or more in this area.

This thickness of Cenozoic sediments is also shown to be present off the Louisiana coast in the same figure. If any Mesozoic sediments are included (i.e., Cretaceous limestones and Jurassic evaporites), it seems quite possible to have a total sediment thickness of as much as 17 km in both areas. Hardin's map also shows a thinner section of Cenozoic sediments over the San Marcos arch as would be expected.

Shallow Structure of the South Texas Continental Shelf

The major structural features inferred to be present on the south Texas continental shelf are salt or shale ridges (Beall, et al., 1973, p. 700, Fig. 1; Bruce, 1972, p. 24) and salt and shale domes (Murray, 1961, p. 203, Fig. 5.1; Uchipi and Emory, 1968, p. 1191, Fig. 19; Atwater, 1959, p. 137, Fig. 9; Lehner, 1969).

Bruce describes the shale ridges as being formed by "down to the coast" faults, both differential compaction and gravity sliding, on the seaward flanks of underlying low density shale masses. The initial high angle of this fault plane appears to become less steep with depth (p. 29). Many of the ridges appear to be examples of regional contemporaneous faulting and are consequently quite complex.

The salt ridges indicated by Beall, et al., (1973) may, in fact, not be salt but rather the low density high pressure shale as described by Bruce. However, Bryant and others (1968) have found sets of salt ridges, approximately parallel to the coast, on the Upper Mexican Continental Slope. They do not show these features to continue up onto the Texas continental shelf although there is a possibility they may trend into the continental slope east of Port Isabel.

Apparent salt domes on the lower Texas shelf are few in number and appear to be concentrated along the shelf edge below 28° N lat. On the continental slope at this latitude the hummocky topography would indicate the presence of many individual salt domes and connected ridges (Gealy, 1955). Atwater (1959, p. 137, Fig. 9) locates a set (20) of individual "structures unrelated to salt uplift", which parallel the coastline within 30 km of land beginning at $28^{\circ}30'$ N lat. and continuing south to Baffin Bay. Although it is not stated by Atwater, these features could also be due to shale diapirism.

Stratigraphy and Lithology

Introduction

The stratigraphy and lithology of the area in the vicinity of the crustal section and the continental shelf south of 28° N lat., in the vicinity of the gravity minima (Fig. 5) is described and summarized by Waters et al. (1955), Williamson (1959), Murray (1961, pp. 277-450), and Preston (1970, pp. 14-18).

All stratigraphic control in this region, as previously mentioned, is from outcrops far inland projected through boreholes on the coastal plain, offshore. Consequently the thicknesses, composition, or even existence of some of the units described may be questionable.

Pre-Upper Jurassic

Murray (1961, pp. 282-287) assigns the Morehouse formation of late Paleozoic age as being the base of the pre-Jurassic sedimentary section. Stratigraphically above it are the Eagle Mills and Werner formations, capped by the Louann salt. The Eagle Mills formation is of possible Upper Triassic age, while the Werner formation and the Louann salt are probable middle to late Jurassic. The Eagle Mills-Werner-Louann strata are inferred to be, respectively, dark fine clastics, carbonates, and evaporites in the south Texas area (p. 282). The true thickness of the Louann salt, by far the most important of the group in terms of their contribution to the physiography and structure of the coastal plain and continental slope, may be as much as 5000 feet in some areas. However, the salt is usually not inferred to be present in large volumes under the south Texas continental shelf and only in a localized area of the south Texas coastal plain. This inference is primarily due to the absence of salt domes in these areas.

Upper Jurassic

The upper Jurassic is represented by the Louark and Cotton Vally groups (Williamson, 1959, p. 1825). Their composition or presence is not documented in the south Texas area, but again by updip well control, they are inferred to be composed primarily of limestone, shales, sandstones, and some evaporites.

Cretaceous

The Cretaceous in the south Texas area is represented by the lower Cretaceous Commanche Series, from oldest to youngest, the Trinity, Fredricksburg, Washita, and Woodbine groups, and the Upper Cretaceous Gulfian Series, the Eagle Ford, Austin, Taylor, and Navarro groups. The lithology

of the Commanche series varies from calcareous-argillaceous strata in the Trinity group, to dense limestones in the Fredricksburg, to argillaceous-calcareous strata in the Washita. Gulfian series strata vary from arenaceous in the Woodbine, to calcareous-arenaceous in the Eagle Ford, while the Austin group is predominantly marly calcareous with the Taylor group being predominantly an alternating argillaceous-calcareous sequence and the Navarro being arenaceous-argillaceous strata.

Cenozoic

Paleocene - The Paleocene in the east Texas area, represented by the Midway group, consists of several hundred feet of shale (Williamson, 1959, p. 16). In the Rio Grande embayment, the equivalent of the Midway group, the Velasco, may reach a thickness of up to 3,000 meters (Murray, 1961, p. 372).

Eocene - The Eocene is represented by the Wilcox, Clairborne, and Jackson groups with respective lithologies of deltaic sands and shales, deltaic sands and shales grading upward to predominantly marine sands, and predominantly marly shales with marine sands (Waters, et al., 1955, p. 1839). Williamson (1959, p. 21, Fig. 8) indicates over 24,000 feet of Eocene strata (including the Midway) in the Corpus Christi-Baffin Bay area.

Oligocene - Oligocene strata is represented by the Vicksburg and Catahoula groups with a lithology of predominant marine shale for the Vicksburg and non-marine grading into marine argillaceous strata for the Catahoula (Williamson, 1961, p. 17). The thickest section of Oligocene strata shown by Williamson is over 16,000 feet at a distance of approximately 30 miles offshore extending from the Brazoria-Matagorda county line south to the Mexican continental shelf.

Miocene-Recent - Miocene-Pliocene (undifferentiated) strata are the Fleming and Citronelle groups which are characterized by marine shales offshore into transitional neritic sands and shales onshore. Williamson (1959, p. 24, Fig. 13) shows as much as 15,000 feet of Miocene and younger strata in the south Texas area.

DESCRIPTION OF THE MARINE GRAVITY MEASUREMENTS

The marine data used in this thesis were obtained from the United States Department of Defense Gravity Library, St. Louis, Missouri. This depository holds a large proportion of the gravity data available in the public domain as collected world-wide by government agencies and many public and private institutions.

The specific data used were collected by the U.S.N.S. George B. Keithly, a Naval Department research vessel, during five cruises conducted from January, 1970 to May, 1970 (see Table 1). Since the primary mission of these cruises was to collect high quality gravity data, careful navigation and ship handling techniques were used (Krivoy and Pyle, 1972, p. 107). The data were supplied on magnetic tape reels U3245 and U3478. Exact formats, reference base stations, and descriptions of features of the data package are given in Appendix 1, a copy of the information supplied by the DOD.

Locations of the actual shiptracks are shown in Figure 2 with the exact positions of the ends of the tracks given in Table 2.

Land data furnished by the DOD was also available for this project but was used mainly as a spot check of values taken from the regional gravity maps.

Brief Explanation of the Gravity Meter and Raw Data Corrections

A LaCoste and Romberg stabilized platform gravity meter was used on all cruises. This type of meter applies the principle of a mass suspended from a zero-length spring. The magnitudes of vertical accelerations are limited by the use of air damping while the mass is primarily restricted to vertical movements by additional fine wire suspensions (LaCoste and

TABLE 1

Cruises of the USNS KEITHLY contributing data to the thesis

Cruise Number	Dates
3337	4 Jan - 24 Jan 70
3440	11 Jan - 24 Jan 70
3339	12 Feb - 28 Feb 70
3438	18 Apr - 13 May 70
3439	17 May - 12 Jun 70

FIGURE 2

Locations of ship tracks of the "George B. Keithly" showing the free-air gravity anomalies. Black represents positive anomalies.

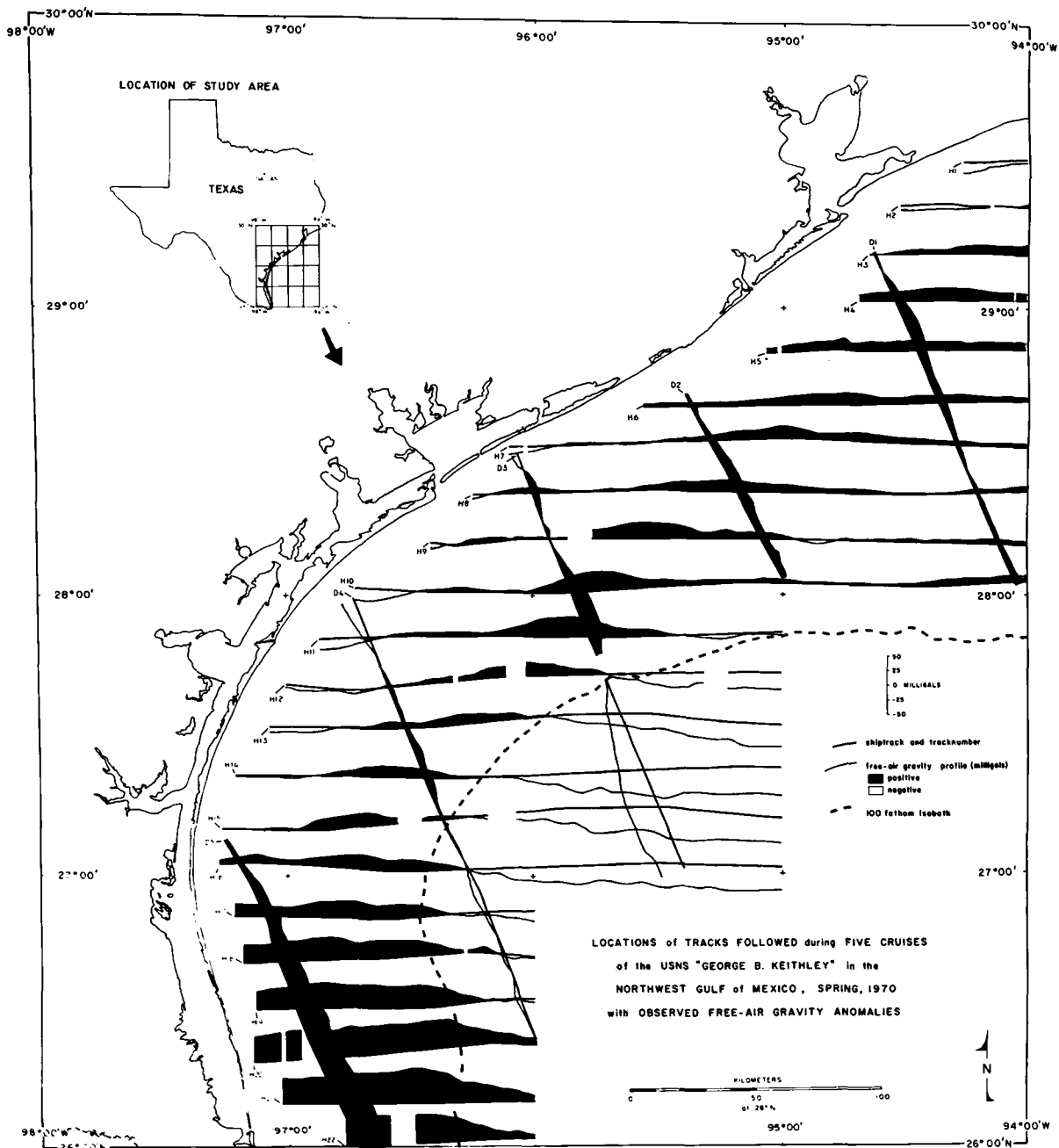


TABLE 2

Locations of Ship Tracks

Track	Number of Stations	Cruise Number	W-NW Origin	E-SE Terminus
H1	106	3337	29 ⁰ 30.10N 94 16.30W	29 ⁰ 31.10N 94 0.50W
H2	133	3337	29 21.00N 94 31.60W	29 29.90N 94 9.20W
H3	206	3337	29 10.90N 94 38.90W	29 10.90N 94 9.10W
H4	206	3337	29 1.10N 94 41.40W	29 10.90N 94 9.10W
H5	393	3440	28 50.00N 95 3.70W	28 51.00N 94 9.20W
H6	476	3337	28 38.60N 95 33.40W	28 39.90N 94 9.10W
H7	658	3339	28 30.20N 96 6.20W	28 30.00N 94 0.20W
H8	658	3339	28 20.20N 96 15.20W	28 30.00N 94 0.20W
H9	1001	3339	28 10.20N 96 25.20W	28 9.30N 94 9.10W
H10	848	3439	28 9.20N 96 43.70W	28 1.10N 94 0.20W
H11	588	3439	27 49.20N 96 52.50W	28 9.70N 94 52.00W
H12	644	3439	27 39.90N 97 1.60W	28 9.40N 95 41.40W
H13	644	3439	27 30.70N 97 4.40W	27 30.50N 95 0.10W
H14	728	3439	27 20.50N 97 12.80W	28 0.10N 94 22.40W

TABLE 2 (cont'd)

Track	Number of Stations	Cruise Number	W-NW Origin	E-SE Terminus
H15	672	3439	27° 9.30N 97 16.10W	27° 21.80N 95 7.30W
H16	728	3439	27 1.70N 97 16.90W	28 0.10N 94 22.40W
H17	393	3439	26 50.50N 97 13.00W	27 0.60N 96 5.30W
H18	392	3438	26 40.40N 97 10.90W	27 0.60N 96 5.30W
H19	369	3438	27 30.30N 97 7.90W	26 32.40N 96 0.20W
H20	336	3438	26 19.20N 97 8.70W	26 32.30N 96 5.80W
H21	336	3438	26 10.20N 97 1.50W	26 32.30N 96 5.80W
H22	204	3438	26 0.10N 96 46.50W	26 1.90N 96 0.20W
D1	417	3337	29 11.40N 94 38.10W	28 0.10N 94 2.70W
D2	280	3337	28 40.80N 95 23.60W	28 21.50N 94 13.40W
D3	524	3440	28 28.70N 96 4.40W	27 9.20N 95 23.80W
D4	679	3339	27 57.80N 96 44.10W	26 23.80N 96 0.10W
D5	392	3438	27 6.80N 97 15.50W	27 5.00N 96 19.20W

13,010 Total Stations

Romberg publication). The function of the stabilized platform is to prevent rotation of the meter in space and to keep it level. These stabilizing functions are accomplished by the use of feedback loops connecting inertial quality gyroscopes, high response torque motors, and accelerometers. The precession of the gyroscopes is optimized by the accelerometers which sense off-leveling. The resultant response by the high torque motors connected to the gyroscopes allows the platform to operate like a long period pendulum which, in effect, cancels out most of the shorter period wave motion (LaCoste, et al., 1967, pp. 101-105). The overall accuracy of this meter under favorable sea states is within one mgal (Lafehr and Nettleton, 1967, p. 116).

The individual gravity stations were taken as successive samples from the continuous output of the gravity meter. The sample intervals range from 800 to 1200 feet. Track spacing was variable, between 15 and 25 km for the east-west tracks and 70-80 km for the northwest-southeast tracks. Positioning was obtained by use of satellite and other navigational systems. Since usable satellite fixes are dependant on the satellites height above the horizon, the frequency of usable fixes may be considerably less than one per hour depending on the latitude. In 1966 the average time between a fix was 90 minutes (Guier, 1966, p. 5904). Other navigational aids such as Loran and Lorac, along with dead-reckoning were used to interpolate between the absolute satellite fixes. The positions and velocities being necessary for computation of corrections applied to the raw data since the gravity meter is responsive to components of accelerations other than the normal component of the earth's field.

The corrections made to the raw data may be divided into those performed by the meter and those performed after the data are collected.

The cross coupling correction, performed by a specially designed computer, is necessary since even though the meter is kept level and restricted from vertical motions by the stabilized platform the ship and consequently the meter is still affected by horizontal motions from sea swells (LaCoste and Harrison, 1961). This effect is sensed as positive or negative motion, depending upon centrifugal force and the center of mass of the meter (LaCoste, et al., 1967, p. 106).

Corrections made after the data are acquired are the Eötvös and drift corrections. The Eötvös correction (Glicken, 1962; Nettleton, 1970) compensates for the change of the measured gravity field caused by the ship's motion. The correction is proportional to the component of velocity in the east-west direction and is dependant on latitude. Drift corrections are applied to the final data to account for any change in the value of absolute gravity measured at the base station before and after a cruise.

ACCURACY OF THE MARINE GRAVITY MEASUREMENTS

Provision is made in the data supplied by the DOD to include a statistical parameter which defines the confidence interval of the free-air anomaly (Appendix 1). Unfortunately, the gravity measurements available in the author's study area did not include this parameter. However, some idea of the repeatability of the data may be gained from analyzing the ship-track-crossing discrepancies. These errors, mainly due to navigation, are listed in Table 3. This table lists the main tracks (D1-D5) and the crossing tracks (H1-H22), the position at the crossing in degrees and minutes of latitude and longitude, the free-air anomaly of the main and cross tracks, and their cruise numbers. For 20 of the 35 crossings, identical positions were not given for both the main and cross tracks so the listed position and free-air anomaly is the interpolated crossing point and anomaly respectively at that position for each track. The interpolated crossings are marked with an asterisk (*).

For each of the five main tracks (D1-D5) the cumulative frequency of error vs. the absolute value of error were plotted on probability paper. From these graphs the graphic means and graphic standard deviations (5th-95th percentile) were computed. This procedure was also used on the total errors. The results of these computations are listed in Table 4.

If the graphic means and graphic standard deviations from Table 4 are plotted on log log paper (Graph 1) then it becomes apparent that track D4 has an anomalous standard deviation. As is seen in Table 3, track D4 has five crossings with errors less than one mgal, three crossings with errors between 3-4 mgals, and one crossing with an error greater than seven mgals. If track D4 is disregarded and the mean and standard deviation of

TABLE 3

Locations and Magnitudes of Crossing Errors

Main Track	Cross Track	Position of Crossing		Free-Air Anomaly At Track Crossing		Cruise Number Main	Cruise Number Cross
		Deg.	Min.	Main	Cross		
D1	H3	29 ⁰	10.90 94 37.90	- 2.5	- 0.1	3337	3337
D1	H4	29	1.10 94 33.20	13.25	14.5	3337	3337
D1	H5	28	50.60 94 27.90	15.85	13.4	3337	3337
D1	H6	28	39.50 94 22.40	11.4	12.4	3337	3337
D1	* H7	28	30.50 94 17.90	5.8	6.6	3337	3339
D1	H8	28	20.40 94 12.90	4.2	5.9	3337	3339
D1	* H9	28	9.50 94 7.40	6.8	8.6	3337	3339
D1	* H10	28	0.90 94 3.10	14.15	10.15	3337	3439
D2	* H6	28	30.70 95 22.40	7.15	4.7	3337	3337
D2	* H7	28	31.60 95 18.10	7.9	7.85	3337	3339
D2	* H8	28	20.80 95 11.60	16.4	17.55	3337	3339
D2	* H9	28	10.80 95 5.60	11.2	9.5	3337	3339
D3	* H8	28	20.60 96 0.80	11.6	8.9	3440	3339
D3	* H9	28	11.00 95 56.55	0.65	0.6	3440	3339

TABLE 3 (cont'd)

Main Track	Cross Track	Position of Crossing		Free-Air Anomaly At Track Crossing		Cruise Number	
		Deg.	Min.	Main	Cross	Main	Cross
D3	H10	27 ⁰ 59.20		22.6	26.1	3440	3439
		95 51.30					
D3	H11	27 49.70		23.4	27.8	3440	3439
		95 47.10					
D3	H12	No Data					
D3	* H13	27 33.20		-21.7	-20.55	3440	3439
		95 39.30					
D3	* H14	27 21.20		-44.4	-42.3	3440	3439
		95 33.60					
D3	* H15	27 13.20		-50.9	-45.3	3440	3439
		95 29.90					
D3	* H16	27 1.20		-39.15	-36.5	3440	3439
		95 24.30					
D4	H11	27 49.70		- 8.7	- 4.8	3339	3439
		95 40.40					
D4	H12	27 39.00		5.2	1.3	3339	3439
		96 35.60					
D4	H13	27 30.20		5.2	8.8	3339	3439
		96 31.70					
D4	* H14	27 19.70		12.5	11.8	3339	3439
		96 27.10					
D4	H15	27 10.90		3.1	3.9	3339	3439
		96 22.70					
D4	H16	27 0.30		- 2.4	- 2.0	3339	3439
		96 16.30					
D4	H17	26 51.00		- 6.4	- 6.1	3339	3439
		96 11.70					
D4	* H18	27 41.80		- 4.3	- 3.65	3339	3438
		96 7.60					
D4	H19	26 32.30		- 7.4	- 0.3	3339	3438
		96 3.60					

TABLE 3 (cont'd)

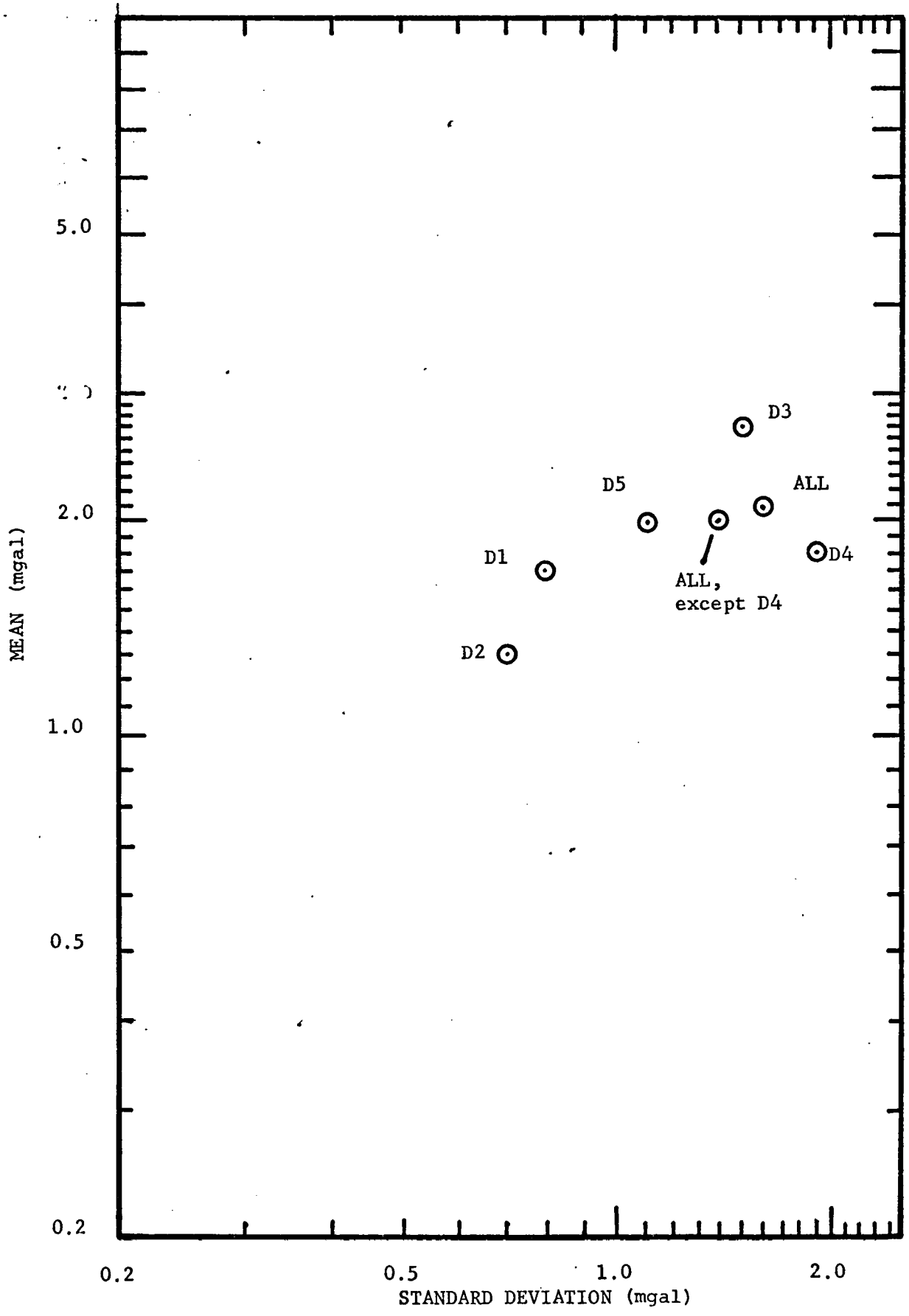
Main Track	Cross Track	Position of Crossing		Free-Air Anomaly At Track Crossing		Cruise Number	
		Deg.	Min.	Main	Cross	Main	Cross
D5	* H16	27 ⁰ 97	1.90 12.10	6.5	9.35	3438	3439
D5	* H17	26 97	50.30 5.70	17.8	17.75	3438	3439
D5	* H18	26 97	40.60 2.40	29.5	30.7	3438	3438
D5	* H19	26 96	30.50 58.20	37.2	36.95	3438	3438
D5	H20	No Data					
D5	H21	26 96	10.10 47.90	46.7	49.1	3438	3438
D5	* H22	26 96	0.20 42.60	46.8	50.4	3438	3438

TABLE 4

Statistics of Crossing Errors

Main Track	Number of Crossings	Range of Absolute Error from Table 3 (mgals)	Graphic Mean of Absolute Error (mgals)	Graphic Standard Deviation of Absolute Error (mgals)	Graphic Range of Absolute Error (5th-95th) Percentile
D1	8	0.8 -4.0	1.7	0.8	0.9-2.5
D2	4	0.05-2.45	1.3	0.7	0.6-2.0
D3	8	0.05-5.6	2.7	1.5	1.2-4.2
D4	9	0.3 -7.1	1.8	1.9	0.0-3.7
D5	6	0.05-3.6	2.0	1.1	0.9-3.1
All Tracks	35	0.05-7.1	2.1	.16	0.5-3.7
All Tracks (except D4)	26	0.05-5.6	2.0	1.4	0.6-3.4

the combined remaining 26 crossings are then computed, one finds that the crossing error is 2.0 ± 1.4 mgals, that is to say, for a normal distribution 90% of the crossing errors are between 0.6 - 3.4 mgals. These errors only apply to the absolute accuracy of the free-air anomaly as the relative error between successive stations on the same line is probably much less than one mgal.



Graph 1 - Mean vs. Standard Deviation of the Crossing Errors

ANOMALY COMPUTATION

Once all corrections have been applied to the raw data the absolute gravity at a station can be determined as the absolute gravity measured at a base station plus the meter difference at the measuring station. For geological interpretation of the results it is necessary to compute the free-air and Bouguer anomalies.

For gravity stations taken from a ship the free-air anomaly is simply

$$g_f = g_a - g_t$$

where

g_f = free-air anomaly

g_a = observed absolute gravity

g_t = theoretical gravity for the station latitude

computed using the 1930 International formula,

$$g_t = A (B + C \sin^2 \phi + D \sin^2 2\phi)$$

where

g_t = theoretical gravity

A = 978049.0 mgal

B = 1.0

C = 0.0052884

D = 0.0000059

ϕ = latitude of gravity station.

Since the meter is at sea level, no elevation correction is necessary.

The Bouguer anomaly is given as,

$$g_b = g_a - g_t + E h$$

where

g_b = Bouguer anomaly

g_a = observed absolute gravity at the station

g_t = theoretical gravity for the station

E = Bouguer correction for infinite slab which is equal to $0.0762 (\rho - 1.03)$ if h is in fathoms

h = water depth at the station

ρ = density assumed for material below water bottom.

For marine gravity studies it is possible to use either the free-air anomaly or the Bouguer anomaly for models of the crustal structure. Valid arguments may be proposed for the use of either anomaly, however, while the calculation of the gravity effects of a localized body, especially in areas of rapidly changing water depth, is often easier if the Bouguer anomaly is used, for long cross-sections which may encompass substantial changes in water depth, the use of the Bouguer anomaly could produce spurious results. This is because the Bouguer anomaly replaces the water layer with material of the same mass as the near surface lithology. This replacement has the effect of eliminating the water-sediment interface. The method assumes knowledge of the densities of the sediments at moderate distances below the water bottom with topography of rather low relief. In areas of fairly constant near-surface lithology this is not a major problem. An example of the possibility of errors is if a Bouguer anomaly is computed for a depth of 100 fathoms in part of a survey area and then computed for a depth of 1000 fathoms in another part of the same area. The large difference in water depths suggests, especially in areas of sediment density increasing with depth, that the reduction density should be larger for the larger water depths (Talwani, 1966).

The free-air anomaly, on the other hand, makes no density assumptions. When computing gravity models the water depths and density are known parameters used in the calculation of the regional gravity anomalies. For

this reason the free-air anomaly, interpreted with knowledge of the topography, is probably best for marine gravity computations on a regional scale.

In calculating the gravity effect of the crustal section the Bouguer anomalies were used for the land stations and the free-air anomalies were used for the marine stations.

The local anomaly on the South Texas continental shelf, on the other hand, was computed from a residual anomaly derived after the Bouguer correction had been applied to the free-air anomaly on line H16.

PROCEDURE USED IN PREPARING THE GRAVITY MAP

The preparation of the gravity map required the following steps:

- (1) Determination of density of gravity stations in the area of study.
- (2) Extraction of data from storage and reordering the gravity measurements to their original positional sequence.
- (3) Plotting the individual tracks as free-air anomaly vs. distance.
- (4) Posting all ship tracks with their gravity values on a base map.
- (5) Contouring the Marine data.
- (6) Adding the land gravity contours and tying the land contours with the marine contours.

A description of each of these procedures is listed below:

(1) The density of gravity stations in the study area was determined by using a FORTRAN program, DATACOUNTER (Appendix 2) which searches the data tape and counts the number of gravity stations present within each degree of latitude and longitude. The degree is broken into ten-minute areas and the number of stations within each area is listed. A sample of the output is shown in Appendix 2. A listing of the actual data was obtained by using DATALISTER.

(2) Extracting the data and reordering the measurements into the original positional sequence was performed by DATAPROCESOR (Appendix 2). Reordering the data was necessary since the data had been sorted by increasing latitude within a degree of increasing longitude. While this is an efficient manner of cataloging large masses of data, it does not allow the easy extraction of data along a particular ship track. In all, portions of 27 tracks were used in the preparation of the map. To provide a rapid method of reforming these lines, the program DATAPROCESOR was written.

Analysis of the "contents of a logical record" (Appendix 1) containing the necessary data for one gravity station shows that there is no one specific characteristic of a particular track which could distinguish it from all other tracks. The cruise number however, contained in word six, does provide some degree of uniqueness. This results from the fact that the data used for the study was acquired during five different cruises. By specifying the maximum and minimum coordinates along with the cruise number, both available from a listing of the data, obtained by using DATALISTER and DATACOUNTER one is able to extract the gravity stations which comprise an individual track plus any pieces of other tracks which may intersect it from the same cruise. These data are then arranged in their original order and punched onto cards, each card indicating the relative position for the station, its latitude, longitude, free-air gravity, and the cruise number. Along with the cards a listing of the same data is provided for each station plus a line printer graph of the free-air anomaly vs. station. The problem then becomes the simple one of physically separating the few crossing points from the resulting card deck.

(3) Once the actual ship tracks had been reconstructed it was found advantageous to plot the free-air anomaly vs. distance precisely to have a hard copy for later reference. The program PROFILEPLOT was written to perform this operation. A Benson-Lehner 48 inch flatbed plotter belonging to the University of Houston Electrical Engineering department was used for this purpose. PROFILEPLOT uses software (on permanent storage at the U of H Computer Center) written specifically for this apparatus.

The spherical coordinates of the gravity stations were converted to rectangular coordinates and the cumulative distance from the origin of the track (taken as the first data point from the west) to each gravity station

was computed. The individual stations were plotted as a continuous line, unless the spacing was greater than a specified minimum, to indicate intervals of missing data, with the horizontal scale being given in kilometers. Necessary annotations were supplied to the software to obtain constant output format for the profiles.

(4) Next, a suitable base map was chosen (U.S. Coast and Geodetic Survey Chart No. 1117, Galveston to Rio Grande) for plotting the ship tracks. The program MAPPLOT was used to plot the location of the ship tracks plus the free-air gravity anomaly as a continuous curve (except the intervals where data were missing). The chart chosen for the base was drawn using a Mercator Projection. The plotted lines however, were drawn using a constant scale at 28° N lat. Consequently there is a small amount of compression of the point spacing below 28° N lat. and extension of the actual locations above 28° N lat. This distortion is not considered critical at the scale of the map and the resolution for which it will be used.

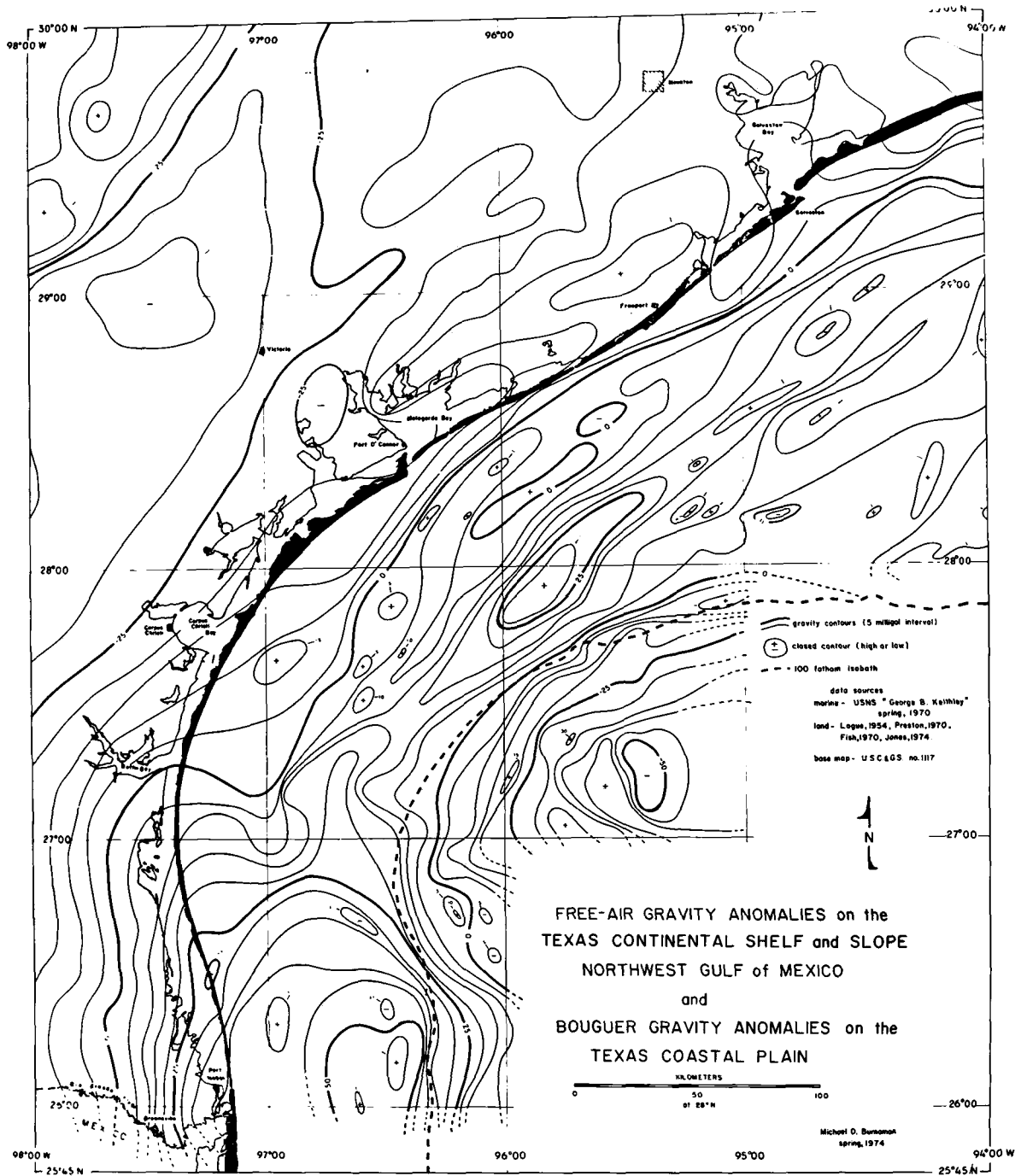
(5) The map was contoured with a five-mgal interval. The intervals were first located on a listing of the data for the ship tracks and these values were transferred to the base map by locating the individual stations, each represented by a discrete point, on the map. An overlay was used for drawing the contours.

(6) The portion of the Bouguer gravity map by Logue (1954) that was of interest was enlarged to the same scale as the marine base map by using a Kale projector and the contours transferred to the overlay directly by hand. The same procedure was used for the map of Preston (1970). The land and marine contours were then joined together. This process did not require changing the contouring of the marine data as the seaward extension of the Bouguer values was very smooth.

The regional gravity map prepared by the method previously outlined is shown in Figure 3 and Plate II.

FIGURE 3

Regional gravity map of part of the Texas coastal plain and the Northwest Gulf of Mexico. Contour interval is five milligals.



LOCATION, MAGNITUDE, AND EXTENT OF THE MAJOR GRAVITY ANOMALIES

The significant anomalies that can be resolved within the five mgal contour interval of the gravity map are shown in Figure 4. Five regional anomalies are present, in addition to many local minima (not resolvable on the contoured map but easily seen on a plot of the ship tracks) on the southern continental shelf (Fig. 5).

A description of each of the anomalies is given below:

(1) The Ouachita Structural Belt Bouguer maximum (AA) is located in the northwest corner of the map. It trends northeast-southwest and has an amplitude of as much as 20 mgals above the regional trend. This anomaly is part of a much larger feature which parallels the Ouachita Structural Belt, from southeastern Oklahoma south to San Antonio, Texas, where it veers west toward Uvalde, Texas and on into the Marathon Uplift region of West Texas (see Fig. 1) (Logue, 1954; Watkins, 1961, p. 28).

(2) The Rio Grande Bouguer and free-air maximum (BB) dominates the southern part of the map. It is a broad maximum associated with the Rio Grande delta; consequently it continues farther west and south than is shown on the map. Maxima of as much as 57 mgals are associated with this anomaly on the continental shelf. The overall size of this anomaly is probably as much as 230 km north-south and over 300 km east-west, covering more than 70,000 square kilometers.

(3) The Continental Shelf free-air maximum (CC) is a curvilinear feature extending from the northeast margin of the map southwestward possibly as far as the southern margin. In the area above 28°N lat. the anomaly follows the coastline between 50-70 km offshore. At $27^{\circ}30'\text{N}$ lat. the anomaly bifurcates with the western portion trending northeastward

FIGURE 4

Regional gravity map showing the locations of the five major regional anomalies discussed in the thesis. These anomalies are coded as follows:

- AA - Ouachita Structural Belt Bouguer Maximum
- BB - Rio Grande Delta Bouguer and Free-air Maximum
- CC - Texas Continental Shelf Free-air Maximum
- DD - Freeport Bouguer Maximum
- EE - Texas Continental Slope Free-air Minimum

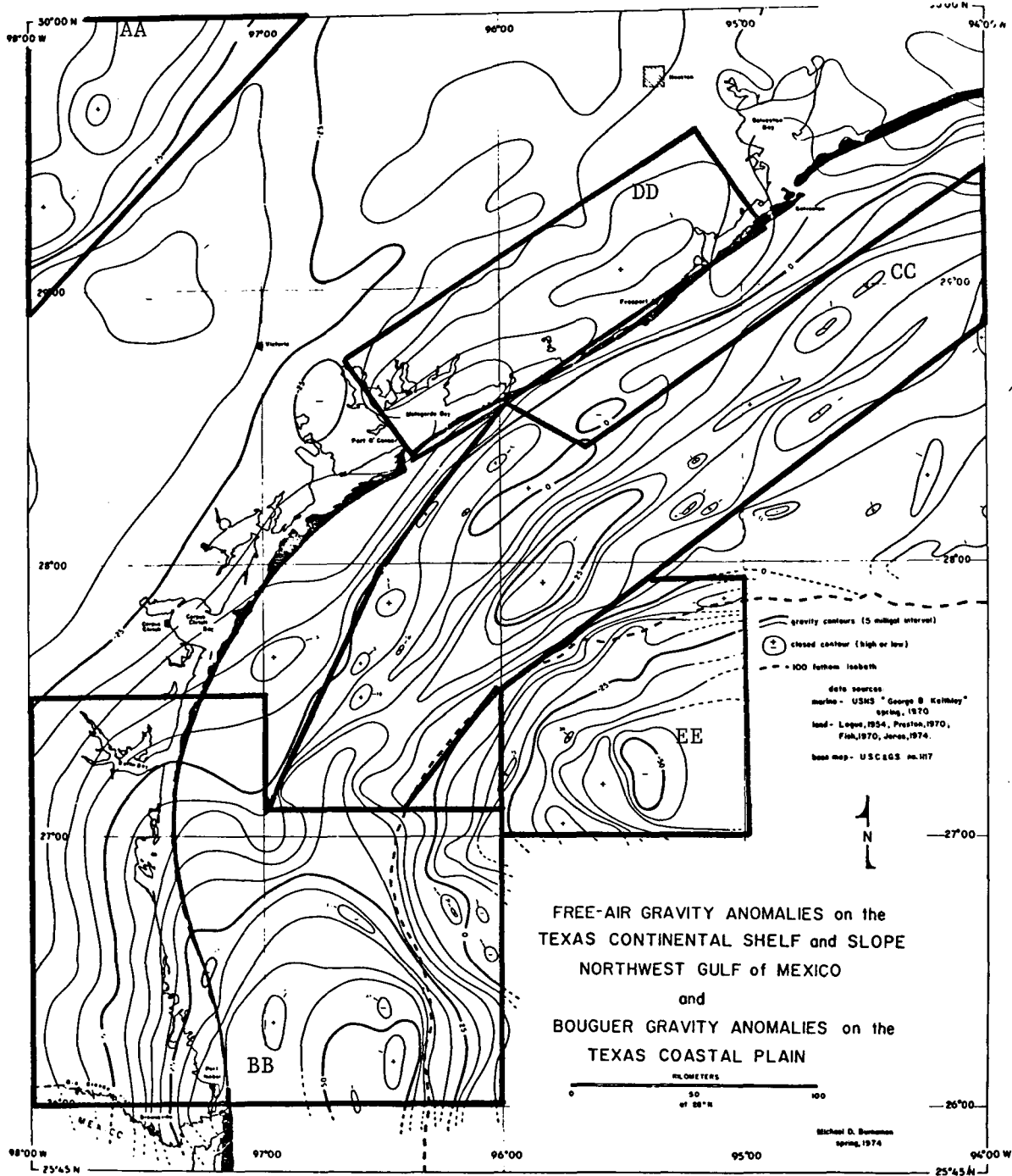
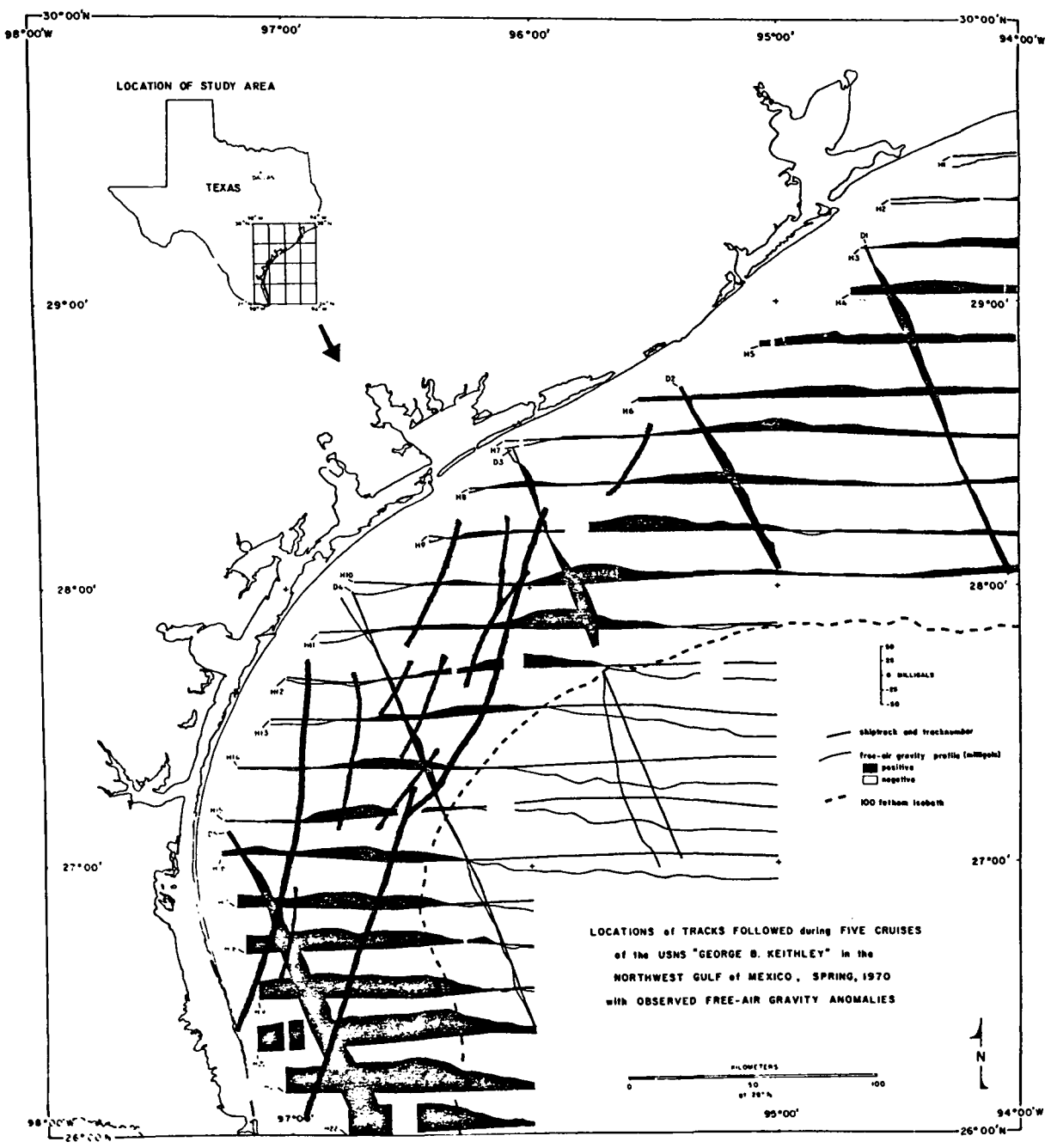


FIGURE 5

"Keithly" ship tracks showing the locations of curvilinear gravity minima south of 29° N lat. and west of 95° W long. Red denotes the most obvious anomalies (possibly due to low density, highly pressured diapiric shale). Blue denotes similar anomalies which appear to be localized. Yellow denotes a possible salt ridge.



LOCATIONS OF TRACKS FOLLOWED during FIVE CRUISES
of the USNS "GEORGE B. KEITHLEY" in the
NORTHWEST GULF of MEXICO, SPRING, 1970
with OBSERVED FREE-AIR GRAVITY ANOMALIES

toward the mouth of the Colorado River while the original portion appears to continue southwest from the point of bifurcation and trend toward the coastline into Port Isabel where it leaves the area of control; alternatively, the maximum could trend toward the continental shelf edge as it is followed south. The continuations of the trend south of the point of bifurcation should be considered speculative, at best. On the major anomaly southwest of Galveston are isolated highs of 15-20 mgals. These highs merge offshore Port O'Connor, giving a maximum anomaly of 32 mgals. This maximum decreases toward the south to the point of bifurcation where it is 10-15 mgals and becomes superposed with the Rio Grande maximum to the south. The total length of this anomaly (on this map), excluding the bifurcation and including the extension to 26°N lat. is almost 550 km. There is evidence (Joesting and Frautschy, 1947; J. C. Weyand, personal communication, 1974) that the maximum extends 110 km east of the Texas-Louisiana border, still on the continental shelf.

(4) The Freeport Bouguer maximum (DD) is located southwest of Freeport, Texas and extends southwestward into Matagorda Bay. The length of this anomaly is approximately 200 km and the magnitude above the regional is as much as 15 mgals in the southwestern portion, decreasing in magnitude and broadening to the northeast. Another positive anomaly is located 85 km northwest of the Freeport anomaly. This anomaly has a magnitude of less than seven mgal and a linear extent of 100 km.

(5) The Continental Shelf free-air minimum (EE) is located within 27° - 28°N lat, 95° - 96°W long. This is a negative anomaly of as much as -50 mgals. The true extent of this anomaly is not shown on the map due to the lack of data to the south and west; however, the free-air anomaly map of the Gulf of Mexico (contour interval of 25 mgals) by Rabinowitz in

Worzel (1973, p. 745) shows this minimum anomaly to extend as far south as 21°N lat with the width varying between 50 and 200 km.

(6) The minimum anomalies on the southern continental shelf (Fig. 5) appear to be both of a local and regional nature. One of these minima (shown as the longest red line in Fig. 5) is over 300 km long with negative anomalies of as much as -12 mgal and may be indicative of a major near-surface (less than 5 km) structural trend. Another major minimum anomaly (shown as the other red line in Fig. 5) is located farther inshore and trends onshore on the southern end (Jones, 1974). The largest magnitude of this anomaly is probably no more than -6 mgals below the regional trend. Numerous other negative anomalies (blue lines on Fig. 5) are present. Most of these are concentrated between the two regional minima.

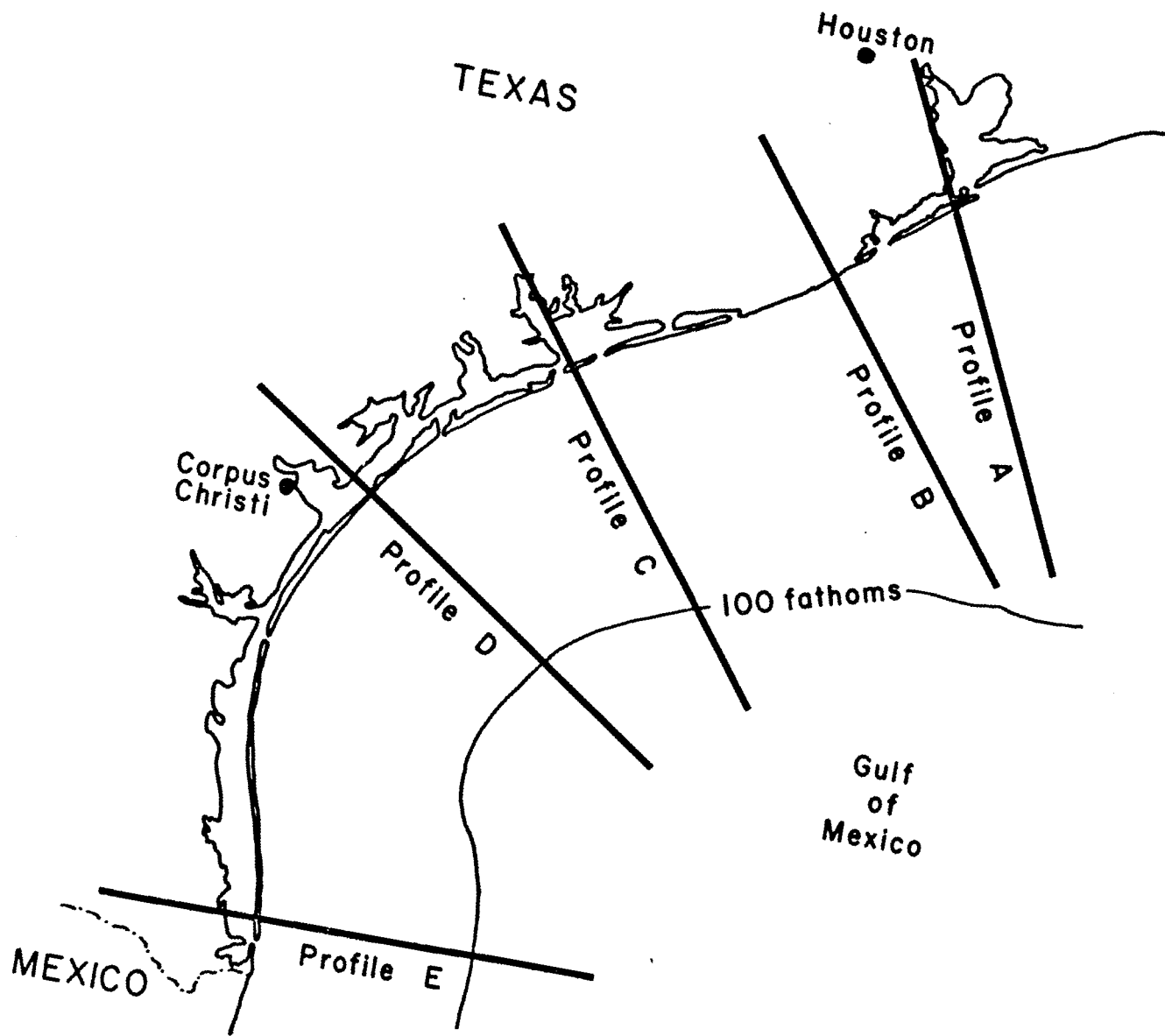
To better show the spatial relationships between the regional gravity anomalies, shown in Figure 4, and the coastal physiography, five profiles perpendicular to the coastline were made from the regional gravity map. Their locations are shown in Figure 6 and the actual profiles are shown in Figure 7.

Each profile begins 70 km inland and extends 150 km offshore. The position of the coastline is shown on each profile at its geographical location. All coastlines are aligned for reference.

The presence of the Texas continental shelf gravity maximum (TCSGM) (CC of Fig. 4) can be seen on profiles A-D and may be inferred on profile E. The TCSGM can be seen to have two components (M1 and M2) in profiles C and D. To the west in profiles A-C the Freeport Bouguer Maximum (FBM) (DD of Fig. 4) (M3 of Fig. 7) can be seen to have its largest amplitude on the Matagorda Peninsula profile (C). It can be seen from the regional gravity map (Fig. 3) that the southwestern termination of the FBM has

FIGURE 6

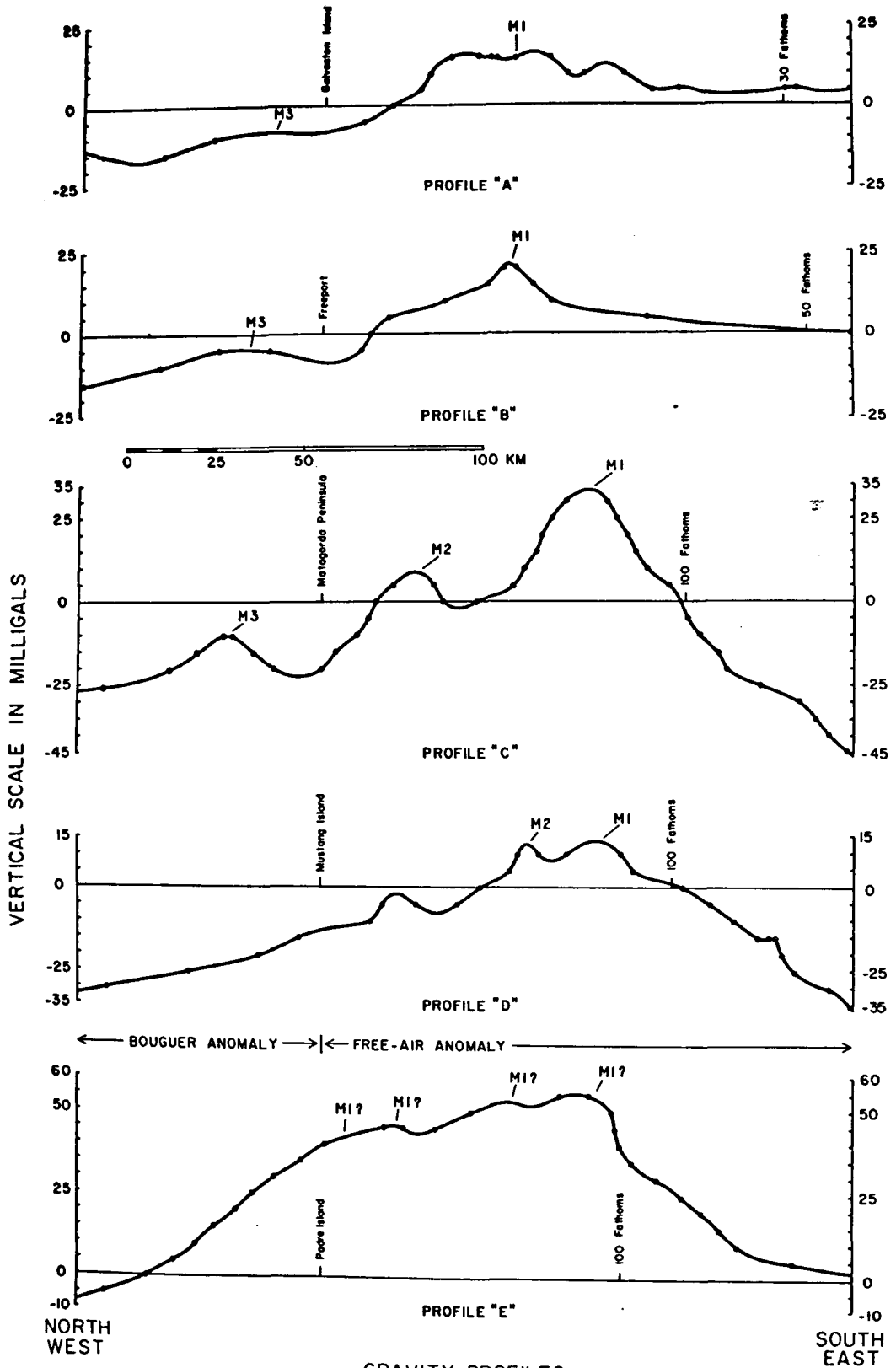
Location of five profiles taken from the regional gravity map
in Figure 3.



Location of Profiles A-E taken from the Gravity Map

FIGURE 7

Five profiles taken from the regional gravity map of Figure 3. The locations of these profiles are shown in Figure 6. The geographic reference denotes the coastline. Bouguer anomalies are west of the coastline. Free-air anomalies are offshore. M1, M2, and M3 represent inferred correlations of the Texas continental shelf gravity maximum and the Freeport maximum.



GRAVITY PROFILES
ACROSS TEXAS COASTAL PLAIN
AND CONTINENTAL SHELF

a much steeper gradient than the northeastern termination.

The regional Bouguer gravity field (excluding the FBM) can be seen in profiles A-D as varying from -12 to -33 mgals 70 km inland with a smaller gradient toward offshore to the north.

The continental slope gravity minimum (CSGM) (EE of Fig. 4) can be seen on profiles C and D where the 100 fathom water depth is characterized by a free-air anomaly of approximately zero, indicating approximate isostatic equilibrium, decreasing rapidly farther offshore. A bathymetric high, possibly a salt diapir, can be seen 25 km from the eastern termination of profile D.

The remarkable gravitational effect of the Rio Grande delta (the Rio Grande Delta gravity maximum (RGDGM) of Fig. 4) is shown in profile E. The distance along the continental shelf from profile D to E is 160 km. Comparison of the anomalies at the coastline and the center of the continental shelf on profiles D and E indicate a gradient of 0.3 mgal/km increasing from D to E. While profiles A-D do not encounter the zero Bouguer anomaly contour until approximately 400 km inland, in the vicinity of the Llano uplift area, profile E shows it to be present less than 20 km from the coast.

QUALITATIVE ANALYSIS OF THE RIO GRANDE DELTA GRAVITY MAXIMUM

The term "Rio Grande Delta" as used in this discussion applies not only to the geographical area covered by the emerged delta but also the submerged portion. The term also applies to the delta as it has existed throughout the Quaternary.

Location and Association with other Gravity Anomalies

The Rio Grande Delta gravity maximum, RGDGM) as has been previously defined, is enclosed by the area shown in Figure 4 (BB). This maximum extends westward out of the map area (Logue, 1954; Murray, 1961, p. 50) as a positive nose trending west-northwest at $26^{\circ}30'N$ lat. culminating in a large negative anomaly of -50 mgals along the Texas-Mexico border extending into Mexico just west of McAllen, Texas (Murray, 1961, p. 63; Fig 1, this thesis).

Modern Deltas and Isostasy

The regional warping of the crust by widely distributed loads such as continental glaciers (Walcott, 1970a) and point loads such as volcanic islands (Walcott, 1970b), are often cited as evidence of isostatic adjustments. However, application of isostasy to explain the vast thicknesses of modern and ancient deltaic sequences, while being accepted as the proper mechanism, does not account for the apparent limiting thicknesses of sediments (Barton, et al., 1933, p. 1458). In a classic paper, Lawson (1942, p. 1238) proposes that for the Mississippi delta, the thicknesses of sediment (more than 36,000 ft.) could be explained by the initial loading that took place on an isostatically balanced surface, approximately four km deep, a depth arrived at by studying continental margins off Africa,

India, Australia, and North and South America (p. 1239). While the depth of four kilometers which Lawson proposes may be too great, the mechanism of subsidence of deltas can be explained qualitatively on this basis.

Comparison of the Gravity Effects of the Rio Grande with other Modern Deltas

The association of a high positive free-air gravity anomaly offshore and a low negative anomaly farther offshore is a common characteristic of modern deltas. In a north-south geophysical cross-section through central Louisiana published by Nettleton (1952, p. 1224) a negative Bouguer anomaly of -30 mgals is centered 90 km inshore from the present coastline. A regional Bouguer anomaly map (with 10 mgal contour interval) of the western Gulf of Mexico continental shelf, made available to the author by Mr. Jack Weyand of Sidney Schafer and Associates, shows a positive anomaly of 40-50 mgals along the offshore portion of the Mississippi delta (not to be confused with the eastern extension of the Texas continental shelf gravity maximum) with the highest values being just offshore from the present delta distributary channels. The distance between this maximum and the minimum shown by Nettleton (also shown on the map by S.S.A.) is 160-250 km depending on positions chosen on the offshore maximum.

The Niger delta is presently prograding into the Gulf of Guinea and has been actively building since the Tertiary. A Bouguer anomaly map of the emerged portion of the delta by Hospers (1965, p. 411) shows a broad minimum anomaly of -37 mgals located 130 km inland. At the coastline is a positive anomaly of just over 40 mgals. Although no data are given in the paper it is possible that the positive anomaly extends farther offshore.

The Nile delta is another example of a positive gravity anomaly offshore coupled with a negative anomaly onshore. Active during Plio-Pleistocene

and Recent time, the Nile delta has extended the Egyptian coastline 100 km into the Eastern Mediterranean (Harrison, 1956, pp. 320-323). Isostatic anomalies reveal a minimum of -20 to -22 mgals centered 80 km inshore and a maximum of 43 mgal centered 45-55 km offshore giving a maximum to minimum distance of 130 km. The minimum thickness of the deltaic sediments, assuming no subsidence, is estimated by Harrison (p. 321), to be 7000 feet. Subsidence is indicated, however for after computing the attraction of this prism of sediments and subtracting it from the observed anomaly, Harrison observed that the remaining anomalies are all negative (-20 to -60 mgals) which was considered indicative of crustal displacement by loading.

Another modern delta, the Amazon, described by Cochran (1973, p. 3261) is characterized by a positive free-air anomaly of 48 mgals just inside the 100 fathom isobath. The distance from the anomaly peak to the center of a large negative anomaly inshore does not appear to be more than 100 km.

The distance from the coastline inland to the center of the McAllen Bouguer minimum (previously discussed) associated with the RGDGM is 150 km. The total distance between the center of the McAllen anomaly and the center of the RGDGM is 220 km. Thus the McAllen minimum anomaly is 60 km (average of inland distances for the Mississippi delta minimum with respect to the offshore positive anomaly further to the east) and 20 km further inland than the Mississippi and Niger delta minima and the magnitude of this minimum also exceeds that of both the Mississippi (-30) and the Niger (-30 to -40) anomalies. The total minimum to maximum distance of the Rio Grande anomalies is then approximately 20-30 km (average) greater than that for the Mississippi delta anomalies.

The Nile and Niger deltas could represent the minimum separation of anomaly peak and troughs at 130 km while the Mississippi could represent

an extreme of up to 250 km (if the greatest separation between the maximum and minimum is considered). The Rio Grande anomalies with separation of 220 km fall between the extremes.

Walcott's Hypothesis about Flexural Rigidity of the Lithosphere

A possible hypothesis to explain the observed Rio Grande anomalies can be patterned after Walcott (1972). In his discussion of the flexural rigidity of the lithosphere, he proposes that early stages of deltaic loading along undeformed continental margins will produce a set of characteristic free-air gravity anomalies with an intermediate stage having a positive anomaly over the continental shelf which will be flanked by negative anomalies, caused by lithosphere flexure, over the emerged delta and continental slope. As examples of this theory he uses, with convincing argument, the previously discussed Mississippi and Niger deltas. This argument allows the gravity maximum to be centered over the present deltaic continental shelf with the inland anomaly being centered at or close to the original edge of the depocenter.

Before further analysis of the data, however, reference should be made again to the McAllen gravity minimum. Conservative estimation of the depth to the basement in the vicinity of the McAllen anomaly from contours on the AAPG Basement Map of North America (Flawn, 1967) results in a depth value of 12-13 km. Mean elevations in this area are much less than 100 meters. The only other area in Texas having similar elevations and gravity anomalies is the "East Texas" Bouguer minimum located 160 km into the East Texas embayment (Fig. 1, this thesis; Murray, 1961, p. 50). This minimum anomaly is more than -40 mgals and the depth to basement in this area (Flawn, 1967) is 7.5 km. Examination of Figure 3 reveals that there is no broad offshore maximum anomaly associated with the East Texas minimum.

Considering the overall similarity between the Rio Grande and East Texas embayments, the likelihood of radically dissimilar origins for the minimum anomalies associated with them is remote, yet the East Texas minimum does not have a maximum associated with it while the Rio Grande does.

The apparent similarity in the morphology of the gravitational effects of deltaic loading in widely separated continental margins suggests a similar mechanism of development for the various deltas. If Wallcott's flexural hypothesis is accepted for that mechanism and applied to the Rio Grande, McAllen, and continental slope anomalies the following order of events may be proposed (Walcott, 1972, p. 1846):

- (1) Formation of an initial edge-effect anomaly on the sediment-free continental margin.
- (2) Initial loading of the continental margin by the delta, producing a downward flexure of the lithosphere. The rigidity of the lithosphere causes this flexure to be transmitted inland and further offshore. The gravity effect is a wide negative anomaly caused by the downwarp of the crust, but with a positive anomaly centered over the present sediment prism which by itself has not been compensated. In order these anomalies are the McAllen minimum, the Rio Grande maximum, and the continental slope minimum.
- (3) As the delta progrades the anomalies move further toward the basin.
- (4) When deposition ceases the positive anomaly directly over the uncompensated sediment prism approaches zero as the crust spreads to distribute the load. The minimum anomaly inland will probably not approach zero as it was not an area of maximum deposition in

the original sequence and is still depressed from the loading.

The negative free-air anomaly offshore will still remain as it is caused partly by the increase in water depth, although some isostatic adjustment may take place to cancel this effect.

The East Texas minimum anomaly can be explained in the same fashion.

The absence of the associated broad maximum anomaly over the upper Texas continental shelf is simply due to the length of time since the last major deposition being such that local compensation of the load has taken place.

PREPARATION OF THE CRUSTAL SECTION

Introduction

Before preparing the crustal section, several factors, each of which has a significant contribution to the validity of the section, must be evaluated. Among these are:

- (1) Proper location, including an area which best displays the Texas continental shelf gravity maximum and the Gulf Coast geosyncline with its structural relationships and which optimizes the other available data.
- (2) Determination of how well the gravity computation procedure applies to the area of interest.
- (3) Determination of the optimum number of layers which will best present any known or presumed structural features and also have the least ambiguity.
- (4) Assumption of geologically realistic densities for the layers which are compatible with other available data and investigations.
- (5) Selecting a depth of compensation for the section which will be both applicable to the problem and also be comparable to crustal sections computed at other locations.

A discussion of each of these factors is presented in the following text.

(1) Selecting the Location

The siting of the crustal section should be determined by the following priorities:

- (a) The location should be as close as possible to the refraction lines used by Ewing et al. (1955), Cram (1961), and Dorman et al. (1972).
- (b) The section chosen should be representative of the deep crustal

structure of the Texas coastal plain, continental shelf, and continental slope.

(c) To obtain the most realistic regional gravity field, the section should be located in an area free from the effects of abnormally shallow low density sediments.

(d) The section should be located coincident with or adjacent to previous crustal sections so as to facilitate comparison.

(e) To minimize isostatic effects, the section should be located in a region which has not been subject to large amounts of recent sedimentation.

The optimum location of the crustal section, chosen on the basis of these criteria, is shown in Figures 1 and 8. The line extends from $29^{\circ} 1'N$ lat. $96^{\circ}58.50'W$ long. southeast 276 km to $27^{\circ} 0'N$ lat. $95^{\circ}16.75'W$ long.

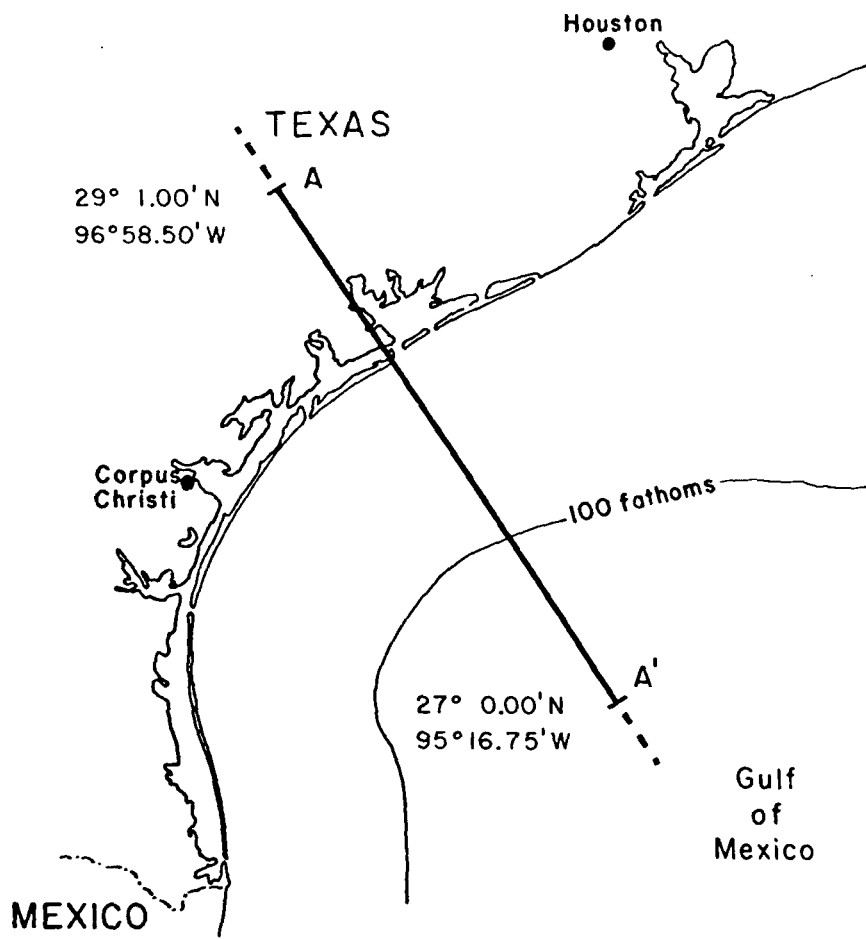
This location is within the zone of overlap of both the Cram and Dorman, et al. refraction profiles and allows projection basinward to the refraction station of Ewing (V-24) as an anchor. Lack of precise gravity data, however, prevents actual extension of the crustal section to Ewing's station.

As can be seen in Figures 3 and 9, the section is located across the significant gravity anomalies (both the Freeport maximum and both components of the Texas continental shelf maximum as well as extending into the continental slope minimum), so it should show the structural significance of these anomalies.

The proximity of the section to and parallelism with the San Marcos arch (Fig. 1) and its possible basinward extension should result in a thinner section of Mesozoic evaporites and should also minimize the effects

FIGURE 8

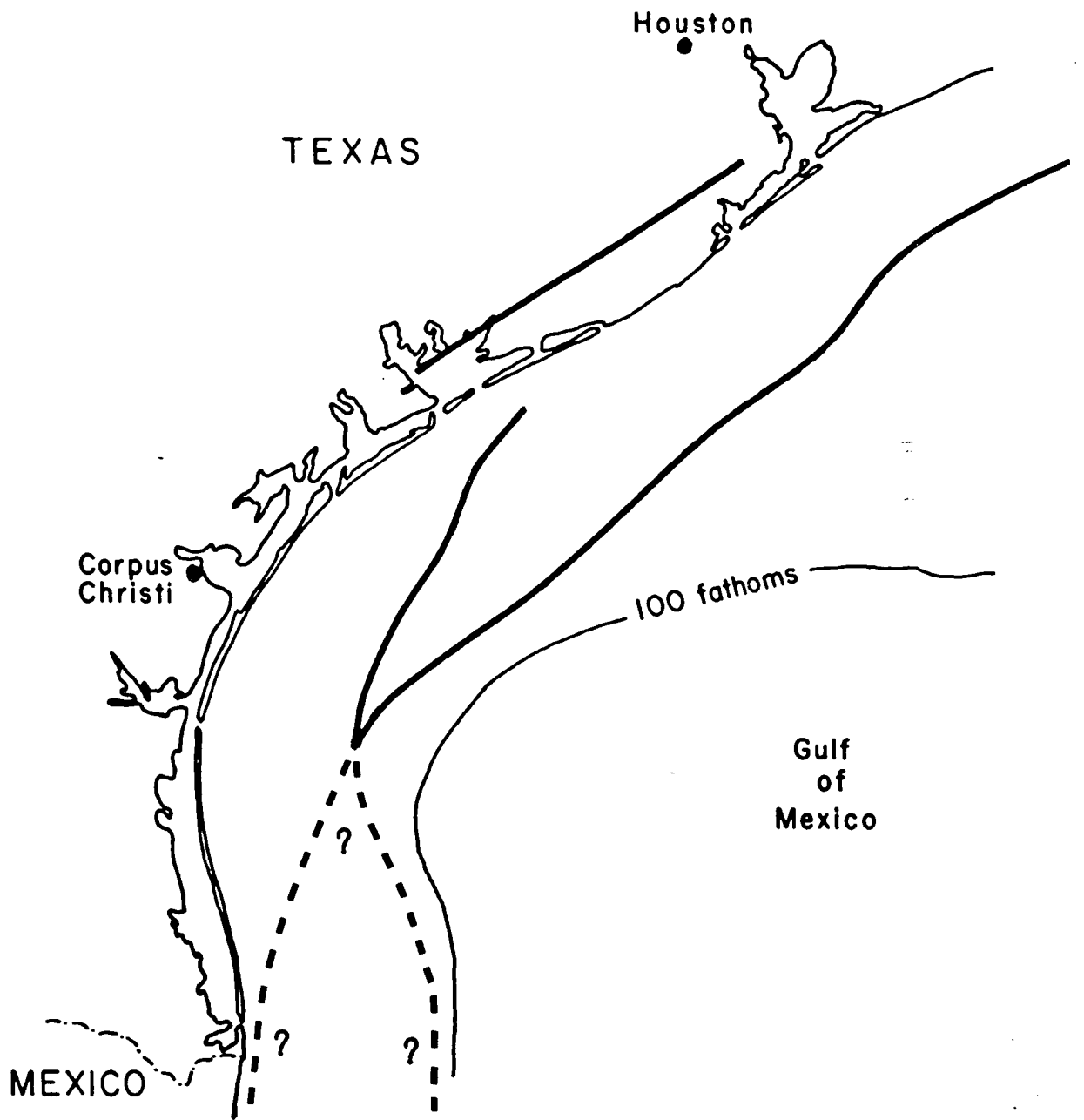
Location of the crustal section shown in Figure 10.



Location of Crustal Section

FIGURE 9

Location of gravity maxima on the Texas coastal plain and continental shelf. The broad line represents the location of continuous gravity maxima on the Texas coastal plain and continental shelf. The dashed portion represents speculative continuance of the Texas continental shelf maximum.



Locations of Free-Air and Bouguer Gravity Maxima

of the Tertiary low density shale as the location appears to be on the edge of that depositional province. Thus the negative anomalies resulting from these lower density materials should be minimized along the section.

Several other crustal models have been prepared parallel to this line, among these are Keller and Cebull (1973), Fish (1971), Cram (1962), Dorman et al. (1972), and Worzel and Watkins (1973). The two former models are actual computed gravity models while the later three represent models derived from seismic and well control which are projected out into the Gulf to tie with the refraction stations of Ewing et al. (1955).

A significant factor that might explain the popularity of this location with different workers is that the area probably represents the thinnest sediment cover along the Texas coast (as interpreted from isopachs by Williamson (1959), Waters et al. (1955)) and has not been an area of significant deposition since the Miocene (Murray, 1961).

(2) Validity of the Computation Method

The procedure used in computing the gravitational attraction of the crustal section is that outlined by Talwani et al. (1959a and b) and in Appendix 2. This is a two-dimensional technique, i.e., the geometry and densities of the assumed layers may vary laterally and vertically, but the third dimension (into the section) must remain constant. This technique is valid along the crustal section, since the trend of the axis of the major structural feature, the Gulf Coast geosyncline, closely follows the present coastline. The mantle and oceanic crust extend in all horizontal directions while the strike of the continental crust and any Paleozoic sediments closely approximates the coastline although inland from it. The only variations of the structure of these main layers occurs along strike. Any major discrepancy in computing the anomaly probably then results from

lateral density variations and thinning in the sedimentary layer. These effects however, are probably minimal.

(3) and (4) Lithologic Characteristics and Geometry of the Layering

Perhaps the most important assumptions in the computation of gravity anomalies are the number and geometry of layers and their densities or density contrasts. It can be shown that as the number of layers increases the ambiguity inherent in the solution of any potential field problem also increases, unless there is sufficient seismic control to establish the depths of the interfaces. Yet use of too few layers for a particular problem may result in a geologically unrealistic solution. The optimum geometry then will be that which can be established by well control, or by seismic or magnetic data or which can be inferred by analysis of regional structural and stratigraphic trends. These same statements apply to the choice of densities. The final result is to obtain as many interface locations and densities as possible through the use of well, seismic, and magnetic data and then to apply the gravity interpretation to solve for the other variables that cannot be determined from such data.

In the construction of the crustal section, six layers are used. They are the water layer, sediments, Paleozoic "Metasediments", continental crust, oceanic crust, and the mantle. The thicknesses and extent of the various layers is given at the three refraction stations along the crustal section. From the indicated depths at these stations it is possible to "hang" the interfaces on the known control points and project their lateral extensions by use of the observed gravity anomalies. Since the number of layers is approximately known from the refraction data, it remains to assign densities to each. However, since it is the contrast between the assigned density and the average density of a theoretical "standard section"

that is used in the calculations, its relationship to the computation of regional gravity anomalies should be given.

(5) Selecting the Depth of Compensation and a "Standard Section"

The total attraction of a crustal column depends on the average density of the column and its total thickness. The depth at the bottom of the column is known as its "depth of compensation" or the depth at which isostatic equilibrium prevails (Heiskanen and Vening Meinesz, 1958, p. 124); below this depth it is assumed that densities are laterally uniform.

A "standard section" is an ideal crustal column whose total attraction represents the average for large areas such as continents or ocean basins (Worzel and Shurbet, 1955b). These sections, of course, are synthetic, being derived from the study of large numbers of seismic refraction stations and their corresponding gravity anomalies. While the layering of a particular standard section is immaterial, the total attraction (corrected for observed gravity anomalies) of all standard sections around the world should be the same (Talwani, 1964, p. 34).

Using the "standard section" the computed regional gravity anomaly at a station is then the total attraction of the crustal column at that point minus the attraction of the standard section. This anomaly is attained by using the density contrasts which result from subtracting the average density of the standard section from the known or presumed density of each layer. These computed anomalies should then show the variation in structure at a particular location with respect to an assumed column of mass representing the average throughout the world.

To compute the standard section of an area, knowledge of the number of interfaces, obtained from seismic refraction data in the area, and knowledge of the densities of the layers, achieved by comparing the P-wave

velocity of the layer to the empirical Nafe-Drake curve (Menard, 1967, p. 3065, Fig. 3), by study of the literature, and by inferring its composition on the basis of whatever other data might be available.

Description of each Layer and its Inferred Density

(1) Mantle - Compressional velocities assumed to be representative of the upper mantle were observed by Cram (8.18 km/sec), by Dorman et al. (8.41 km/sec) inland and along the south Texas coastal plain. Warren et al. (1966) report a mantle velocity of 8.38 km/sec in southern Mississippi while Ewing et al. (1955) report a mantle velocity of 8.3 km/sec south of the Sigsbee Escarpment (V-24) on the northern edge of the abyssal plain in the Gulf of Mexico.

These recorded velocities, ranging from 8.18 to 8.41 km/sec are anomalously high when compared to the western United States and most of the east coast or for the rest of the world for that matter (Herrin, 1969, p. 243, Fig. 1). Only in the central U. S. and along the coast of southern California are the compressional velocities greater than 8.2 km/sec. The low mantle velocities in most of the western United States have been attributed to a lower density mantle (3% deficiency) by Thompson and Talwani (1964, p. 4813). A normal mantle density for that region should be 3.4 gm/cc. Since the western United States is characterized by anomalously high heat flow, the result of geologically recent tectonic activity (Simmons and Roy, 1969, p. 81) the observed low mantle velocities and density are not surprising.

Heat flow in the northern Gulf of Mexico ranges from 0.7-1.0 cgs units while the average of all continents and oceans is 1.45 and 1.46 cgs units respectively (Von Herzen and Lee, 1969, pp. 90-92). This may be in part due to the large sediment thicknesses or to the absence of seismic activity.

Considering the length of time (over 10^8 years) since regional tectonic movements have taken place in the northwest Gulf of Mexico the presence of a normal mantle density of 3.4 gm/cc should be expected. There does not appear to be complete agreement on this value, as shown by Table 5, which tabulates crustal sections or isostatic computations and assumed densities that have been used by other investigators in the western Gulf of Mexico. The mantle densities range from 3.3 to 3.4 gm/cc.

The density assigned to the mantle in the computed crustal section is 3.4 gm/cc. This density satisfies the high observed compressional velocities, low heat flow, and an inferred upper mantle of peridotite, eclogite, or pyrolite composition (Wyllie, 1971, p. 29).

(2) Oceanic Crust - Compressional wave velocities of 6.45-6.94 km/sec were recorded for the "oceanic crust" along four refraction lines (Cram, Dorman et al., Hales et al., and Ewing et al.). They are interpreted as representing a basaltic composition. Table 5 shows that the range of densities that have been assigned to the oceanic crust is 2.8 to 3.0 gm/cc. Use of the Nafe-Drake curves (Menard, 1967, p. 3065, Fig. 3) for a velocity of 6.61 km/sec (mean of seven refraction values, including four from Hales et al.) results in a density of 2.91 gm/cc. The mean of oceanic crust densities for Table 5 is 2.93 gm/cc.

The density for the oceanic crust should then be at least 2.91 to 2.93 gm/cc from the previous analysis. Mass balancing, used in later attempts to construct the standard section indicated that a higher density for this layer would be appropriate; this conclusion was also born out in attempts to compute the gravitational attraction of the southeastern end of the crustal section. A compromise density of 2.97 gm/cc was chosen as it gives good results in the mass balancing, the computation of the crustal

TABLE 5

LAYER DENSITIES USED FOR CRUSTAL SECTIONS AND ISOSTATIC COMPUTATIONS IN AND ADJACENT TO THE
WESTERN GULF OF MEXICO

Investigator (s)	Densities			Mantle	Location
	Sediments	Continental Crust	Oceanic Crust		
Dehlinger and Jones, 1965	2.00-2.50	2.70	3.00	3.40	Galveston, Texas to Yucatan
Shurbet, 1969	2.00-2.70	2.84	2.84	?	Galveston, Texas to Sigsbee Scarp
Preston, 1970	2.30-2.50	2.84	2.84	3.35	Rio Grande Embayment to Continental Shelf
Hales, Helsey, and Nation, 1970	2.16-2.67	2.84	2.84-3.10	3.30	Texas-Louisiana Coastal Plain to Continental Slope
Fish, 1971	2.10-2.67	2.80	2.90	3.30	San Marcos, Texas to Indianola, Texas
Keller and Cebull, 1973	2.51	2.75	3.00	3.30	Odessa, Texas to Port O'Conner, Texas
Worzel and Watkins, 1973	2.30	-	-	3.40	Isostatic Computations
Moore and Castillo, 1974	2.00-2.40	2.80	2.80-3.00	3.40	Veracruz to Compeche Bank
Burnaman, 1974	2.53	2.88	2.97	3.40	Texas Coastal Plain to Continental Slope

section, and is well within the range of densities chosen for this layer by previous investigators (Table 5).

(3) and (4) Continental Crust and Paleozoic Metasediments - Velocities indicative of continental crust (inferred granitic composition) were recorded on the Cram and Dorman et al. profiles. Cram found a thickness of 12.5 km of 5.38 km/sec material which he interpreted as being "Paleozoic and Precambrian metasediments and acidic igneous rocks" (Cram, 1961, p. 569). Dorman et al. estimated a thickness of 6.48 km of 5.22 km/sec material which they correlated with Cram's 5.38 km/sec layer (Dorman et al., 1972, p. 332, Fig. 5, p. 335, Fig. 7). Contrary to these interpretations Hales et al. (1970) in his refraction survey along the Texas-Louisiana border identified approximately 6.5 km of 5.76 km/sec material 30 km inland thinning to 5 km of 5.81 km/sec material 30 km offshore. This layer was also identified 300 km inland (at a speed of 5.75 km/sec), but the bottom interface was not recorded. This 5.75 - 5.76 km/sec velocity was interpreted as "may correspond to the Cretaceous-Tertiary interface" (p. 2042), implying that the 5.75 km/sec layer is the Cretaceous limestone and not the "crust". They further show on p. 2049, Fig. 8 this boundary along the offshore section as corresponding to the top of the Cretaceous inferred by Williamson (1959).

The probable existence of Paleozoic "metasediments" under the Texas coastal plain has previously been noted. Yet, Cram, Dorman et al., and Hales et al. failed to discriminate any boundary between these "metasediments" and the continental crust (thus assuming that the next lower layer with velocities over 6 km/sec is not continental crust). It should be mentioned, though that in the area along Hales' profile the "metasediments" may be missing entirely.

This paradox may be resolved if it is assumed that the intense heat and pressure to which the Paleozoic sediments have been subjected has increased the seismic velocity to one resembling the continental crust. Any compositional and/or textural changes which have taken place are most probably gradational, resulting in the absence of an easily distinguishable seismic or textural boundary. For simplicity however, these may be treated as two distinct layers with the continental crust terminating somewhere under the coastal plain and the metasediments extending on to the coast as envisioned by Flawn (1964, p. 275).

This same argument can be stated for the absence of a clearly defined seismic boundary between the Cretaceous limestone of Hales et al. and the continental crust as velocities of 5.75 km/sec are not uncommon for deeply buried, highly compacted limestones.

Using a mean velocity for the continental crust of 5.30 km/sec (obtained from the Cram and Dorman et al. profiles only) with the Nafe-Drake curve results in an apparent density of 2.63 gm/cc. This density is 0.16 gm/cc lower than the mean of densities used for this layer by other investigators (Table 5). For this reason, higher densities for these two layers should be considered.

A representative average density for the continental crust is probably 2.84 gm/cc as described and used by Worzel and Shurbet (1955a and b). Table 5 gives a range of 2.70 to 2.84 for continental crust densities. Using 2.84 gm/cc as an average continental crust density, it could be possible to assign the metasediments a density of 2.80 gm/cc and the continental crust a density of 2.88 gm/cc.

The 2.80 gm/cc density of the metasediments is 0.03 gm/cc less than that used by Fish (1971, p. 15) for the same layer, while the 2.88 gm/cc continental crust is generally higher than any other investigator has used

for crustal sections in the area. However, if equal thicknesses of continental crust and metasediments are considered, their average density would be 2.84 gm/cc and a general increase of density with depth is assumed. The exact density of the continental crust is not crucial to the calculation of the crustal section since this portion of the crust appears to truncate far inland and its resulting gravitational effect on the model is minimal.

(5) Mesozoic and Cenozoic Sediments - Probable sediment velocities vary from 2.3 to 3.9 km/sec along the Cram (1961) profile, 2.20 to 4.49 km/sec along the Dorman et al. (1972) profile, and 1.78 to 2.84 km/sec along the Hales et al. (1970) profile. Accepted sediment densities (Table 5) in the Gulf Coast geosyncline vary from 2.0 gm/cc for near surface sediments. The true representation of sediment density in this region is probably best shown by Musgrave and Hicks (1966, p. 717, Fig. 13). They describe the sediment density under the Louisiana continental shelf as increasing linearly from 1.95 gm/cc at a depth of 1,000 feet to 2.60 gm/cc at a depth of 20,000 feet. This is a simplification but it does show the fundamental relationship of sediment density to depth of burial in the Gulf Coast as described by Nettleton (1934, p. 1179, Fig. 1).

The absence of well data along the major portion of the crustal section precludes assuming individual layers for the major lithologic groups, Late Triassic - Jurassic evaporites (predominantly salt), Cretaceous limestones, and Tertiary sands and shales. Consequently, the determination of a density for the entire post-Paleozoic sequence should take into account the unknown thickness of evaporites (2.15-2.20 gm/cc), the upper Cretaceous limestones (2.40-2.70 gm/cc), and the Tertiary sand-shale sequences (1.95-2.60 gm/cc). The sands and shales comprise the majority of the sedimentary section, with the limestones probably being more

prevalent to the northwest than to the southeast and the evaporites being more abundant to the southeast than to the northwest (Murray, 1961). Any average density chosen should reflect these abundances and should also include the increase of density with increasing depth of burial displayed by the dominant Tertiary lithology.

Dehlinger and Jones (1965, p. 105) in discussing the density assumptions used in constructing their crustal section state:

"A deviation from the Nafe-Drake curves was assumed for the major thickness of the Gulf Coast geosyncline, where average densities of 2.5 gm/cc were used instead of the 2.4 gm/cc obtained from the curves. This change was based on known densities from well data in South Texas".

The average density over the total thickness of each sediment layer measured at the deepest portion of the geosyncline in the Dehlinger and Jones section is 2.41 gm/cc, as is the case for the section of Shurbet (1969, p. 244). The average sediment density for the crustal section of Moore and Castillo (1974, p. 614) is 2.30 gm/cc while that for the sections by Fish (1971, p. 17), Preston (1970, p. 24), and Keller and Cebull (1973, p. 1664) are 2.49, 2.50, and 2.51 gm/cc respectively. The average sediment density of all seven crustal sections is 2.41 gm/cc. This density appears to be low in light of the thick sequence of sediments (presumably greater than 15 km) and the fact that both the Musgrave and Hicks curve and the Nettleton curve show a density of 2.45 gm/cc at 16,000 feet (4.8 km). This depth is less than one third of the total estimated thickness of sediments at the deepest part of the geosyncline.

Left out of these calculations are the higher density carbonates and the lower density evaporites possibly present at the bottom of the sediment

section. If densities of 2.54 gm/cc and 2.20 gm/cc are assumed for the carbonates and evaporites respectively, their average is 2.37 gm/cc, also assuming equal thicknesses. Furthermore, if a total thickness of sediments of 16 km is assumed, including 2 km of 2.37 gm/cc material and 14 km of 2.50 gm/cc material, the average density of the entire column is 2.48 gm/cc.

As was the case for the density of the oceanic crust, after several attempts at mass balancing for the standard section and finally many crustal models, a density of 2.53 gm/cc was considered to be most representative of the total thickness of sediments.

(6) Water - The water column is assigned a density of 1.03 gm/cc, its actual density at the temperature and salinity it possesses.

Computing the Standard Section

Once the layers have been specified and their densities have been assigned, it remains necessary only to select the total thickness and average density of the standard section.

Talwani et al. (1959b) used a column of strata 32 km deep with an average density of 2.87 gm/cc in their investigations of the Puerto Rican trench through the use of gravity anomalies. This same section was again used by Talwani et al. (1965) to compute gravity anomalies over the Mid-Atlantic ridge, south of Iceland. Worzel and Shurbet (1955a) describe standard sections for both continental and oceanic areas with each section having an average density of 2.84 gm/cc and depth of 33 km. These sections were subsequently used to compute gravity anomalies along the eastern continental shelf of the United States (Worzel and Shurbet, 1955b). It remains to be seen which of these sections, if any, most resembles the mass distribution of the Texas coastal plain and continental shelf, which constitute a transition zone between the continental and oceanic areas (Menard, 1967, p. 3061).

A description of possible standard sections for the Texas portion of the Gulf of Mexico transitional area is shown in Table 6. This table lists the seismically determined layering for both the Cram and Dorman et al., refraction stations, along with the assumed densities for the layers and their mass/unit area, adjusted for gravity anomalies, computed by the method of Hayes (1966, p. 336). For each station the total areal mass is computed down to 32 and 33 km (by the sum of products of the layer thickness and assumed density) and the average densities are then determined.

The average density for the Cram column is 2.85 gm/cc for both the 32 and 33 km depths of compensation. Average densities for the Dorman et al., column are 2.85 and 2.86 gm/cc for 32 and 33 km depths respectively. These two Texas crustal columns are 0.01-0.02 gm/cc heavier than the Worzel and Shurbet columns and 0.01-0.02 gm/cc lighter than that of Talwani et al. It should be noted that the standard sections of Worzel and Shurbet use a mantle density of 3.27 gm/cc, while that of Talwani et al. use a mantle density of 3.40 gm/cc.

In computing regional gravity anomalies, the effect of a thicker crustal column is to increase the attraction while a thinner column decreases it. Thus, whether a 32 or 33 km column is used should be of critical importance. However, since the attraction of the theoretical column is subtracted from the total computed anomalies, the effect of a thicker column can be minimized by lowering any or all of the interfaces to decrease total attraction (assuming a continual increase of density with depth) or raising it if the theoretical column is shortened.

For the crustal model computed in this investigation, a standard section of 32 km with an average density of 2.87 gm/cc was chosen. This section, while admittedly having a mass excess per unit area of 0.64×10^5 gm/cm² (0.02 gm/cc X 32 km) greater than the column computed for the two

available refraction profiles (Table 6), is comparable to crustal sections computed at other localities, i.e. Talwani et al. (1959b), Talwani et al. (1965), Dillon and Vedder (1973), and Henderson (1963).

The density discrepancy between the computed sections and the one assumed for the model may be described as follows: assuming that the depth of the chosen standard section is correct, then subtracting a higher average density (2.87 instead of 2.85 gm/cc) from the assumed densities for the layers has the effect of decreasing the positive attraction of those densities greater than 2.85 gm/cc and increasing the negative attraction of those densities less than 2.85 gm/cc. These changes will result in slightly higher interfaces than computed otherwise. Any changes in interface depth, however, are immaterial, due to the ambiguities inherent in the original assumptions as to number of layers, densities, and depth of compensation.

Computing the Model

After the number of layers, their densities, and the standard section were determined, the next step was to prepare the crustal model for input to the computer program (GRAVITYMODEL, Appendix 2). The seismic refraction depths from Dorman et al. (1972) 47 km inland and Cram (1961) 124 km inland were posted on centimeter graph paper (1 cm = 4.6 km, horizontal; 1 cm = 1 km, vertical). Gravity computation station (field points of GRAVITYMODEL) spacing was 4.6 km with 61 stations used for a total model length of 276 km. The first station was 92 km inland and was used as the zero ordinate and abscissa for the coordinates of the layers. The observed gravity at each computation station was obtained from the regional gravity map (Fig. 3 or Plate II). Water depths were determined from the United States Coast and Geodetic Survey Chart 1117 and from Gealy (1955). All applicable layers were extended a maximum of 1800 km on either side of the zero ordinate to

TABLE 6

STANDARD SECTIONS FOR THE SOUTH TEXAS COASTAL PLAIN

Seismic Station	Observed Gravity Anomaly (mgals)	a. Equivalent mass/unit area ($\times 10^5$ gm/cm ²)	Layer	Velocity (km/sec)	Thickness (km)	Density (gm/cc)	b. Mass/unit area ($\times 10^5$ gm/cm ²)	Total Adjusted Mass (a + b)	Average Density (gm/cc)
Cram, 1961	-25	+0.60*	Sed	2.20	2.30	2.53	5.06		
			Sed	3.94	5.30	2.53	13.41		
			Cont. Crust and Metased.	5.38	12.50	2.86**	35.75		
			Oceanic crust (to 32 km)	6.92	13.20	2.97	36.23	91.05	2.85
			(to 33 km)				39.20	94.02	2.85
			Mantle (to 32 km)	8.18	-0-	3.40	-0-		
Dorman et al. (1972)	-27	+0.64*	Sed	2.20	3.30	2.53	3.36		
			Sed	3.40	4.26	2.53	10.78		
			Sed	4.49	2.28	2.53	5.67		
			Metased.	5.22	6.48	2.80	18.14		
			Oceanic crust	6.45	13.62	2.97	40.45		
			Mantle (to 32 km)	8.41	2.06	3.40	7.00	91.13	2.85
			(to 33 km)		3.06	3.40	10.40	94.53	2.86

* 42 mgals $\cong 10^5$ gm/cm²

** includes 9 km continental crust and 3 km metasediments

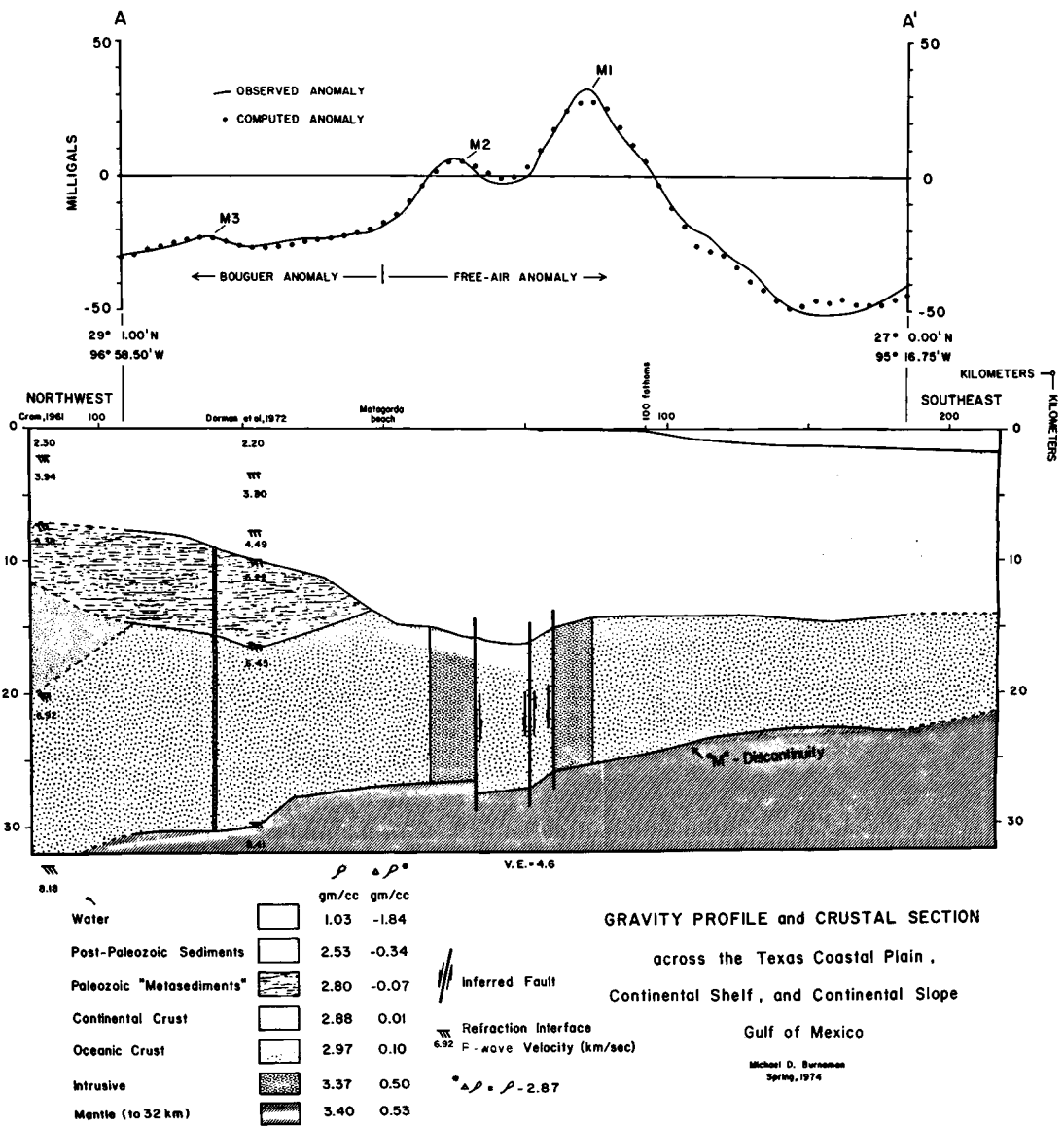
obtain realistic gradients for the ends of the model. Density contrasts ($\rho - 2.87$) used were: water, -1.84; sediments, -0.34; metasediments, -0.10; continental crust, +0.01; oceanic crust, +0.10; and mantle, +0.53. Total attraction to 32 km was then computed. The coordinates of all layers are given in revised MODEL of Appendix 2.

Figure 10 shows the final model which represents the results of approximately 350 program executions using variations of the layering geometry. It can be seen that the depths at the seismic control were changed, in some cases a few tenths of a km to obtain a better fit to the observed gravity. Of greater importance, however, was the necessity of including three vertical intrusions ($\Delta\rho = +0.50$) at positions to correspond to anomalies M1, M2, and M3. The reasons for including these high density intrusions are discussed in the next section of this thesis.

The actual input parameters for the final gravity model are listed in Datafile REVISEDMODEL. in Appendix 2.

FIGURE 10

The computed crustal section. The location is shown in Figure 8. Anomalies M1, M2 and M3 are from Figure 7. The intrusive corresponding to anomaly M3 has been exaggerated in width for presentation purposes. It's actual width is 0.75 km.



DISCUSSION OF THE CRUSTAL SECTION

Introduction

The three positive regional anomalies along the computed crustal section (Fig. 10) may be caused by continental edge effects, "basement" topography, shallow high-density intrusions, "basement" intrusions, or any combination of these features. Each of the possibilities is discussed in the following text along with a discussion of general features of the section.

The Relation of the M-Discontinuity and Water Depth to a Continental "Edge" Effect

The attraction of the observed gravity field along the crustal section may be thought of as being caused by five major components: variations in depth to the M; lateral variations in the crustal thickness or density; relief on the crust-sediment interface; variation in the density of near surface material; and variations in water depth of the offshore area.

Along continental margins the regional gravity field is influenced primarily by rapid changes in the depth to M coupled with rapid changes in the bathymetry. Considering only Bouguer anomalies, the change in depth to M across the continental margin from the interior continental area results in an increasing anomaly whose value is generally negative in areas of high elevation, zero in areas at or close to sea level, and positive over marine areas where the water is deep (Nettleton, 1971, p. 66, Fig. 50). Using the free-air anomaly only for the offshore portion will result in a positive anomaly over shallow water depths and an absolute or relative negative anomaly over the deeper water which may then become positive further offshore where the M is shallowest.

This positive free-air anomaly (on the continental shelf), coupled with a negative anomaly further offshore is a result of the continental "edge" effect (Worzel and Shurbet, 1955b, p. 466). It is similar to the effects already noted in the discussion of the Rio Grande Delta gravity maximum.

Using models of simplified continental margins Worzel (1965, p. 348, Fig. 135) showed that "edge" effect anomalies with an absolute difference of 100 mgals could result from a change in mantle depth of 18 km over a distance of 150 km coupled with an increase of water depth from zero to five km in the same section. The positive anomaly is wholly a function of the gradient of the crust-mantle interface while the negative anomaly is wholly explainable on the basis of the crust-water interface. The "edge" effect then connotes no deep structural significance other than these depth changes.

Is the Texas Continental Shelf Gravity Maximum
Caused by an Edge Effect?

It became apparent after studying the first few preliminary computer models of the crustal section that the crust-mantle interface could not have the steep gradients previously discussed if the observed gravity and the depths and assumed densities of the seismically determined horizons were to be honored. To test the hypothesis that the Texas continental shelf gravity maximum (TCSGM) is not caused by an "edge" effect and to isolate local anomalies for further study, simple Bouguer anomalies (no terrain correction), described in a later section, were computed for tracks H16 and D3 (Figs. 11 and 12). The procedure used to compute these anomalies is described in the later section on minimum anomalies. Track H16 is perpendicular to the coastline and crosses track D3 (also perpendicular)

FIGURE 11

Observed free-air gravity anomaly, simple Bouguer anomalies for various correction densities, and bathymetry along track H16. Bathymetry is from Gealy (1955). Location of the local minimum anomaly of Figure 17 is at "MODEL". Carets represent locations of inferred near surface salt masses as evidenced by both bathymetry and local gravity minima.

NOTE: Coordinate of eastern terminus should be $27^{\circ} 0.10'$ N.

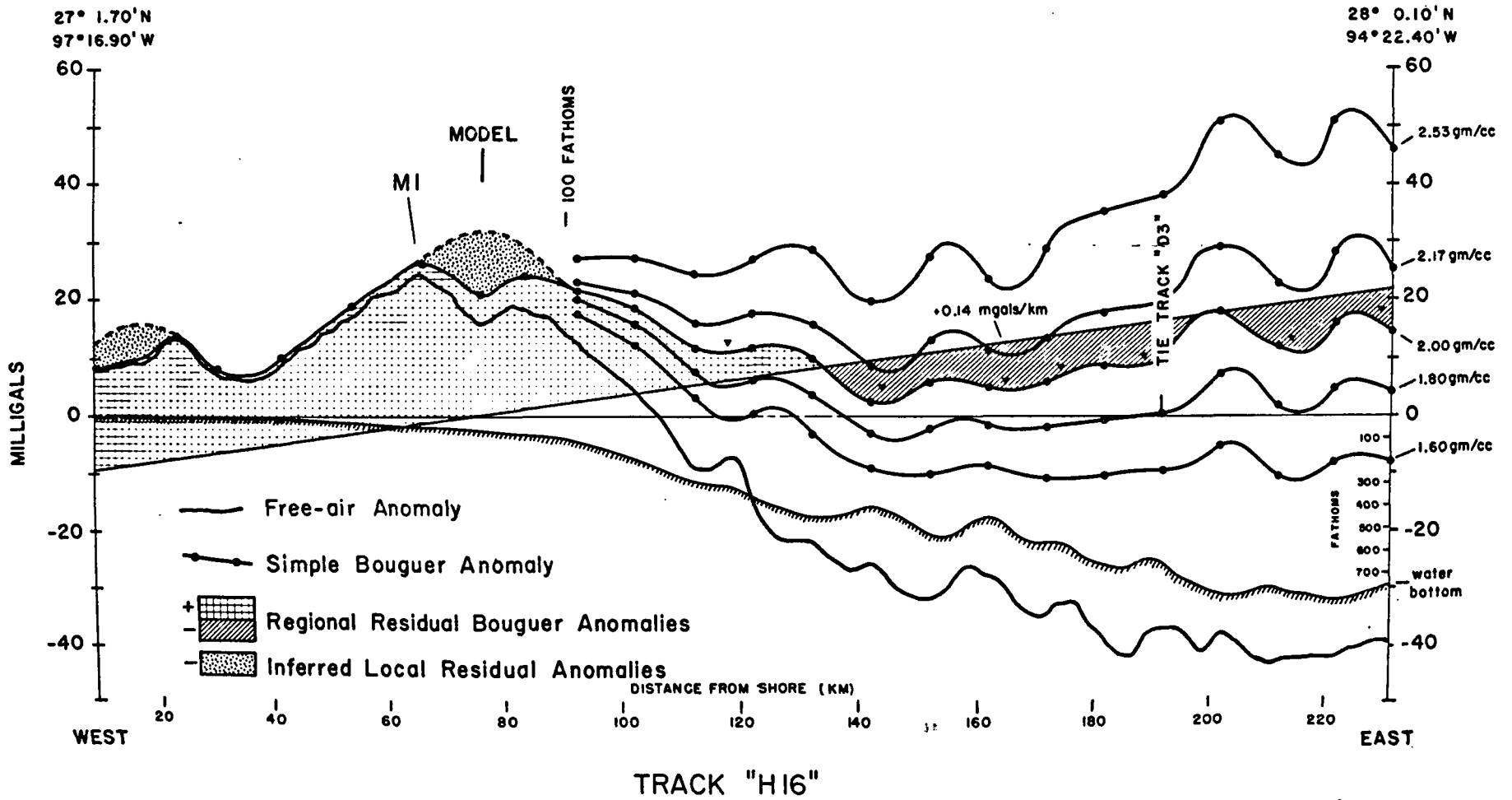
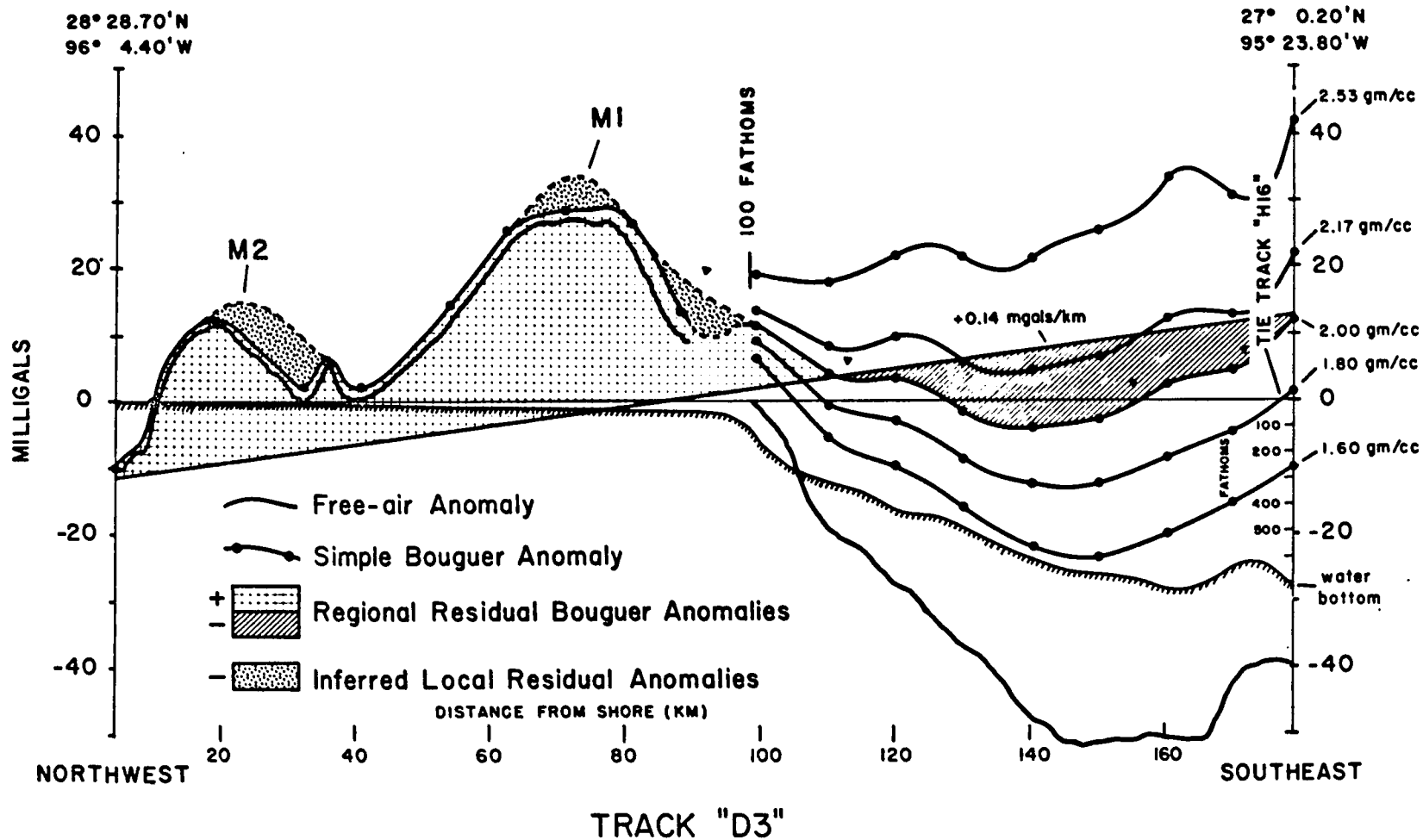


FIGURE 12

Observed free-air gravity anomaly, simple Bouguer anomaly for various correction densities, and bathymetry along track D3. Bathymetry is from Gealy (1955). Carets represent locations of inferred near surface salt masses as evidenced by both bathymetry and local gravity minima.



at a distance of 175 and 190 km respectively from the coast. Comparison of the free-air anomalies of D3 and H16 indicates that the TCSGM (M1 on Figs. 11 and 12) is centered on each profile at 75 km offshore. There is a minimum anomaly on H16 (at "model") which furrows the shelf maximum. This minimum anomaly may be traced south of Port Isabel, Texas.

Drawing attention to track D3 we see that the two components (M1 and M2 of Fig. 12) of the TCSGM represent the only positive anomalies. At the northwestern termination, the Bouguer anomaly (using 2.0 gm/cc) is -10 mgals, while at the southeastern end it is +11 mgals. The northwest end of the track is located 41 km east of the crustal section, where the gradient of the Bouguer anomaly along the land portion of the crustal section is 0.14 mgal/km.

Using the 0.14 mgal/km gradient, it can be seen on Figure 12 that the two components of the TCSGM (after correcting for negative anomalies inferred from Figure 5) represent substantial variations from the regional Bouguer gradient. Anomaly M2 is 24 mgals high while anomaly M1 is 35 mgals high. Essentially the same results can be seen on track H16 (Fig. 11). Here if the effects of the Rio Grande gravity maximum are subtracted from the Bouguer value at the coastline and the anomaly there is taken as 14 mgals, then using the 0.14 mgal/km gradient results in a positive anomaly of 32 mgals at M1, above the linear Bouguer regional trend, if allowance is made for the gravity minimum at 75 km. While these computed Bouguer anomalies are similar at the tie point, the resulting regional anomalies are 12 and 17 mgals for D3 and H17 respectively.

The computed M depth rises 3.5 km from 50 km inshore of the coastline and continues to rise (excluding the inferred down faulted section under the continental shelf, shown in Fig. 10) in an undulatory fashion to 22 km

at the end of the computed section 184 km into the Gulf of Mexico. It probably continues its undulatory rise to station V-24 of Ewing et al. (1955) where it is measured at 19.3 km. If the M does in fact rise to the 19.3 km depth for V-24 at a closer distance to shore than shown in Figure 10, the effect of the resulting excess positive gravity anomalies along the crustal section could be minimized by increasing the sediment thickness to greater than 14 km at a distance of 100 km offshore. This would be only a minor adjustment and would not violate the geometry of the measured interfaces at V-24.

The major flexure on the M (excluding the down faulted block) occurs just east of the Dorman et al. (1972) profile at a depth of 27.8 km. The resulting M gradient (0,03 km/km, within 50 km either side of the coastline) apparently conflicts with gradients measured from the computed sections of Dehlinger and Jones (1965) and Shurbet (1968). Gradients of the M on these sections are 0.085 km/km and 0.155 km/km respectively, within 50 km either side of the shoreline.

Since computation of the Bouguer anomaly should, in theory, "continentalize" the observed free-air gravity anomalies most of the "edge" effect should be removed and the smoothed regional gravity field should increase toward the basin. As was shown, both in Figures 11 and 12 and, although not shown for the gravity profile associated with the crustal section, the components of the TCSGM are still present after computing the Bouguer anomaly. Considering the lack of correlation between the TCSGM and the bathymetry above 28°N lat., the complexity of the TCSGM, and the apparent low gradient of the M, it appears that a continental edge effect cannot explain the TCSGM completely.

Are the Components of the Texas Continental Shelf Gravity Maximum the Result of Basement Topography?

The existence of a "basement" ridge or high under the Texas Continental shelf or slope has been postulated extensively in the literature. Logue (1954), by extrapolating land gravity isogals, projected the Appalachian gravity trend through southern Alabama and Florida into the Gulf of Mexico just south of the Mississippi delta and over to the Rio Grande delta. This gravity maximum was inferred to be caused by a buried extension of the Appalachian mountain chain called "Llanoria".

J. Ewing et al. (1960, p. 4089) show a ridge feature on the "basement" (5.4 km/sec) on a cross-section across the Gulf of Mexico based on available seismic refraction measurements. This "ridge" is located under stations V-28 and V-29 (V-29 is northwest of V-28 shown in Fig. 1., this thesis).

In discussing this feature they state,

"after examination of all the data, it now appears more likely that the 5 km/sec material is part of a large ridge which separates the Sigsbee deep from the Gulf Coast geosyncline".

Hardin (1962, p. 13, Fig. 17), in a schematic cross-section through central Louisiana to link up with the Ewing et al. (1955) and J. Ewing et al. (1960) seismic refraction data shows a pre-Jurassic basement ridge with local relief as great as 5.8 km composed of "folded Paleozoic Metasediments".

He states that this feature may, in part, be caused by downfaulting to the northwest. This ridge is located under V-28. Cram (1962, p. 1726), also using J. Ewing et al. (1960) data, infers a ridge under station V-28 in his schematic cross-section through the Texas portion of the Gulf Coast geosyncline. He also states that this feature may be caused by sediment loading (p. 1726).

Antoine and Ewing (1963, p. 1979, Fig. 3), in another schematic

section across the Gulf Coast geosyncline off Galveston, show dip reversals under refraction station V-28 and interpret the deepest mappable layer of 5.3 km/sec to be upper Cretaceous. However, on page 1983, while discussing this cross section they state:

"The results can be interpreted to indicate the existence of a prominent ridge or uplift in the deeper layers which forms the southern margin of the Gulf Coast geosyncline and separates it from the Sigsbee Deep... However, we emphasize once more that we have only a limited number of profiles for the area and the evidence from them is far from overwhelming". Dorman et al. (1972, p. 335, Fig. 7), in their approximate crustal section along the same line as the crustal section in this thesis, show a high point on the oceanic crust under the upper continental slope from projections of Hales et al. (1970).

After reviewing these data and their authors' interpretations, it is this authors' contention that the 5.3 km/sec velocity measured 240 km offshore from Galveston at V-28 at 5.0 km depth is actually salt, which is now accepted as being present under this area but was not at the time these previous references were published. Consider, for example, Uchipi and Emery (1968, p. 1191, Fig. 19), as they show that the entire continental slope, from Texas to Mississippi, is strewn with structures, both topographic and seismic, which may be attributed to salt diapirism.

Consequently there does not appear to be any confirmed evidence of substantial relief on the surface of the oceanic crust below the continental shelf and slope, other than that suggested by the crustal section of Figure 10. Here, the deepest portion of the Gulf Coast geosyncline is inferred to be located 51 km offshore. The depth to the oceanic crust at this point is 16.3 km (53.5 k ft). This surface rises to 14.3 km

25 km further offshore and going toward shore it has a depth of 15 km at 19 km from the coastline. This depression in the crust terminates the dip of the basement surface which began in the vicinity of the Llano Uplift.

Are the Components of the Texas Continental Shelf Gravity Maximum Caused by Shallow High Density Material?

Simple Bouguer anomalies were computed from the free-air anomalies along the crustal section. Using the 0.14 mgal/km gradient observed on the land portion of the section allowed isolation of residual anomalies for both M1 and M2 of Figure 10. Use of the "half-width" method of Nettleton (1940) on these two residual anomalies results in depths of 13.8 and 12.9 km respectively for the depth to the center of an infinite horizontal cylinder. Assigning a $\Delta \rho$ of 0.50 gm/cc gives a cylinder with a diameter of 10.5 km centered at a depth of 13.8 km for M1 and a cylinder with a diameter of 7.4 km centered at a depth of 12.9 km for M2.

The dimensions resulting from Nettletons' formula should be considered only as an approximation since, among other things, it assumes that the residual anomaly being used is caused only by the assumed model (i.e. a true residual). Since the depth to M, which greatly affects the observed gravity anomalies, is only known from the present gravity calculations; it would be fortuitous to expect that the simple 0.14 mgal/km gradient truly represents the actual regional gravity field. However, the depths and widths which were obtained do appear to rule out that anomalies M1 and M2 are caused by shallow high-density igneous or sedimentary rocks, rather, the calculated depths and widths infer sources in the basement, in this case the oceanic crust, with widths of the order of those shown for M1 and M2 in Figure 10. It should be noted that lowering the density contrast in the calculations has the effect of increasing the diameter of

the cylinder whose center has been located by the half-width of the residual anomaly.

The previous discussion should not infer that intrusive igneous rocks (within the sedimentary section) are not present in the South Texas area. Murray (1961, p. 126) states that the San Marcos arch: "differs somewhat from that of adjacent embayments and salt dome areas in the presence of different predominant structural types, in the absence of known salt or at least an insufficiency of salt to produce diapiric intrusions, and in the presence of relatively common serpentine masses and associated igneous phenomena".

Lyons (1957, p. 8, Fig. 5) infers igneous intrusives from isolated gravity and magnetic anomalies on the San Marcos arch and also a predominantly east-west line of Cretaceous volcanics at the latitude of Uvalde, Texas. Upper Cretaceous igneous rocks are present at the base of many boreholes on the Monroe uplift in northeastern Louisiana (Murray, 1961, p. 116, Fig. 31.5b). None of these areas of intrusive or extrusive igneous rocks, whether Upper Cretaceous or Tertiary in origin, exhibits the breadth, extent, or continuity of the Texas continental shelf gravity maximum.

Discussion of the High Density Intrusions Associated with the Texas Continental Shelf Gravity Maximum

Once all of the previously discussed possibilities had been considered and ruled out as the primary cause of the Texas continental shelf gravity maximum (TCSGM), crustal models were constructed using basement intrusions coupled with a minimum amount of basement topography to account for the +33 mgal free-air anomaly at M1 and the +7 mgal anomaly at M2 (Fig. 10).

To simplify the model and the later interpretation it was felt that the intrusions for both M1 and M2 should have identical or, if that is not possible, similar densities. The magnitude of the density contrast was

originally considered to be quite large, since if the contribution of the continental edge effect is considered to be minimum and the very large thickness (apparently greater than 15 km) of sediments in the vicinity of the crustal section is taken into account, then the fact that positive free-air anomalies are observed over the continental shelf is surprising.

As can be seen from Figure 10, the density contrasts which best fit the observed gravity were large, $\Delta\rho = 0.50$, with an apparent density of 3.37 gm/cc; a density approaching that of the mantle. The width of intrusion M1 is 11.6 km while that of M2 is 13.8 km. The apparent contradiction in the relative sizes of the two intrusions may be explained by noting that the mantle is substantially higher around M1 than around M2 which may lead to a more complex regional gravity anomaly, as discussed previously. This complexity of the gravity field in the area of M1 resulted in displacing the center of intrusion M1 2.5 km farther inshore than the location of the apparent maximum appeared to warrant. This displacement is probably due to unresolvable low relief on the basement surface, tilting of the intrusion, relief of M around the intrusion, or any combination of these factors. Whatever the case, any model of anomaly M1 must include the high density material at depth equal to or below the surface of the crust.

The three faults inferred between intrusions at M1 and M2 are merely to show a possible mechanism to account for the relief of 1.5 km within a horizontal distance of only 29 km between the two intrusions. Consequently the faulting should be considered only speculative as its inclusion is neither confirmed or denied by the available data.

The high apparent density of the intrusions should be considered in the context in which it was obtained, as a parameter chosen to harmonize

best with the other unknown but assumed parameters of the complete crustal model in Figure 10. For example, if the gravitational attraction of the intrusives could be truly separated from the "noise" contributed by the other rock layers (i.e. obtained a true residual anomaly for the intrusives) then one would probably find that the density contrast necessary for the geometry of the intrusions now inferred, would probably be less than +0.40 gm/cc, possibly even +0.30 gm/cc. This observation is partially confirmed since the intrusives shown in Figure 10 both have a maximum computed anomaly of 48 mgal, the only difference being that intrusion M2 has a broader anomaly due to its greater width. The residual anomalies which were obtained during calculation of the half-width distances were 23 mgal for M2 and 44 mgal for M1. In both cases the anomaly computed in the crustal section for the intrusives was greater than the residual anomaly obtained by assuming a simple linear regional gravity field.

Other Features of the Crustal Section

Besides the presence of the intrusions under the continental shelf, other important, and possibly significant structural features are present.

Although the gravitational effect directly above it was not computed, the observed gradients imply that the continental crust terminates approximately 90 km inshore. The Paleozoic metasediments, directly above both the continental and oceanic crusts appear to pinch out at the present coastline.

The interface described by the connection of the continental and oceanic crusts and the Paleozoic metasediments contains two significant structural "highs"; one approximately 90 km inshore and the other at the coastline. The actual existence of these highs may be suspect since the lowest position of the metasediment-oceanic crust interface is located

where Dorman et al. (1972) have seismic control. It would be a rare coincidence that the location of the seismic control just happened to be at the point where the surface of the oceanic crust was lowest. Any alteration of the surfaces in this area would significantly alter the computed gradients. Perhaps the structure is more complex than that assumed. This may be the case, as an extension of the Freeport gravity maximum is inferred to be present west of the location of the Dorman et al. (1972) profile. The width of this intrusion (M3 on Fig. 10) is exaggerated on the crustal section as it is actually 0.75 km wide. Extension of the intrusion through both the oceanic crust and the Paleozoic meta-sediments is speculative, and it was done mainly to provide a maximum age of the intrusions. As can be seen, it has the density of intrusions at M1 and M2.

Slight depressions are shown to be present in the oceanic crust and the M at distances of 160 and 184 km respectively, offshore. These were necessary to account for the negative free-air anomaly over this region. Such a change amounts to no more than ten mgals at most. This area represents an enigma. Figures 11 and 12 show that the area is characterized by a negative regional Bouguer anomaly of -8 to 110 mgals. This value is unusual as oceanic areas are usually characterized by positive Bouguer anomalies. Perhaps a better explanation than a change in shape of the crustal surface or of M is that the negative Bouguer anomaly is due to the massive thickness of salt which has previously been mentioned as being present under the Texas continental slope, extending to the Sigsbee Escarpment. It should not be incorrect to assume that this salt layer could produce a regional Bouguer gravity low.

ANALYSIS OF THE MAGNETIC ANOMALY SOUTHEAST OF GALVESTON, TEXAS

A description of the total intensity aeromagnetic anomaly profile shown in Figure 13 has been given in the section on Previous Investigations.

The magnetic low of Figure 13 at 53 km offshore coincides with the free-air maximum (M1) of track D1. This gravity maximum of 21 mgals is shown in Figures 3 and 4. It is part of the Texas continental shelf gravity maximum.

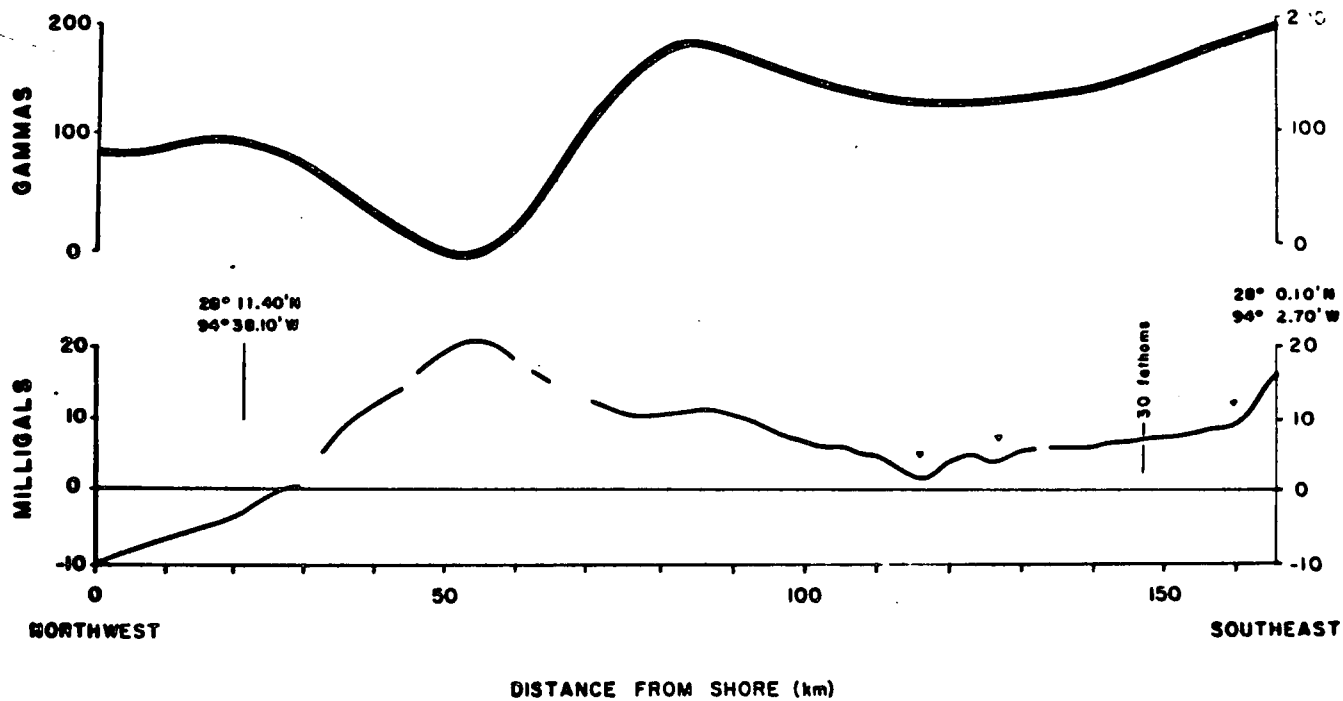
As has been previously mentioned, a magnetic anomaly of similar character as that found on track D1 can be inferred to be associated with the gravity maximum M1 of Figure 10 from the magnetic anomaly map of Heirtzler et al. (1966, p. 521, Fig. 2). In this case the magnetic maximum is displaced 16 km farther offshore than the gravity maximum. Similar measurements on the magnetic and gravity anomalies in Figure 13 show that the magnetic maximum is 32 km farther offshore than the gravity maximum. This apparent difference in the width of the magnetic anomaly between the location southeast of Galveston and the location of the crustal section may not be real if the poor resolution of the Heirtzler et al. (1966) data is considered.

Assuming that the magnetic and gravity anomalies are caused by the same feature, an igneous intrusive body, a regional gradient of 0.30 gammas/km increasing toward the southeast was subtracted from the magnetic anomaly profile in Figure 13 to a separate anomaly which could be interpreted using a dike model. This residual anomaly is shown in Figure 14(A).

Inspection of Figure 14(A) reveals that the minimum is to the northwest of the maximum and the max-min positions are separated by 32 km. If it is assumed that the dike is two-dimensional, that it strikes $N45^{\circ}E$,

FIGURE 13

Track D1 showing the free-air gravity anomaly and total intensity aeromagnetic anomaly. Flight elevation is 500 feet. Aeromagnetic profile courtesy of Mr. Jack Weyand of Sidney Schafer and Associates, Houston, Texas. Gravity anomaly M1 (shown in Fig. 7) is located on the gravity maximum approximately 53 km offshore. Carets represent locations of probable salt domes.



TRACK "DI"

— Total Magnetic Intensity (regional removed)

SOURCE : Sidney Schofer and Associates , Houston , Texas

— Free-Air Gravity Anomaly

SOURCE : USNS "George B. Kellnley" , 1970

that it has vertical dip, that it has induced magnetization with a positive susceptibility contrast, and that it is at a magnetic latitude of 52 degrees with normal polarity, then the observed max-min positions are those that would be expected from the assumed model.

The possibility that reversely polarized remanent magnetization accounts for most of the observed residual anomaly should not be discounted. Magnetic profiles in the area just offshore of the gravity maximum of track D1 as shown by Heirtzler et al. (1966, p. 522, Fig. 3) indicate low amplitude anomalies (50-75 gammas peak to trough) with wave lengths varying from 35 to 45 km trending parallel to the Texas coast and into Louisiana. These have been inferred by Yungul (1971, p. 2640) to be possible examples of the polarity reversals that are associated with the present mid-ocean ridges (Talwani, et al., 1965). The profiles of Heirtzler et al. show a change in the character of the magnetic anomalies as the anomaly associated with the gravity maximum of track D1 is approached from the east indicating that the source of the magnetic anomaly associated with the gravity anomaly may be of a fundamentally different nature as compared to whatever causes the apparent polarity reversals to the east.

Depth estimates using the Peters "slope" method as outlined by Dobrin (1960, pp. 312-313) on the anomaly in Figure 13 yield values to the magnetic basement of 12.2 and 20.8 km for both sides of the anomaly with the mean being 16.5 km. This depth must be considered in light of a magnetic depth estimate in the same vicinity by Nettleton (1952, p. 1224, Fig. 1) of 10.6 km. Nettleton used data from an aeromagnetic survey by Balsey (1949). In discussing the magnetic depth estimates along the Texas coastal plain, Nettleton (p. 1223-1224) states:

"Probably the most reliable single value is the depth of 35,000 ft. (10.6 km)

just offshore at the southeast corner of Texas. This is based on the air-borne magnetic survey carried out recently by the United States Geological Survey (Balsey, 1949)".

Since the distance between Nettleton's depth estimate and the author's is less than 30 km, an apparent contradiction appears since it is doubtful that the basement surface could vary six km in depth over a horizontal distance of less than 30 km. The aeromagnetic survey for Sidney Schafer and Associates was conducted in 1963, 14 years after Balsey's work, and this author believes that the most credance should be given to the more recent data.

The depth of 16.5 km to the magnetic basement at a distance of approximately 50 km offshore agrees with the prior assumption that the total thickness of sediment offshore Galveston is greater than that in the vicinity of the San Marcos area (although not by much) as implied by Hardin (1962, p. 4). Hales et al. (1970, p. 2049, Fig. 8) show a depth to the oceanic crust of 17.5 km inland, rising to 15.5 km at a distance of 35 km offshore, a depth substantially greater than that estimated by Nettleton.

Considering the previous arguments, the computed depth to the magnetic basement, in this case the top of the oceanic crust, at the location of the gravity maximum of track D1 does not appear excessive.

To test the hypothesis that the magnetic anomaly could be caused by an intrusive body in the oceanic crust, models were constructed and their anomalies were computed using the equations for induced and remanent magnetization of Reford and Sumner (1964, p. 505). This method assumes a uniformly magnetized dike extending to an infinite depth, with horizontal top, parallel sides, and infinite extent in the strike direction. The dike is

assumed to strike $N45^{\circ}E$ and to have vertical dip. Further, the width is assumed to be 14 km (the approximate width of one of the intrusives in Fig. 10) and have a depth to the top between 15 and 16.5 km (within the range of depths as determined from the magnetic depth estimates and from the gravity model of Fig. 10) with the inclination of the earth's field 52° , a declination of $8^{\circ}W$, and a total ambient magnetic field of 0.5×10^5 gammas. If it is further assumed that no change has occurred in the inclination of the earth's field with time, the equations for remanent and induced magnetization become equal. As any speculation on remanent magnetization would probably lead to further error such an assumption seems prudent. Susceptibility contrasts of +0.002 and +0.003 cgs units are chosen although there is no quantitative evidence that these are correct. However these appear to conform to suitable susceptibilities for an ultramafic intrusion into a mafic rock.

Figure 14 shows the original magnetic anomaly (A), the free-air anomaly (F), the residual magnetic anomaly after subtracting a gradient of 0.30 gamma/km (B), the computed anomaly for $\Delta k = +0.002$ cgs units at 15 km depth (C), the computed anomaly for $\Delta k = +0.003$ cgs units at 16.5 km depth (D), and the computed anomaly for $\Delta k = +0.002$ cgs units at 16.5 km depth (E).

While the computed anomalies do not coincide exactly with the residual anomaly the similarity, considering the simplicity of the models, is striking. The best fit appears to be either C or E, implying a susceptibility contrast of +0.002 cgs units at a depth of 15 to 16.5 km. There are two discrepancies. First, the computed anomalies do not have the magnitude of the observed positive anomalies; secondly, the models appear to be skewed three km to the west. Both discrepancies could be due to

FIGURE 14

A portion of the aeromagnetic anomaly and free-air anomaly shown in Figure 13. Also shown are computed magnetic anomalies from the assumed models. M1 represents the correlation of the Texas continental shelf gravity maximum shown in Figure 4, 7 and 13.

remanent magnetization, relief on the surface of the body, or dip of the dike. Whatever the cause of the discrepancies, the apparent good correlation in magnitude and position between the observed and computed anomalies warrants the following conclusions:

- (1) The top of the anomalous magnetic body lies between 15 to 16.5 km below sea level.
- (2) The anomalous magnetic body can be modeled as a two-dimensional dike.
- (3) The susceptibility contrast of +0.002 cgs units is well within the possible contrasts for mafic-ultramafic rocks.
- (4) The width of the modeled dike compares favorably with the width of the intrusive bodies shown in the crustal section (Fig. 10).

While the resolution of available data does not necessarily justify our concluding that the anomalous magnetic body with the characteristics just listed is the body responsible for the almost coincident gravity anomaly on the crustal section of Figure 10, it seems reasonable to infer a common origin for both bodies.

EVIDENCE FOR HORIZONTAL OFFSETS ALONG PART OF THE TEXAS CONTINENTAL SHELF
GRAVITY MAXIMUM

While plotting positions of tracks H15 and H16 on Figure 16, it became apparent that the positions of the Texas continental shelf gravity maximum (TCSGM) showed substantially more horizontal offset, as much as 15 km, than one would expect for a smoothly curved feature even when the 20 km track separation is taken into account.

Inspection of the regional gravity map (Fig. 3 or Plate II) showed that tracks H15 and H16 are located at the position where the TCSGM appears to make an abrupt turn toward the 100 fathom isobath. Another area of anomalously rapid curvature of the TCSGM is found at the closed 25 mgal contour offshore Port O'Conner. This location also corresponds to a rapid change in the direction of the inshore portion of the TCSGM, as outlined by the five mgal contour.

To test the hypotheses that the TCSGM could indeed show abrupt horizontal displacement, a procedure was designed to accentuate the true locations of the TCSGM along the individual ship tracks. This was most useful on tracks H16 - H19 as a large minimum anomaly (shown as the longest red line in Fig. 5) could be correlated across the tracks and its location corresponded rather closely to the inferred location of the TCSGM along these profiles. The procedure used is as follows:

- (1) Profiles of the free-air anomaly vs. distance, obtained by use of PROFILEPLOT (Appendix 2), with horizontal scale of 4 km/cm and vertical scale of 4 mgal/cm were studied separately and also as a group in order to determine where the TCSGM was located along each track, since in some cases minimum anomalies obscured its true position. Tracks H1 - H3, H5, and D1 were not used due to either

"noisy" data (H5) or the TCSGM not being well defined. Tracks H20 - H22 and D5 were also deleted since the Rio Grande Delta gravity maximum coupled with minimum anomalies (as shown in Fig. 5 and Fig. 7, profile E) rendered a definitive choice of location doubtful.

(2) The inferred regional field (the true TCSGM) was sketched on each profile.

(3) The position of the TCSGM was located on each profile and the coordinates of those positions were obtained from a listing of the latitude, longitude, and free-air anomaly for the individual gravity stations along each profile by comparing the value of the actual free-air anomaly on the plotted profile with the values in the data listing.

(4) The positions of the maxima, including the inshore bifurcation were located on an appropriate map with the inferred lineations shown and possible offsets shown as faults.

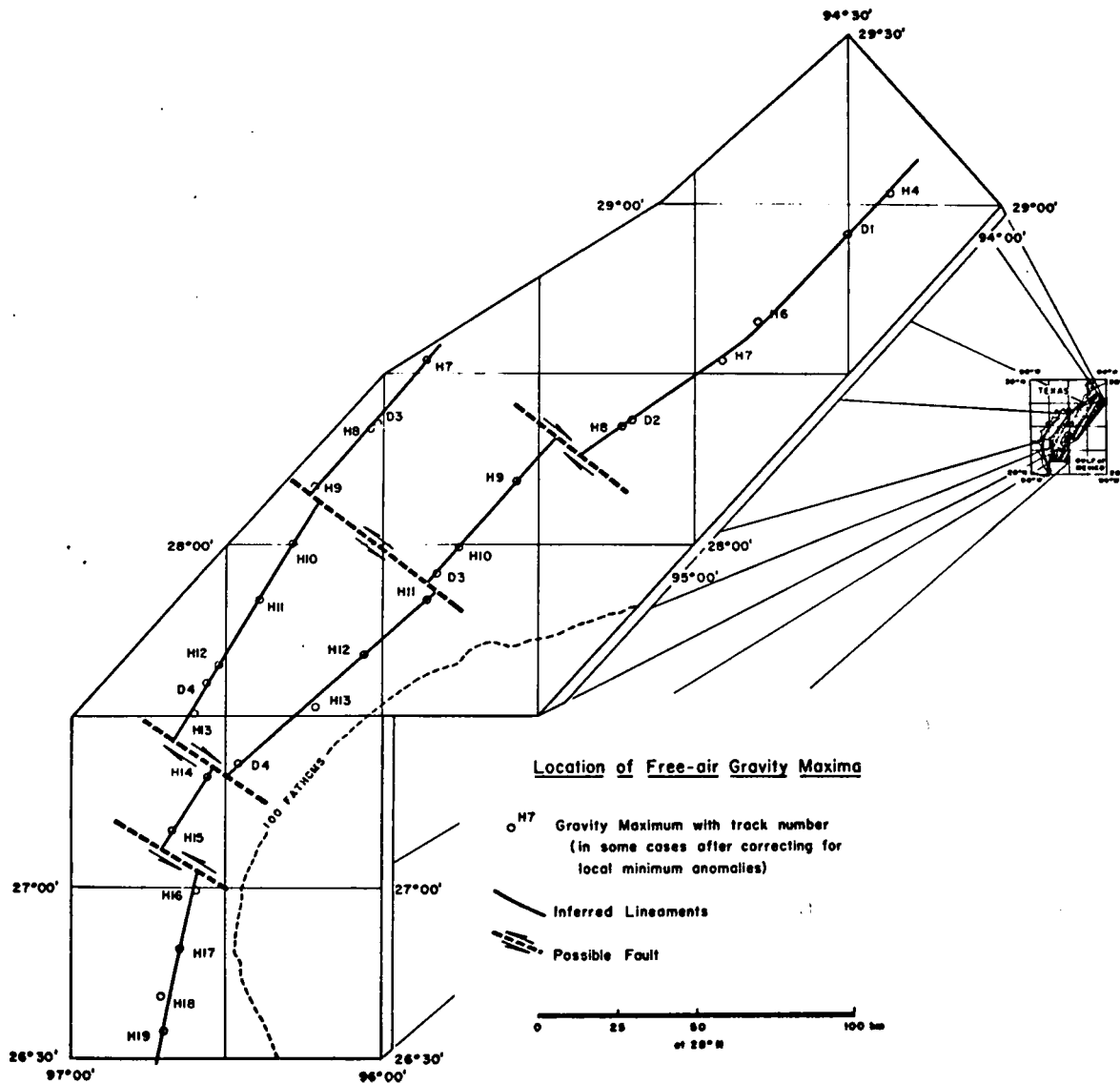
The completed map is shown in Figure 15. Although the aforementioned procedure does involve subjectivity in the location of the maxima, efforts were made to minimize the subjective aspects. In any event, the only tracks where corrections greater than a few milligals were necessary, were H16 - H19, where as Figure 5 shows, a large minimum anomaly is indicated.

The lineations were determined by drawing the best fit straight line through as many data points as possible, with the exception of the points north of H8 where a slight bend is shown. Another fault could be drawn between H6 and H7 although the evidence does not appear conclusive. Four offsets result from this procedure, which will be referred to as faults A to D respectively from the northeast. The strike of the inferred faults is somewhere between $N50^{\circ}W$ and $N60^{\circ}W$, having been arbitrarily drawn as

FIGURE 15

Location of possible horizontal offsets along the Texas continental shelf gravity maximum.

NOTE: The positions of some of the maxima were determined after correcting for assumed minimum anomalies similar to those shown in Figure 5.



parallel to fault B where close control is available.

The largest displacement involves 14 km of left-lateral motion on fault D. Fault B shows at least six km of left-lateral movement across both portions of the TCSGM. The most interesting fault is "A", between H8 and H9. The apparent motion is right-lateral for a distance of nine km. Lack of data north of H7 precludes extension of this fault to the northwest onto the coastal plain. There does appear to be a shift in the -10 mgal contour on the southern portion of the Freeport gravity maximum (DD of Fig. 4) which shows a right-lateral displacement of approximately 10 km. Possibly fault A could be extended to intersect the Freeport anomaly.

Discussion of the Significance of the Inferred Faults

The TCSGM has been inferred to result mainly from high density intrusions in the oceanic crust along a fracture system having a trend closely approximating the trend of the present coastline. If this hypothesis is even partially correct the apparent strike-slip faults shown in Figure 15 probably formed during or after the emplacement of the intrusions. There is little, if any, literature on observed strike-slip faulting on the Texas coastal plain and especially on the continental shelf to support this statement. This is not unexpected as the inferred displacements in Figure 15 are small (less than 15 km) and the horizontal movement probably does not extend upward into the Cretaceous and Tertiary sediments. If it is assumed that there is little relief associated with the faulted surfaces, then only very detailed magnetic and gravity surveys could hope to show these relatively small horizontal offsets. This is further complicated by the extreme depths encountered on the coastal plain and continental shelf coupled with the presence of only two relatively distinct positive linear

gravity anomalies which would be likely to show offsets this small. These are the Ouachita Structural Belt maximum (AA of Fig. 4) and the Freeport maximum (DD of Fig.4). To this author's knowledge, neither of these features has been studied with the detail needed to isolate the geophysical anomalies which would be expected if this hypothesis were correct.

Some thought has been given to the presence of strike-slip or wrench faulting in the "basement" of east Texas and northern Arkansas where Fowler (1964) discusses basement faulting and corresponding Smackover Limestone that might be associated with petroleum structures. Some of his conclusions are:

- (1) Vertical basement faults do not produce normal fault systems in the overlying layers that are in any sense similar to the Gulf coastal plain grabens.
- (2) Based on the result of his analysis of seismic, gravity, and well log data from some petroleum-producing structures of east Texas and southern Arkansas, that the Smackover limestone and the overlying Buckner Formation, both Upper Jurassic, show both horizontal (as much as 3 km) and vertical movements.
- (3) Deformation of the Louann salt, stratigraphically below the Smackover and Buckner, by gravity tectonics, cannot account for the apparent horizontal displacements.
- (4) Using a principal stress field with azimuth of 330° results in a conjugate set of first order faults and folds. This could explain strike directions of dominant structural trends in the Ouachita-Mid-continent area of N-S, $N60^{\circ}W$, and $N60^{\circ}E$.
- (5) The time of movement along these strike-slip faults could have been as early as the time of deposition of the Eagle Mills formation

(Upper Triassic) as extensive faulting preceded the deposition of the Werner formation (Upper Jurassic) which rests unconformably upon the Eagle Mills.

The type, time, and magnitude of faulting inferred by Fowler may be similar to that inferred for the TCSGM and the Freeport gravity maximum.

TECTONIC IMPLICATIONS OF THE FREEPORT AND TEXAS CONTINENTAL
SHELF GRAVITY MAXIMA

The great length of the Texas continental shelf gravity maximum (TCSGM), at least 450 km and possibly as much as 600 km, suggests that its origin is intimately related to the regional tectonic history of the Texas continental margin.

Trends of the Ouachita Structural Belt (Flawn, 1961, Plate 2) indicate that the TCSGM does not show any obvious relation to the stress system present when the Ouachitas were formed during the Late Paleozoic. The existence of the TCSGM prior to the formation of the Ouachita Structural Belt is highly doubtful, considering generally accepted mechanisms of the interaction of lithospheric plates and their relation to the formation of folded mountain belts (Dewey and Bird, 1970).

What little specific information that exists in the literature on the relationship of plate tectonics to the evolution of the Ouachita Structural Belt is summarized in papers by Yungul (1971) and Keller and Cebull (1973). Yungul (p. 2641) on the basis of magnetic data published by Heirtzler et al. (1966), suggests that the Ouachita Structural Belt is the result of subduction along a continental margin and infers that the now inactive trench formed during such convergence could be the Gulf Coast geosyncline. Keller and Cebull (pp. 1661-1664) suggest that the Ouachitas were formed in the same manner as the classic Dewey and Bird (1970) model of oceanic crust being consumed in a subduction zone adjacent to continental lithosphere with resulting thrust faulting and emplacement of an igneous core within the structural belt. The Ouachita gravity maximum of Figure 4 is the geophysical expression of this "mobile core". The time span for this orogenic activity is Late Ordovician through Early Permian.

Reconstruction of the continental plates by Dietz and Holden (1970, p. 4943, Fig. 2) show that at the end of the Permian, prior to the rifting of the North Atlantic during the Late Triassic, Yucatan and Honduras occupied the area now encompassed by the Gulf of Mexico, adjacent to the North American plate. This reconstruction implies that the present Gulf of Mexico has formed since the Late Permian. It also implies that if the structural features which comprise the TCSGM existed prior to the present Gulf, they most surely would have undergone considerable alteration during the orogenic activity. If this reconstruction is correct one would infer that the TCSGM and the associated Freeport gravity maximum formed after the emplacement of the Ouachita Structural Belt, possibly at a time coinciding with the Late Triassic opening of the North Atlantic.

A model for the origin of the Gulf of Mexico by Moore and Del Castillo (1974, pp. 612-614) suggests that during the Late Triassic a rift developed inshore along the present Texas-Louisiana coastline and separated the North American and Yucatan-South American-African plates along two large transform faults extending adjacent to the present Mexico-Gulf coastline and western Florida. The rift is implied to be an extension of that developed in the North Atlantic during the same time period. By Late Jurassic time, they conclude, Yucatan had moved to its present position, movement along the transform faults had ceased, and the active spreading center had shifted south of Yucatan to connect directly with the Mid-Atlantic ridge. The authors do not give any evidence for the spreading center to have moved, during rifting, toward the southeast away from the Texas-Louisiana coastline or whether it remained stationary, at the original site of rifting, as a single convection cell with movement only toward the southeast.

The high density ultramafic intrusions which are inferred to be the cause of both the TCSGM and the Freeport gravity maximum appear to have the location and length they would need to fall within the area where the Moore and Del Castillo model calls for an initial rift. A peridotite composition for the intrusions would account for the high apparent densities. This rock type would also be compatible with the assumed magnetic susceptibility of 0.002-0.003 cgs units (fig. 14).

While peridotite intrusions in the oceanic crust, having widths of as much as 14 km and extending continuously for over 450 km appear highly speculative, they are not without modern analogues. Vogt et al. (1971) consider the large magnetic anomalies of several hundred gammas present in the Tyrrhenian Sea in the western Mediterranean to be due to isolated ophiolites extruded onto the sea floor, diapirs of serpentized peridotites within the oceanic crust, or a combination of both. This area of the Mediterranean is thought to be a zone of underthrusting of the African plate below southern Europe. Analysis of earthquake epicenters by Caputo et al. (1970) indicates that the stresses of the thrusting are being concentrated in southern Italy, possibly causing the oceanic crust of the Tyrrhenian Sea to be highly fractured (p. 4920). This may explain the large number of individual magnetic anomalies observed by Vogt et al. Models of some of the magnetic anomalies show that they have lengths of up to 200 km with widths ranging between 20-150 km. Interestingly, the models assuming peridotite diapirs are assumed to have magnetizations of 0.002 cgs units and are believed to be as much as 10 km thick, dimensions similar to those chosen for the magnetic and gravity models of the TCSGM. Vogt et al. (p. 3226) conclude that the emplacement of the ophiolites or serpentized peridotite diapirs "... is controlled by the continental-basin

boundary, a region of major change in crustal structure and hence very likely a zone of weakness".

Cochran (1973, p. 3260, Fig. 6) in a study of fracture zones in the Guiana basin, West Equatorial Atlantic infers an ultramafic intrusive, probably serpentinized peridotite, with a density contrast of 0.30 gm/cc, a thickness up to four km, width of as much as 60 km, and a length over 600 km to be the cause of the positive free-air anomaly associated with the Romanche fracture zone. This density contrast, although 40% less than that assumed for the intrusions in Figure 10, is comparable since the 0.50 gm/cc density contrast used in the crustal section is too large if only the true residual anomaly due to the intrusive is considered. Since the Romanche fracture zone is the surface expression of a large east-west trending transform fault along the Mid-Atlantic ridge, the source of the peridotite would be from the upper mantle through the fractures and then onto the sea floor.

The TCSGM and the Freeport gravity maximum, if considered in the light of the previously discussed investigations, could represent evidence of ancient plate movements in the northwest Gulf of Mexico. The high density ultramafic intrusions inferred from Figure 10 could, in fact, be peridotites intruded along fractures formed parallel to an area of weakness, caused by the Oauchita subduction, along the Texas-Yucatan boundary. A crustal section across the Campeche Escarpment by Henderson (1963) shows that the continental crust extends to the Escarpment. Matching the edge of the continental crust along the Campeche Escarpment with the edge of the Paleozoic metasediments shown in Figure 10 could show the general location of this post-Oauchita orogeny zone of weakness in the crust.

Considering the regional extent of the TCSGM, it would not be overly speculative to associate the location of the initial rift, in the late

Triassic as envisioned by Moore and Del Castillo (1974), with the line of peridotite intrusions emplaced along the line of weakness marked by the Paleozoic metasediments on the Texas margin and the continental crust on the margin of the Yucatan-South America-Africa plate. Horizontal offsets, shown in Figure 15, could represent transform or transcurrent faults, now inactive, which formed after the separation of the two plates. The magnetic polarity reversals described by Heirtzler et al. (1966) which parallel and appear to die out to the east of the TCSGM could have been formed during the period of axial accretion. Absence of the polarity reversals is to be expected on the eastern side of the transform fault assumed to have been present west of Florida. The graben, inferred in Figure 10, could be similar to the Triassic grabens present on the eastern continental margin of North America (Murray, 1961, p. 81, Fig 3.2)

An alternative hypothesis is that the intrusions and graben system could represent the site of a spreading center instead of marking the boundary of plate separation. Conclusive arguments to disprove this hypothesis rest on the location of a spreading center, active from the Late Triassic to the Late Jurassic in the Sigsbee Deep between the Texas continental slope and the Campeche Escarpment. A corollary to this hypothesis is that the TCSGM is not caused by high density intrusions, but by topography on the oceanic crust. The available data, as has been previously discussed, preclude the existence of any relief on the crust having the magnitude necessary to explain the observed gravity anomalies.

Both of these hypotheses differ from a model proposed by Beall (1973, p. 113). He concludes that a rift opened between Yucatan and the Texas continental margin in the Precambrian. The associated convection cells were active throughout the Paleozoic, forming the Ouachita and Marathon

mountains and the oceanic crust of the Gulf of Mexico. At the end of the Paleozoic, the convection cells became inactive and the Gulf region began to subside forming regional crustal fractures. Stress relaxation along these fractures allowed formation of the Mesozoic aged intrusions and large fault systems such as the Balcones and Mexia-Talco grabens.

The data presented in this thesis appear to refute Beall's interpretation, especially if the time of emplacement and the apparent continuity of the TCSGM are considered. Emplacement of the intrusions during the active Ouachita subduction would result in deformation and fracturing of the intrusives, similar to that described presently as occurring in the Tyrrhenian Basin, destroying the continuity that the TCSGM appears to possess. If, on the other hand, the ultramafic material was intruded into fractures forming during relaxation of stress, as Beall contends, horizontal offsets, such as those shown in Figure 15 would have to be incipient with the ultramafic material intruding exactly along the fracture zones to form the gravity anomalies now present. It is doubtful whether horizontal displacements as small as those shown in Figure 15 would be preserved if intrusion did, in fact, occur by this mechanism.

Further speculation concerning the relation of the TCSGM to plate tectonic activity in the northwest Gulf of Mexico is dependant on acquisition of high quality magnetic data on the Texas continental shelf, particularly in those areas shown in Figure 15, whose horizontal offsets are suggested by the gravity data. Likewise, a detailed magnetic and gravity survey over the southern portion of the Freeport gravity maximum is necessary to determine if the horizontal offset inferred to extend through the feature actually exists.

INTERPRETATION OF GRAVITY MINIMA ON THE SOUTH TEXAS CONTINENTAL SHELF AND UPPER CONTINENTAL SLOPE

Introduction

Gravity minima, as determined from the available data in the south Texas offshore area, may be divided into two categories: curvilinear anomalies which may be correlated along the continental shelf continuously for distances of over 200 km (Fig. 5) and isolated anomalies which may or may not be correlated with topography along the upper continental slope (Fig. 16).

The curvilinear minima on the continental shelf are easily discerned by using only the free-air anomaly while the relief of the topography on the continental slope is such that Bouguer anomalies are necessary for correct interpretation.

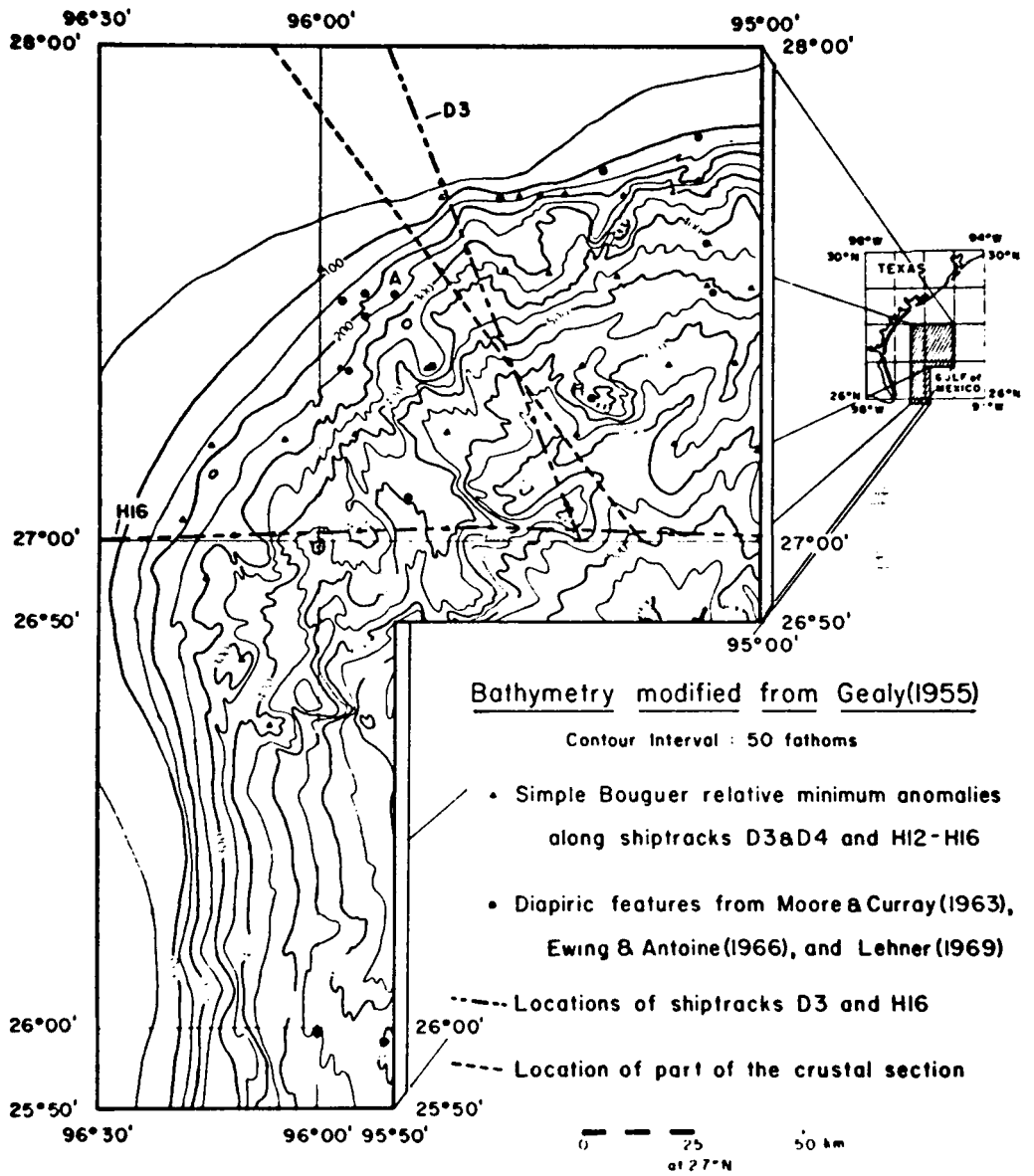
Computing the Bouguer Anomalies

Simple Bouguer anomalies (no terrain correction) were computed using the formula previously given for profiles H12-H16 and D3-D4. It was necessary to obtain the water depths from another source as they were not included with the gravity data.

Gealy (1955) compiled maps of submarine topography in the northwest Gulf of Mexico. Part of her Plate 1 is shown in Figure 16. Her maps are contoured at 25 fathom intervals; for convenience only contours at 50-fathom intervals are shown in Figure 16. Accuracy of her map is stated to be within 25 fathoms in water depths greater than 250 fathoms and within one fathom in water less than 100 fathoms deep. This error in depth corresponds to a maximum error (for 25 fathoms) of 2.9 mgal for a density of 2.53 gm/cc and 1.10 mgal for a density of 1.60 gm/cc. While this error is large for detailed petroleum exploration, it is well within the range

FIGURE 16

Bathymetry of part of the Texas upper continental slope showing residual Bouguer minimum anomalies along tracks H12-H16 and D3-D4 indicated by bold carets. Locations of diapirs determined by seismic reflection indicated by carets and Bouguer relative minimum anomalies shown by dots. Bathymetry from Gealy (1955).



of the absolute accuracy of the gravity measurements themselves and, as will be seen, it is satisfactory for the use intended for it here.

Inspection of Figure 16 reveals that the surface of the continental shelf is characterized by smooth, gentle gradients. This generalization ends at the 100 fathom isobath where the gradient begins to vary substantially, forming linear depressions, ridges, and isolated mounts. This is the "hummocky zone" extending from the Texas continental shelf to the Sigsbee Escarpment as described by Gealy (1955, p. 214). The topography in this area has been attributed to be the result of diapirism, most probably salt (Ewing and Antoine, 1966, p. 498). Uchipi and Emory (1968, p. 1191, Fig. 19) show numerous diapiric structures determined by seismic reflection work which are located over the area of Figure 10. The scale of their map is such that the actual locations of the diapirs with respect to the topography cannot be shown. More easily mappable seismic results are available from Moore and Curray (1963, p. 1726, Fig. 1), Ewing and Antoine (1966, p. 499, Fig. 15), and Lehner (1969, p. 2434, Fig. 4) all of which show diapiric structures in the area of Figure 16. These features are indicated as small dots.

Examples of the bathymetric profiles are shown on tracks D3 (Fig. 12) and H16 (Fig. 11). Track D3 crosses several minor topographic features and a major feature at approximately 170 km offshore. The latter has a relief of over 100 fathoms. Track H16 crosses six features which substantially interrupt the gradient, two of them, at offshore distance of 140 and 160 km having relief of 120 and 80 fathoms respectively along the profile.

The free-air anomalies along all the profiles are heavily influenced by the topography, as would be expected. This close correspondence between the free-air anomalies obtained from the DOD data and the bathymetry from

Gealy's map confirms the usefulness of computing and analyzing Bouguer anomalies.

Simple Bouguer corrections were applied to each profile using respective densities of 1.60, 1.80, 2.00, 2.17, and 2.53 gm/cc. No terrain corrections were applied as computation of such a correction for the isolated mound on track D3 produced only 1.5 mgal (for a density of 2.0 gm/cc), which is less than the possible error due to incorrect water depths. The spacing of the topographic highs and lows is such that depth observations at 10 km intervals are sufficient to resolve all topographic changes along the profiles.

Examination of the Bouguer anomalies on Figures 11 and 12 indicates that the anomaly computed for a density of 2.53 gm/cc, the sediment density used in the crustal section, has a strong negative correlation with the topography. This implies that the density is too large, which is to be expected from the previous discussions on near-surface sediment densities. The anomaly computed using a density of 2.17 gm/cc, which closely approximates that of salt (2.15 gm/cc), results in substantial negative anomalies which can be directly associated with the bathymetry, especially on track H16.

The anomaly computed with a density of 1.60 gm/cc shows the least correlation with bathymetry and therefore appears to be the correct density for the reduction. It is possible, however, that if the correct water depths were known with accuracies greater than 25 fathoms and terrain corrections were included for them, the Bouguer reduction density would be larger. Considering the variation in water depth along the profiles and the variation of density with depth of Gulf Coast sediments (Musgrave and Hicks, 1966, p. 717, Fig. 13) the probable Bouguer density should be 1.95 gm/cc on the continental shelf and should increase to 2.1 gm/cc in water depths greater

than 800 fathoms where tracks D3 and H16 intersect. The theoretically correct Bouguer reduction density would then vary with water depth. As this procedure would not be practical without better bathymetric control, a compromise density of 2.0 gm/cc was chosen as most appropriate over the lengths of all seven ship tracks used in preparing Figure 16.

To obtain the residual anomalies along the ship tracks, the regional Bouguer anomaly was sketched on each profile (using the 2.0 gm/cc density). The regional Bouguer anomaly over the continental slope was considered to be in the form of a smooth depression (as seen in Figures 11 and 12) below the 0.14 mgal/km gradient, while the regional anomaly over the shelf was assumed to approximate the Texas continental shelf gravity maximum. The residual anomalies resulting from this procedure are plotted as carets in Figure 16.

Gravity Minima on the Southern Continental Shelf

Lehner (1969, p. 2434, Fig. 3) shows that the growth faults, both onshore and on the continental shelf, which are arranged in belts representing the major axes of Tertiary clastic deposition are subparallel en-echelon with the coastline. These faults are probably equivalent to the contemporaneous faults which Bruce (1972, p. 23) considers to form on the seaward flanks of deeply buried low density, highly-pressured marine shale masses in the south Texas area. This marine shale is thought to be derived from the Jackson and Vicksburg groups (Broomer, 1967, p. 126) whose depocenters are shown in Williamson (1959, pp. 21-22, Figs. 7, 9). He shows that the 6000 ft isopach is centered in Hidalgo and Kenedy counties trending to the northeast along the coast for the Jackson Group while the 5000 ft isopach is centered 30 miles (48 km) inland along the Texas-Mexico border and extending northeast along the present coastline to Galveston Island for the Vicksburg Group.

Moore and Curraý (1963) show reflection profiles on the south Texas continental shelf with usable information down to 1.2 sec., which corresponds to a total depth of 4200 ft (1.28 km), assuming a sediment velocity of 7000 ft/sec. Their Aransas Pass profile (p. 1738, Fig. 8) which extends 160 km southeast of the pass shows a set of normal faults having small displacements at a distance of 77 km offshore.

This area is between tracks H13 and H14 (Fig. 5) where a minimum anomaly of -3 to -4 mgals is indicated and is 53 km north of the minimum anomaly of -12 mgal shown on track H16 (Fig. 11 at "MODEL"). These faults probably correlate with the minimum at H16. Since the small displacements on these faults (and on other faults shown on this profile) are not large enough to account for the observed -12 mgal anomaly, a deeper source is indicated.

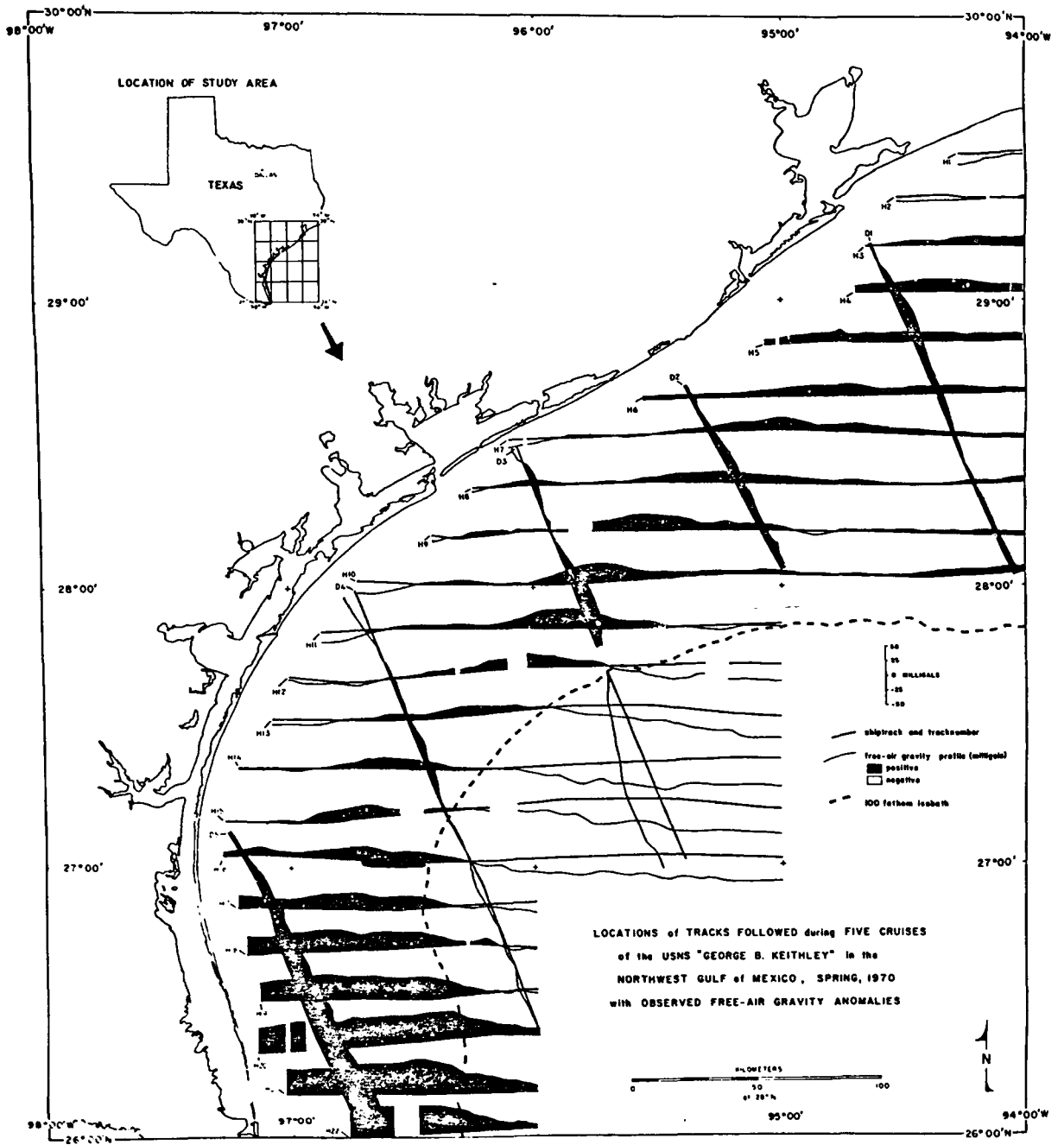
Assuming that the source of the minimum on track H16 is a mass of low density, highly pressured marine shale, a model, whose location is shown in Figure 17, was based on the seismic profiles over these same type features published by Bruce (1972). On page 23, of this paper he describes the shale masses as follows:

"...these masses, commonly tens of miles in length have been observed to range in size up to 25 miles in width and 10,000 ft vertically."

These dimensions allow use of the two-dimensional modeling techniques previously described. Density contrasts were obtained from the graph of Musgrave and Hicks (1966, p. 717, Fig. 13). Bruce's seismic data indicate that the low density shale masses may extend deeper than 20,000 ft (6.1 km) and the high pressure surface which marks the top of the shale mass may come within 8200 ft (2.5 km) of the water bottom. Using this range, the density contrasts were allowed to vary from -0.06 gm/cc at the top of the shale mass (2.1 km depth) to -0.25 gm/cc at 6.5 km depth. The normal density

FIGURE 17

The red line represents the location of the minimum anomaly shown in Figure 11(at "MODEL") and in Figure 18.



at 6.5 km should have the value (assuming the validity of Musgrave and Hicks data for this region) of 2.60 gm/cc at this depth. Three layers were used to model this density distribution. The horizontal coordinates of the mass were determined by trial and error.

The resulting gravity model is shown in Figure 18 with the actual coordinates used in its construction given in the Datafile 3PARTLUMP of Appendix 2. This model is in the shape of a triangle with a base 10.5 km wide and a flattened apex. Similar shapes are shown in Bruce's seismic examples indicating that while this may not be a unique interpretation of the observed gravity data, it is realistic and may closely approximate the actual structure of the shale mass. The dimensions of the actual shale mass most probably vary along strike as evidenced by the decrease in the magnitude of the minimum anomaly to the north of track H16.

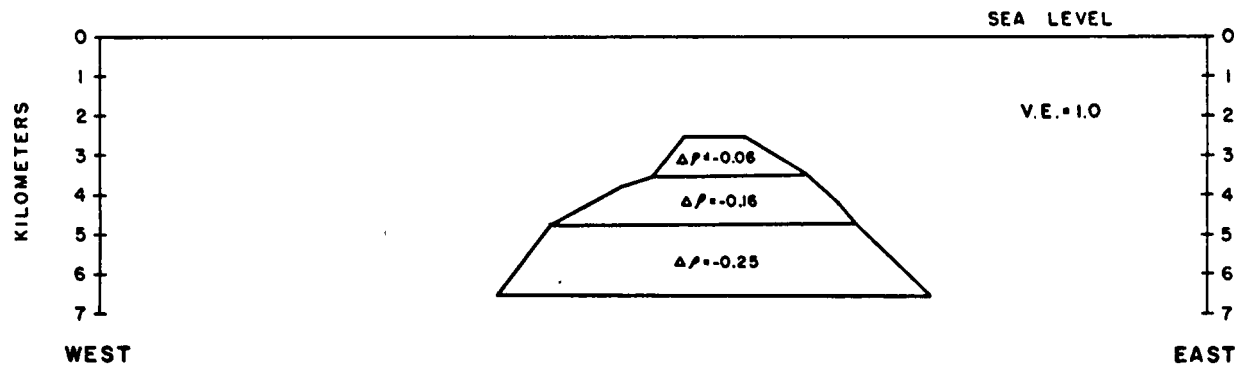
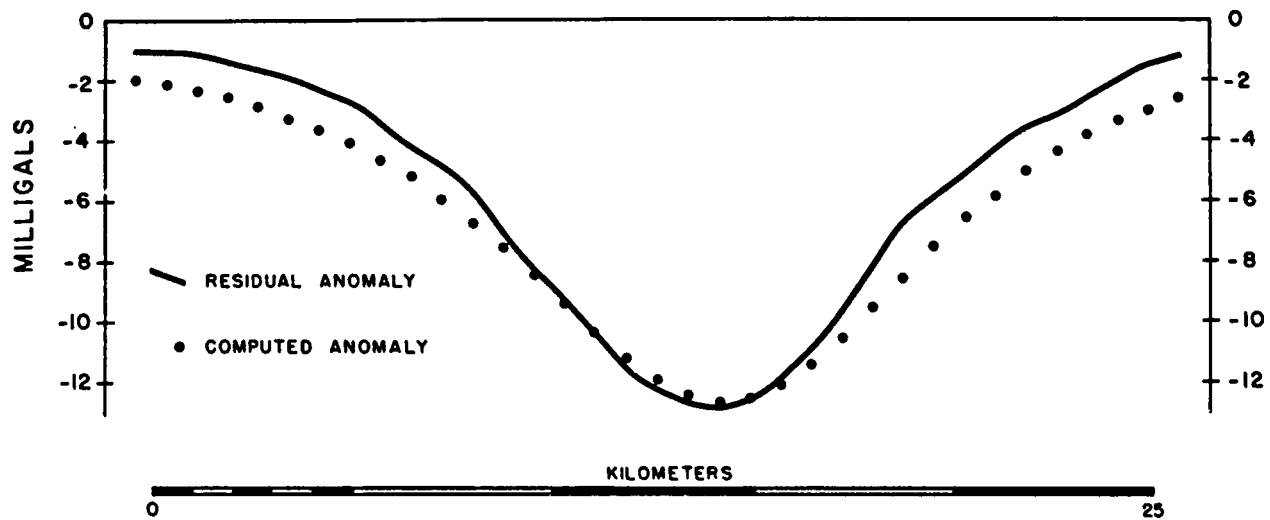
Features similar to that shown in Figure 18 may be responsible for the other linear anomalies shown in Figure 5, as the location of the areas of maximum deposition for the marine shales coincides with the offshore gravity anomalies and with a zone of shale diapirs onshore (Broomer, 1967, p. 128, Fig. 1). The continuity of the offshore minima indicated by the lines in Figure 5 does not infer continuity of associated structural features, which may in fact be discontinuous.

Gravity Minima on the Southern Continental Slope

In stark contrast to the apparent linear anomalies on the continental shelf, the gravity minima on the upper continental slope are isolated and linear only when there are obvious topographic lineations. The magnitude of the residual Bouguer minima present along tracks H12-H16 and D3-D4 vary from -2 to -8 mgal. These values compare favorably with those observed by Nettleton (1957) over a shallow salt dome in 60 fathoms of water along

FIGURE 18

Computed gravity model for the local anomaly shown in Figure 11
(at "MODEL"). The location is shown in Figure 17.



GRAVITY MODEL FOR NEGATIVE
ANOMALY OBSERVED ON TRACK "H16"

the Texas-Louisiana border.

The depth of the salt under the upper continental slope varies considerably, as in most cases the diapirs formed by the salt possess nearly vertical sides. Nevertheless, a large portion of the area shown in Figure 16 is underlain by salt at very shallow depths, especially where there is substantial topographic relief (Lehner, 1969, p. 2435, Fig. 4).

Position A on Figure 16 represents a salt diapir detailed by Lehner. In this case the salt surface was cored at 106 m below the water bottom (600 m total depth) (p. 2447). This position represents a small bathymetric prominence. Position H is a topographic mound (from 11-15 km in diameter) having 305 m relief. Salt was cored here at a depth of 248 m below water bottom with a total subsea depth of 1150 m (p. 2453). Residual anomalies of -4 to -6 mgals are associated with the west flanks of this mound on tracks H14 and H15.

If seismic data were available for all gravity profiles shown in Figure 16 the locations of all the residual gravity minima (38 in all) would probably correspond to the locations of shallow salt diapirs similar to those present at locations A and H. These seven tracks, however, represent gravity coverage of only a small portion of the continental slope; more detailed coverage would probably show many more diapiric features.

As previously mentioned the regional Bouguer low associated with the continental slope may in fact be due to the abnormal thickness of salt present in this area.

Other Comments on the South Texas Offshore Gravity Minima

Interestingly, the 100-fathom contour appears to mark the boundary (in the area south of 29°N lat.) between the "shelf" diapiric shale province and the "slope" salt province. A possible exception to this generalization

is the linear anomaly shown as the yellow line in Figure 5. This feature could be a deep seated continuous salt-ridge, as it appears to extend farther east and out of the shale province. This type of salt feature is common on the Mexican continental slope south of 26°N lat. (Bryant, et al., 1968). Salt ridges similar to those described by Bryant et al. may even be the cause of the gravity minima on the south Texas shelf inferred to be caused by shale. However, none of the ridges described by Bryant et al. are reported to extend onto the continental shelf in this area.

SUMMARY AND CONCLUSIONS

Before overall conclusions are stated, the geological inferences that have been reached from a study of different types of information will be presented. The individual sources of information to be considered in this light are the regional gravity map (Figs. 3 & 4), the crustal section based on the gravity data (Fig. 10), the magnetic model (Fig. 14), and the map showing horizontal offsets of the gravity maxima (Fig. 15).

The Gravity Map

The offshore gravity data show that the regional free-air gravity anomalies on the Texas continental shelf are considerably more complex than those shown on the map by Dehlinger and Jones (1965).

Considering the entire map derived in this study, five regional gravity anomalies are present. Two of them, the Ouachita Structural Belt maximum and the Rio Grande Delta maximum, are inferred to be due to a core of higher density igneous intrusive and metamorphosed sedimentary rocks for the former and temporary sediment loading of an isostatically balanced continental margin for the latter. One of the five anomalies, the Texas continental slope free-air minimum, is caused primarily by the increased water depths over the continental slope and may be partially due to the excessive thicknesses of low density salt present in the area. The other two regional anomalies, the Texas continental shelf free-air maximum and the Freeport Bouguer maximum may be modeled as resulting from high density ultramafic intrusions adjacent to the Texas coastline.

The Crustal Section

The general features shown in the crustal section are:

- (1) Along the Coastal plain, in the vicinity of the crustal section,

the continental crust terminates approximately 90 km inland with the overlying Paleozoic metasediments pinching out at the coastline. The basement under the continental shelf and slope is oceanic crust.

(2) The regional southeastern dip as indicated by the surface of the Paleozoic metasediments and oceanic crust reverses at a distance of approximately 50 km offshore where the depth to the oceanic crust is 16.3 km.

(3) The M becomes shallow away from shore (excluding the local deepening under the continental shelf) and continues an undulatory rise to the southeast terminus of the crustal section where its depth is 22 km. This structure is not in agreement with that shown by Dehlinger and Jones (1965, p. 101, Fig. 2) who show the depth of the M to be at 22 km under the center of the shelf deepening to 30 km further offshore or that by Shurbet (1969, p. 244, Fig 1), who indicates that the M rises to a depth of 16 km at a distance of 50 km offshore, continuing further offshore at this same depth.

(4) The high-density intrusives associated with anomalies M1 and M2 of Figure 10 intrude into the oceanic crust only, while the one at anomaly M3 intrudes into both the oceanic crust and the Paleozoic metasediments, implying that the intrusion took place during post-Paleozoic - pre-Tertiary time.

The Magnetic Model

Analysis of the magnetic profile southeast of Galveston, approximately 175 km northeast of the crustal section, yielded these results:

(1) The Texas continental shelf gravity maximum, at a distance of 53 km offshore is associated with a large, normally polarized magnetic anomaly an unusual feature considering the depth to magnetic basement in this area.

(2) The depth to the top of the magnetic basement, considered to be

the oceanic crust in the area of the magnetic profile may be as much as 16.5 km.

(3) The magnetic anomaly appears to be a two-dimensional feature, striking in a direction similar to that of the shelf gravity maxima.

(4) The susceptibility contrast of the anomalous material is between 0.002-0.003 cgs units.

(5) Calculated widths of the assumed two-dimensional dike model compare favorably with the widths of the intrusions determined from gravity models along the crustal section.

The Horizontal Offsets of the Shelf Gravity Maxima

The reconstructed locations of both components of the Texas continental shelf gravity maximum on 18 of the 27 ship tracks showed as much as 14 km of strike-slip displacement of the gravity maxima, approximately perpendicular to the present coastline. Similar faulting may be inferred for the Freeport maximum. The most recent faulting activity here is inferred to be pre-Cretaceous.

Conclusions

The present study, combining recently obtained high quality marine gravity data with land gravity data available in the literature, of regional anomalies along the margin of the Northwest Gulf of Mexico, infers the existence of an extensive set of peridotite bodies, hitherto unreported in the literature, intruding the oceanic crust under the continental shelf. Previous investigators have been limited in both the quality and quantity of data available in the literature which would have revealed the presence of this structure at an earlier date.

Integration of the intrusive structure with a recently published model, based on modern plate-tectonic theory, for the late Triassic origin of the

present Gulf of Mexico produces a rational explanation for the extent of the gravity anomalies shown in Figure 9, the geometry of the continental crust and the depths to the oceanic crust and to M shown in Figure 10; the magnetic anomaly shown in Figure 14; the linear normal and reversed polarity magnetic anomalies in the area described by Heirtzler, et al. (1966); and the horizontal offsets of the gravity maxima shown in Figure 15.

Finally, the curvilinear minima, some of which extend well over 150 km, present on the continental shelf (Fig. 5) are most probably due to intrusions of low-density, highly pressured marine shale of late Eocene - early Oligocene age. The isolated minima present on the upper continental slope (Fig. 16) are probably due to extremely shallow salt diapirs, which also produce the rugged topography of the slope.

REFERENCES

- Antoine, J. and Ewing, J., 1963, Seismic refraction measurements on the margins of the Gulf of Mexico: *J. Geophys. Res.*, v. 68, no. 7, pp. 1975-1996.
- Atwater, G. I., 1959, Geology and petroleum development of the continental shelf of the Gulf of Mexico: *Gulf Coast Geol. Soc. Trans.*, v. 9, pp. 131-145.
- Balsey, J. R., 1949, Total-intensity aeromagnetic map (survey) of part of Gulf of Mexico, U. S. Geol. Survey, Geophys. Inv. Prelim. Map.
- Barton, D. C., Ritz, C. H., and Hickey, M., 1933, Gulf coast geosyncline: *Amer. Assoc. Petr. Geol. Trans.*, v. 17, no. 10, pp. 1446-1467.
- Beall, A. O., Jr., Laury, R., Dickson, K., and Pusey, W. C. III, 1973, Sedimentology, pp. 699-729 in J. L. Worzel, ed., Initial Reports of the Deep Sea Drilling Project, v. 10, Galveston, Texas to Miami, Florida: U. S. Government Printing Office, 748 p.
- Beall, Robert, 1973, Plate tectonics and the origin of the Gulf coast basin: *Gulf Coast Assoc. Geol. Soc. Trans.*, v. 23, pp. 109-114.
- Broomer, F. J., Jr., 1967, Shale diapirs of the lower Gulf coast as typified by the north Laward diapir: *Gulf Coast Assoc. Geol. Soc. Trans.*, v. 17, pp. 126-134.
- Bruce, Clemont H., 1972, Pressured shale and related sediment deformation: A mechanism for development of regional contemporaneous faults: *Gulf Coast Assoc. Geol. Soc. Trans.*, v. 22, pp. 23-31.
- Bryant, William R., Antoine, J., Ewing, M., and Jones, B., Structure of the Mexican continental shelf and slope, Gulf of Mexico: *Am. Assoc. Pet. Geol. Bull.*, v. 52, no. 7, pp. 1204-1228.
- Caputo, M., Panza, G. F., and D. Postpischl, 1970, Deep structure of the Mediterranean basin: *J. Geophys. Res.*, v. 75, no. 26, pp. 4919-4923.
- Cochran, James R., 1973, Gravity and magnetic investigations in the Guiana basin, western equatorial Atlantic: *Geol. Soc. Amer. Bull.*, v. 84, no. 10, pp. 3249-3268.
- Cram, I. H., Jr., 1961, A crustal structure refraction survey in south Texas: *Geophysics*, v. 26, no. 5, pp. 560-573.
- Cram, I. H., Jr., 1962, Crustal structure of Texas coastal plain region: *Amer. Assoc. Pet. Geol. Trans.*, v. 46, no. 9, pp. 1721-1727.
- Dehlinger, Peter and B. R. Jones, 1965, Free-air gravity map of the Gulf of Mexico and its tectonic implications, 1963 edition: *Geophysics*, v. 30, no. 1, pp. 102-110.

- Dewey, J. F. and J. M. Bird, 1970, Mountain belts and the new global tectonics: *J. Geophys. Res.*, v. 75, no. 15, pp. 2625-2647.
- Dietz, R. S. and J. Holden, 1970, Reconstruction of Pangaea: Breakup and dispersion of continents, Permian to present: *J. Geophys. Res.*, v. 75, no. 26, pp. 4939-4956.
- Dillon, W. P. and John G. Vedder, 1973, Structure and development of the continental margin of British Honduras: *Geol. Soc. Amer. Bull.*, v. 84, no. 8, pp. 2713-2732.
- Dobrin, Milton B., 1960, *Introduction to Geophysical Prospecting*, 2nd Edition: New York, McGraw-Hill, 446p.
- Dorman, J., Worzel, J. L., Leyden, R., Crook, T. N., and Hatziemanuel, M., 1972, Crustal section from seismic refraction measurements near Victoria, Texas: *Geophysics*, v. 37, no. 2, pp. 325-336.
- Ewing, J., Antoine, J., and Ewing, M., 1960, Geophysical measurements in the western Caribbean sea and in the Gulf of Mexico: *J. Geophys. Res.*, v. 65, no. 12, pp. 4087-4126.
- Ewing, M., Worzel, J. L., Frieson, B., and Heezen, B. C., 1955, Geophysical and geological investigations of the Gulf of Mexico: *Geophysics*, v. 20, no. 1, pp. 1-18.
- Ewing, M. and Antoine, J., 1966, New seismic data concerning sediments and structures in Sigsbee Deep and upper continental slope, Gulf of Mexico: *Amer. Assoc. Pet. Geol. Bull.*, v. 50, no. 3, pp. 479-504.
- Fish, J. E., 1971, Crustal structure of the Texas gulf coastal plain: *Corpus Christi Geol. Soc. Bull.*, v. 11, no. 8, pp. 1-29.
- Flawn, P. T., Goldstein, A. Jr., King, P. B., and Weaver, C. E., 1961, The Oauchita System: *Texas Univ. Pub.*, no. 6120, 401 p.
- Flawn, P. T., 1964, Basement rocks of the Texas Gulf coastal plain: *Gulf Coast Assoc. Geol. Socs. Trans.*, v. 14, pp. 271-276.
- Flawn, P. T., 1967, Chairman, Basement Map of North America between Latitudes 24 and 60 N: *U. S. Geol. Sur. and Amer. Assoc. Pet. Geol.*, scale 1:5,000,000.
- Fowler, P. T., 1964, Basement faults and Smackover structure: *Gulf Coast Assoc. Geol. Socs. Trans.*, v. 14, pp. 179-192.
- Gealy, E. L., 1955, Topography of the continental slope in northwest Gulf of Mexico: *Geol. Soc. Amer. Bull.*, v. 60, no. 2, pp. 203-228.
- Glicken, Milton, 1962, Eotvos corrections for a moving gravity meter: *Geophysics*, v. 27, no. 4, pp. 531-533.
- Gough, D. I., 1967, Magnetic anomalies and crustal structure in eastern Gulf of Mexico: *Amer. Assoc. Pet. Geol. Bull.*, v. 51, no. 2, pp. 200-211.

- Grant, F. S. and G. E. West, 1968, Interpretation Theory in Applied Geophysics: New York, McGraw-Hill, 583 p.
- Guier, W. H., 1966, Satellite navigation using integral doppler data-the AN/SRN-9 equipment: J. Geophys. Res., v. 71, no. 24, pp. 5903-5910.
- Hales, A. L., Helsley, C. E., and Nation, J. B., 1970, Crustal structure study on the Gulf coast of Texas: Am. Assoc. Pet. Geol. Bull., v. 54, no. 11, pp. 2040-2057.
- Harden, G., 1962, Notes on Cenozoic sedimentation in the Gulf coast geosyncline, U.S.A., in Geology of the Gulf Coast and central Texas and guidebook of excursions: Houston Geol. Soc., pp. 1-15.
- Harrison, J. C., 1955, An interpretation of gravity anomalies in the eastern Mediterranean: Royal Soc. London. Phil. Trans., Ser. A, No. 947, v. 248, pp. 283-325.
- Hayes, Dennis e., 1966, A geophysical investigation of the Peru-Chile trench: Marine Geol., v. 4, pp. 309-351.
- Heirtzler, J. R., Burckle, L. H. and Peter, G., 1966, Magnetic anomalies in the Gulf of Mexico: J. Geophys. Res., v. 71, no. 2, pp. 519-526.
- Heiskanen, W. A. and Vening Meinesz, F. A., 1958, The Earth and its gravity field: New York, McGraw-Hill.
- Henderson, Garry C., 1963, Preliminary study of the crustal structure across the Campeche Escarpment from gravity data: Geophysics, v. 28, no. 5, pp. 736-744.
- Herrin, E., 1969, Regional variations of p-wave velocity in the upper mantle beneath North America, pp. 242-246 in P. J. Hart, ed., The Earth's Crust and Upper Mantle: Amer. Geophys. Union Mon., no. 13, 735 p.
- Hospers, J., 1965, Gravity field and structure of the Niger delta, Nigeria, West Africa: Geol. Soc. Amer. Bull., v. 76, no. 4, pp. 407-422.
- Joesting, H. R. and Frautschy, J. D., 1947, Reconnaissance gravity map of Gulf of Mexico, U. S. Geol. Survey, Geophys, Inv. Prelim. Map.
- Keller, G. R. and S. E. Cebull, 1973, Plate tectonics and the Ouachita system in Texas, Oklahoma, and Arkansas: Geol. Soc. Amer. Bull., v. 84, no. 5, pp. 1659-1666.
- Krivoy, H. L. and T. E. Pyle, 1972, Anomalous crust beneath West Florida Shelf: Amer. Assoc. Pet. Geol., v. 56, no. 1, pp. 107-113.
- LaCoste, L., Clarkson, N., and Hamilton, G., 1967, LaCoste and Romberg stabilized platform gravity meter: Geophysics, v. 31, no. 1, pp. 99-109.

- Lafehr, T. R. and Nettleton, L. L., 1967, Quantitative evaluation of a stabilized platform shipboard gravity meter: *Geophysics*, v. 31, no. 1, pp. 110-118.
- Lawson, A. C., 1942, Mississippi delta- A study in isostasy: *Geol. Soc. Amer. Bull.*, v. 53, no. 8, pp. 1231-1254.
- Lehner, P., 1969, Salt tectonics and Pleistocene stratigraphy on continental slope of northern Gulf of Mexico: *Amer. Assoc. Pet. Geol. Bull.*, v. 53, no. 12, pp. 2431-2479.
- Logue, L. L., 1954, Gravity anomalies of Texas, Oklahoma, and the United States: *Oil and Gas Jour.*, no. 50, pp. 132-135.
- Lyons, P. L., 1957, Geology and geophysics of the Gulf of Mexico: *Gulf Coast Assoc. Geol. Socs. Trans.*, v. 7, pp. 1-10.
- Menard, H. W., 1967, Transitional types of crust under small ocean basins: *J. Geophys. Res.*, v. 72, no. 12, pp. 3061-3073.
- Moore, D. G. and Curray, J. R., 1963, Structural framework of the continental terrace, northwest Gulf of Mexico: *J. Geophys. Res.*, v. 68, no. 6, p. 1725-1747.
- Moore, G. W. and L. Del Castillo, 1974, Tectonic evolution of the southern Gulf of Mexico, *Geol. Soc. Amer. Bull.*, v. 85, no. 4, pp. 607-618.
- Murray, G. E., 1961, *Geology of the Atlantic and Gulf Coastal Provinces of North America*: New York, Harper and Brothers, 692 p.
- Musgrave, A. W. and W. G. Hicks, 1966, Outlining of shale masses by geophysical methods: *Geophysics*, v. 31, no. 4, pp. 711-725.
- Nettleton, L. L., 1934, Fluid mechanics of salt domes: *Amer. Assoc. Pet. Geol. Bull.*, v. 18, no. 9, pp. 1175-1204.
- Nettleton, L. L., 1940, *Geophysical Prospecting for Oil*: New York, McGraw-Hill, Inc., 444 p.
- Nettleton, L. L., 1949, Geology, geophysics, and oil finding: *Geophysics*, v. 14, no. 3, pp. 273-289.
- Nettleton, L. L., 1952, Sedimentary volumes in the Gulf coastal plain of the United States and Mexico: Part VI, geophysical aspects: *Geol. Soc. Amer. Bull.*, v. 63, no. 12, pp. 1221-1228.
- Nettleton, L. L., 1957, Gravity survey over a Gulf coast continental shelf mound: *Geophysics*, v. 22, no. 3, pp. 630-642.
- Nettleton, L. L., 1971, Elementary gravity and magnetics for geologists and seismologists: *Soc. Explor. Geophys. Mon.*, no. 1, 121 p.

- Preston, R. J., 1970, A gravity study of a portion of the Rio Grande embayment, Texas: Unpublished Master of Science thesis, Texas A. and M. Univ., 87 p.
- Reford, M. S. and J. S. Sumner, 1964, Aeromagnetism: *Geophysics*, V. 29, no. 4, pp. 482-516.
- Shurbet, D. H., 1969, Development of the Gulf coast geosyncline: *Texas J. Sci.*, v. 20, pp. 243-247.
- Simmons, G. and R. F. Roy, 1969, Heat flow in North America, pp. 78-81 in P. J. Hart, ed., *The Earth's Crust and Upper Mantle: Amer. Geophys. Union Mon. no. 13*, 735 p.
- Skeels, D. C., 1947, Ambiguity in gravity interpretation: *Geophysics*, v. 12, no. 1, pp. 43-56.
- Talwani, M., , Description of digital computer program for computing the vertical component of the gravitational attraction of two-dimensional bodies of arbitrary shape: unpublished manuscript, 32 p.
- Talwani, M., Worzel, J. L., and Landisman, M., 1959a, Rapid gravity computations for two-dimensional bodies with application to the Mendocino submarine fracture zone: *J. Geophys. Res.*, v. 64, no. 1, pp. 49-59.
- Talwani, M., Sutton, G. H., and Worzel, J. L., 1959b, A crustal section across the Puerto Rican trench: *J. Geophys. Res.*, v. 64, no. 10, pp. 1545-1555.
- Talwani, M., 1964, A review of marine geophysics: *Marine Geol.*, v. 2, pp. 29-80.
- Talwani, M., X. Le Pichon, and M. Ewing, 1965, Crustal Structure of Mid-ocean ridges: *J. Geophys. Res.*, v. 70, no. 3, pp. 341-352.
- Thompson, G. A. and M. Talwani, 1964, Crustal structure from the Pacific basin to central Nevada: *J. Geophys. Res.*, v. 69, no. 22, pp. 4813-4837.
- Uchipi, E. and K. O. Emery, 1968, Structure of continental margin of Gulf coast of United States: *Amer. Assoc. Pet. Geol. Bull.*, v. 52, no. 7, pp. 1162-1193.
- Vening Meinesz, F. A. and Wright, F. E., 1930, The gravity measuring cruise of the U. S. Submarine S-21: *Publ. U. S. Naval Obs.*, 2nd Ser., Appendix 1, Washington, D. C., 94 p.
- Von Herzen, R. P. and W. H. K. Lee, 1969, Heat flow in oceanic regions, pp. 89-95 in P. J. Hart, ed., *The Earth's Crust and Upper Mantle: Amer. Geophys. Union Mon. no. 13*, 735 p.
- Vogt, P. R., Higgs, R. H., and Johnson, G. L., 1971, Hypotheses on the origin of the Mediterranean basin: magnetic data: *J. Geophys. Res.*, v. 76, no. 14, pp. 3207-3228.

- Walcott, R. I., 1970a, Isostatic response to loading of the crust in Canada: *Can. J. Earth Sci.*, v. 7, pp. 716-734.
- Walcott, R. I., 1970b, Flexure of the lithosphere at Hawaii: *Tectonophysics*, v. 9, pp. 931-937.
- Walcott, R. I., 1972, Gravity, flexure, and the growth of sedimentary basins at a continental edge: *Geol. Soc. Amer. Bull.*, v. 83, no. 6 pp. 1845-1848.
- Warren, D. H., Healy, J. H., and W. H. Jackson, 1966, Crustal seismic measurements in southern Mississippi: *J. Geophys. Res.*, v. 71, no. 14, pp. 3437-3458.
- Waters, J. A., McFarland, P. W., and J. W. Lea, 1955, Geologic framework of Gulf coastal plain: *Amer. Assoc. Pet. Geol. Bull.*, v. 39, no. 9, pp. 1821-1850.
- Watkins, J. S., 1961, Gravity and magnetism of the Ouachita structural belt in central Texas: *Gulf Coast Assoc. Geol. Socs. Trans.*, v. 21, pp. 25-41.
- Wilhelm, O. and Ewing, M., 1972, Geology and history of the Gulf of Mexico: *Geol. Soc. Amer. Bull.* V. 83, no. 3, pp. 575-600.
- Williamson, J. D. M., 1959, Gulf coast Cenozoic history: *Gulf Coast Assoc. Geol. Socs. Trans.*, v. 9, pp. 15-29.
- Woods, R. D. and J. W. Addington, 1973, Pre-Jurassic framework of northern Gulf basin: *Gulf Coast Assoc. Geol. Socs. Trans.*, v. 23, pp. 92-108.
- Woollard, G. P. and Joesting, H. R., 1964, Bouguer gravity anomaly map of the United States: *Amer. Geophys. Union and U. S. Geol. Survey*, scale 1:2,500,000.
- Worzel, J. L. and G. L. Shurbet, 1955 a, Gravity interpretations from standard oceanic and continental crustal sections, pp. 87-101 in A. Poldervaart, ed., *Crust of the Earth*: *Geol. Soc. Amer. Spec. Paper* no. 62, 762 p.
- Worzel, J. L. and Shurbet, G. L., 1955b, Gravity anomalies at continental margins: *Nat. Acad. Sci. Proc.*, v. 41, pp. 458-469.
- Worzel, J. L., 1965, Deep structure of coastal margins and mid-oceanic ridges, pp. 335-361 in W. F. Whittard and R. Bradshaw, eds., *Submarine geology and geophysics*: London, Butterworths, 503 p.
- Worzel, J. L. and W. R. Bryant, 1973, Regional aspects of deep sea drilling in the Gulf of Mexico, Leg 10, pp. 737-748 in J. L. Worzel, ed., *Initial Reports of the Deep Sea Drilling, Project*, v. 10, Galveston, Texas to Miami, Florida: U. S. Government Printing Office, 748 p.

Worzel, J. L. and J. S. Watkins, 1973, Evolution of northern Gulf coast deduced from geophysical data: Gulf Coast Assoc. Geol. Socs. Trans., v. 23, pp. 84-90.

Wyllie, P. J., 1971, The Dynamic Earth: New York, John Wiley and Sons, Inc., 416 p.

" "
Yungul, S. H., 1971, Magnetic anomalies and the possibilities of continental drift in the Gulf of Mexico: J. Geophys. Res., v. 76, no. 11, pp. 2639-2642.

APPENDIX 1

Information supplied with the Department of Defense Gravity Data.

FILE DESCRIPTION FORM

1. FILE NAME (EXTERNAL LABEL NAME)

SELECTFILE13

2. LOGICAL TAPE UNIT

13

3. NUMBER OF REELS

2

4. FORMAT

A. DENSITY (CHECK ONE)

 800 556 200

B. TAPE MODE (CHECK ONE AND FILL IN INFORMATION)

 BINRECORD¹ CONTAINS 23 (NO.) WORDSBLOCK² CONTAINS 230 (NO.) WORDS

STANDARD BUFFER SIZE ALTERED

 YES NO

IF YES SPECIFY SIZE

 BCD

RECORD CONTAINS _____ (NO.) CHARACTERS

BLOCK CONTAINS _____ (NO.) CHARACTERS

C. FILE CONTENT PER RECORD (DESCRIBE, INCLUDING FORMATS OR PICTURES)

All words are integer except words 17 and 23, which are alpha (field data). (See attachment for record description).

D. APPROXIMATE NUMBER OF RECORDS ON FILE

#1 - U3245 - 9840

#2 - U3478 - 58,852

5. FILE ARRANGEMENT (CHECK ONE)

 UNSORTED SORTED (DESCRIBE)

Increasing latitude within each degree of increasing longitude.

6. TERMINATING DEVICE (CHECK ALL APPLICABLE BOXES)

SINGLE REEL

 EOF PADDING (DESCRIBE) OTHER (DESCRIBE)

The last block of data on the reel is filled with words containing six alpha nines.

MULTI-REEL

 EOF PADDING (DESCRIBE) OTHER (DESCRIBE)LEGEND: ¹NUMBER OF UNIQUE ITEMS IN I/O STATEMENT, E.G., ϕ , λ , H (3 WD S.P., 6 WD D. P.)²INFORMATION READ/Written BY ONE I/O STATEMENT

CONTENTS OF A LOGICAL RECORD

Word 1	Security control
Word 2	Security classification
Word 3	Not used
Word 4	Type of elevation
Word 5	Reference base station
Word 6	Source
Word 7	\pm Degrees of latitude
Word 8	Minutes of latitude in hundredths of a minute
Word 9	\pm Degrees of longitude
Word 10	Minutes of longitude in hundredths of a minute
Word 11	Secondary elevation in tenths of a meter
Word 12	\pm Elevation in tenths of a meter
Word 13	Observed gravity in hundredths of a milligal minus 976,000 milligals
Word 14	\pm Free Air anomaly in tenths of a milligal
Word 15	\pm Bouguer anomaly in tenths of a milligal
Word 16	Terrain correction or Isostatic anomaly code
Word 17	Sequence number (A4)
Word 18	Logical counter
Word 19	Sigma Indicator
Word 20	Sigma of Free Air anomaly
Word 21	Sigma of Bouguer Anomaly
Word 22	Reformat Code
Word 23	Reference base station value (A1)

EXPLANATION
of
TAB LIST HEADING

Security Control. Coded as follows:

Blank = Not applicable

- 1 = Limited Dissemination, to full-time employees of Department of Defense, Central Intelligence Agency and Atomic Energy Commission
- 2 = Not releasable to Foreign Nationals
- 3 = Limited Dissemination, not releasable to Foreign Nationals
- 4 = Special Release from originating agency required for dissemination to any third party
- 5 = Modified Handling authorized (includes Foreign "Restricted", NATO, CENTO, SEATO, Etc.)

Security Classification. Coded as follows:

- U = Unclassified material
- F = Material classified FOR OFFICIAL USE ONLY
- C = Material classified CONFIDENTIAL
- S = Material classified SECRET

Reference Base Station:

DoD Gravity Services Branch code number which will represent a general area in which a base station is located. The last digit contains the DoD Gravity Services Code number which will represent a definite site of the base station.

Source of Information:

A code number is provided for each publication from which gravity information has been taken.

Latitude: Degrees, minutes and .01 minute.

Longitude: Degrees, minutes and .01 minute.

Supplemental Elevation:

Depth of instrument, lake or ice; positive downward from surface given to one tenth of a meter.

Type of Elevation. Coded as follows:

- 1 = Land
- 2 = Subsurface
- 3 = Ocean surface
- 4 = Ocean submerged
- 5 = Ocean bottom
- 6 = Lake surface (above sea level)
- 7 = Lake bottom (above sea level)

- 8 = Lake bottom (below sea level)
- 9 = Lake surface (above sea level) with lake bottom below sea level.
- A = Lake surface (below sea level)
- B = Lake bottom (surface below sea level)
- C = Ice Cap (bottom below sea level)
- D = Ice Cap (bottom above sea level)
- E = Transfer Data Given

Elevation of the Station:

The elevation is given to one tenth of a meter.

Observed Gravity:

The observed gravity in milligals to one hundredth milligal minus 976,000 milligals.

Free-Air Anomaly: In milligals to one tenth milligals.

EST. STD: This value is an estimation of the Standard Deviation of the Free-Air Anomaly.

Simple Bouguer Anomaly: In milligals to one tenth milligal. A mean density of 2.67 is used.

EST. STD: This value is an estimation of the Standard Deviation of the Bouguer Anomaly.

Isostatic anomaly or terrain correction given in document. Coded as follows:

- 0 = No isostatic anomaly or terrain correction given in document.
- 1 = Terrain correction given in document.
- 2 = Isostatic anomaly given in document.
- 3 = Both are given in document.

Sequence Number: Gravity station number, sequence of gravity station in source document/or page on which station is listed.

EDGFB is a logical counter for internal use only.

GRAVITY STATION DATA

CARD FORMAT

1 May 1968

DoD Gravity Services Branch

Explanation of DoD Gravity Services Gravity Station Data Card Format Effective 1 July 1968

- I Definitions and Notation
- II Formulas used in Computing Free-Air and Bouguer Anomalies
- III Punch Card Format for Gravity Station Data
 - Contains a complete listing of the data fields as punched in the Gravity Station Data machine card and a definition of all codes for each data field.
- IV Gravity Coding Sheet
 - A graphic representation of the Gravity Station Data machine card showing the position of the data fields and also a listing of the codes for each data field (same as the Punch Card Format listing in III above). This sheet is used to code gravity source documents for keypunching.
- V Gravity Station Data Machine Card
 - Special printed format card used for each gravity station in filling requests for punch card data. Gravity data is punched in this card as shown in the Punch Card Format for Gravity Station Data (III above) and the punched fields are interpreted in the appropriate named blocks at the top of the card.

I. DEFINITIONS

1. Observed (or measured) Gravity (g) is the value of gravity at the site of the gravity instrument referenced to a recoverable base reference station.

2. Theoretical Gravity. The International Gravity Formula is used for theoretical gravity (γ) at sea level:

$$\gamma = 978049.00 (1 + 0.0052884 \sin^2\phi - 0.0000059 \sin^2 2\phi) \text{ mgals.}$$

3. Units of Gravity. The mgal is the unit for our gravity data.

4. Free-Air Anomaly. For many practical purposes, to reduce gravity to sea-level, we use the normal gradient of gravity or "free-air" correction: $+0.3086h$ mgal; h is in meters and positive down to the geoid. The second order terms of the elevation correction will be applied when they are of the magnitude of 0.1 mgal or more. The free-air anomaly is derived from $\Delta g_f (\text{mgal}) = g + 0.3086h - \gamma$

5. Simple Bouguer Anomaly. The simple Bouguer Anomaly is derived from $\Delta g_B (\text{mgal}) = g + 0.3086h - 0.1119h - \gamma$

The term $0.1119h$ is obtained from the attraction of a flat and horizontal plate of infinite radius, thickness h and with standard density $\rho = 2.67 \text{ cm}^3$.

6. Standard Deviation (Error) connotes that there is a 68% probability that the free-air or Bouguer anomalies will fall between the indicated \pm and $-$ value: e.g., if the free-air anomaly is 10 mgal with a ± 2 mgal error or standard deviation, then there is a 68% probability that the value lies between 8 and 12 mgals.

7. The computations of free-air and Bouguer Anomalies with various modes of n observation types of terrain are given in the Anomaly Computation Chart.

II. Formulas Used in Computing Free-Air and Bouguer Anomalies

1. Symbology

<u>Symbol</u>	<u>Definition</u>	<u>Units</u>
Δg_f	Free Air Anomaly	milligals
Δg_B	Bouguer Anomaly	milligals
ϕ	Latitude of Observation	degrees, minutes
γ	Theoretical Gravity	milligals
g	Observed Gravity	milligals
h	Elevation (Col 23-29) of surface of land, ice or water; depth of ocean (positive downward) elevation types 3, 4, and 5. + = above SL; - = below SL.	meters
d	Supplemental Elevation (Col 31-35) = Depth of Ocean, lake, ice or instrument (positive downward)	meters

2. Theoretical Gravity Computation

Using the International Gravity Formula:

$$\gamma = C_1 (1 + C_2 \sin^2 \phi - C_3 \sin^2 2\phi)$$

where: $C_1 = 978049$ mgals

$$C_2 = 0.0052884$$

$$C_3 = 0.0000059$$

3. Anomaly Computations

See following pages

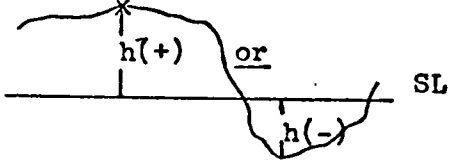
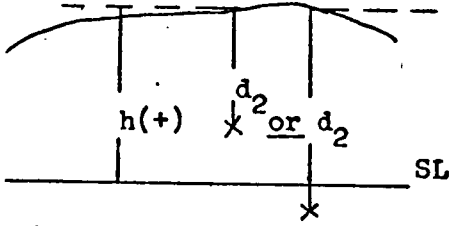
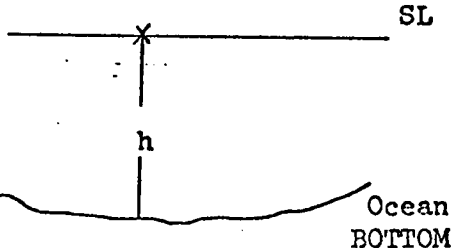
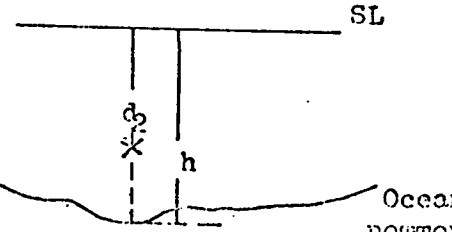
b = Bouguer Correction Factor

$$= 2\pi k\rho = 0.04191\rho$$

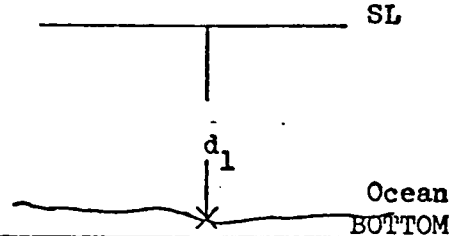
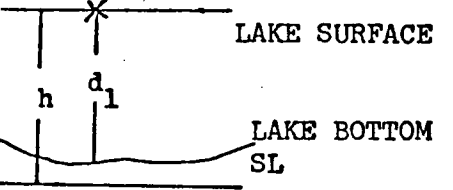
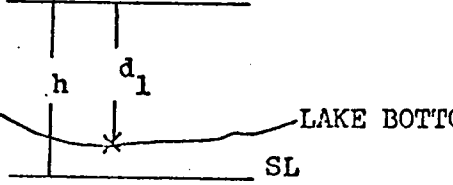
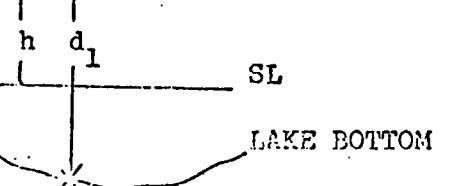
ρ = Density Used in Computations

Substance	ρ	$b = 2\pi k\rho$
Fresh Water	1.0	0.04191
Salt Water	1.027	0.04304
Ice	0.917	0.03843
Land	2.67	0.1119
Land-Fresh Water	1.67	0.06999
Land-Salt Water	1.643	0.06886
Land and Ice	1.753	0.07347

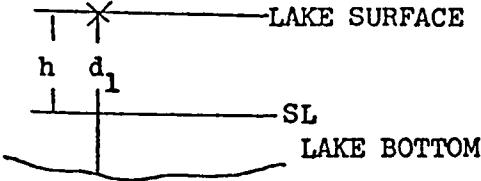
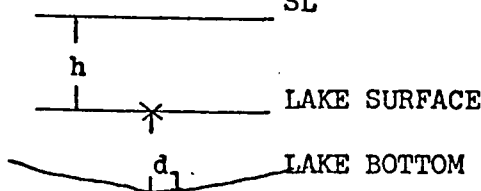
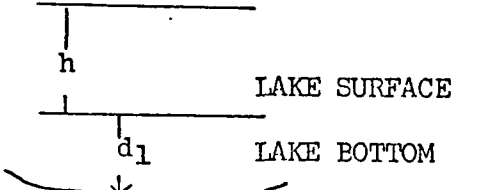
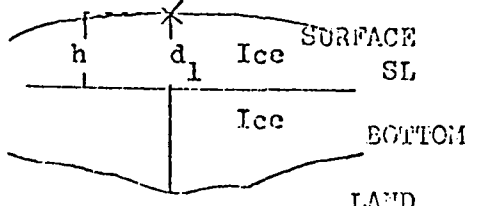
ANOMALY COMPUTATION CHART (p. 1)

Elev. Type Col. 21	SITUATION	FREE-AIR ANOMALY COMPUTATION	BOUGUER ANOMALY COMPUTATION
1	<p>LAND OBSERVATION</p> 	$\Delta g_f = g + 0.3086h - \gamma$	$\Delta g_B = \Delta g_f - 0.1119h$
2	<p>SUBSURFACE</p> 	$\Delta g_f = g + 0.2238d_2 + 0.3086(h-d_2) - \gamma$ <p>NOTE: d_2 = depth of instrument</p>	$\Delta g_B = \Delta g_f - 0.1119h$
3	<p>OCEAN SURFACE</p> 	$\Delta g_f = g - \gamma$	$\Delta g_B = \Delta g_f + 0.06886h$ <p>NOTE: h = depth of ocean positive downward from surface</p>
4	<p>OCEAN SUBMERGED</p> 	$\Delta g_f = g - 0.2225d_2 - \gamma$ <p>NOTE: d_2 = depth of instrument positive downward</p>	$\Delta g_B = \Delta g_f + 0.06886h$ <p>NOTE: h = depth of ocean positive downward</p>

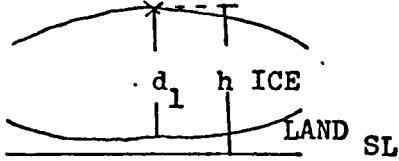
ANOMALY COMPUTATION CHART (p. 2)

Elev. Type Col. 21	SITUATION	FREE-AIR ANOMALY COMPUTATION	BOUGUER ANOMALY COMPUTATION
5	<p>OCEAN BOTTOM</p> 	$\Delta g_f = g - 0.2225d_1 - \gamma$ <p>NOTE: d_1 = depth of ocean positive downward</p>	$\Delta g_B = \Delta g_f + 0.06886d_1$
6	<p>LAKE SURFACE (above sea level)</p> 	$\Delta g_f = g + 0.3086h - \gamma$	$\Delta g_B = \Delta g_f - 0.04191d_1 - 0.1119(h-d_1)$ <p>NOTE: d_1 = depth of lake positive downward</p>
7	<p>LAKE BOTTOM (above sea level)</p> 	$\Delta g_f = g + 0.08382d_1 + 0.3086(h-d_1) - \gamma$	$\Delta g_B = \Delta g_f - 0.04191d_1 - 0.1119(h-d_1)$
8	<p>LAKE BOTTOM (below sea level)</p> 	$\Delta g_f = g + 0.08382d_1 + 0.3086(h-d_1) - \gamma$	$\Delta g_B = \Delta g_f - 0.04191h - 0.06999(h-d_1)$

ANOMALY COMPUTATION CHART (p. 3)

Elev. Type Col. 21	SITUATION	FREE-AIR ANOMALY COMPUTATION	BOUGUER ANOMALY COMPUTATION
9	<p>LAKE SURFACE (above sea level) with bottom below sea level</p> 	$\Delta g_f = g + 0.3086h - \gamma$	$\Delta g_B = \Delta g_f - 0.04191h - 0.06999(h-d_1)$
A	<p>LAKE SURFACE (below sea level)</p> 	$\Delta g_f = g + 0.3086h - \gamma$	$\Delta g_B = \Delta g_f - 0.1119h + 0.06999d_1$ <p>NOTE: d_1 = depth of lake positive downward</p>
B	<p>LAKE BOTTOM (surface below sea level)</p> 	$\Delta g_f = g + 0.3086h - 0.2248d_1 - \gamma$ <p>NOTE: d_1 = depth of lake positive downward</p>	$\Delta g_B = \Delta g_f - 0.1119h + 0.06999d_1$
C	<p>ICE CAP (bottom below sea level)</p> 	$\Delta g_f = g + 0.3086h - \gamma$	$\Delta g_B = \Delta g_f - 0.03843h - 0.07347(h-d_1)$ <p>NOTE: d_1 = depth of ice positive downward</p>

ANOMALY COMPUTATION CHART (p. 4)

Elev. Type Col. 21	SITUATION	FREE-AIR ANOMALY COMPUTATION	BOUGUER ANOMALY COMPUTATION
D	<p>ICE CAP (bottom above sea level)</p> 	$\Delta g_f = g + 0.3086h - \gamma$	$\Delta g_B = \Delta g_f - 0.03843d_1 - 0.1119(h-d_1)$ <p>NOTE: d_1 = depth of ice</p>

SOURCE LISTING
GULF COAST CONTINENTAL SHELF

- 238 VENING MEINESZ, F. A. & WRIGHT, F. E.
The Gravity Measuring Cruise of the US Submarine S-21
Publ of the US Naval Observatory, Sec Series, Vol XIII, App 1,
Washington, 1930
- 2927 NAVOCEANO
Project C-19, SS Sarda SS 488 New London, Conn - New Orleans, La
21 May - 29 May
- 2928 NAVOCEANO
Project C-19, USS Sarda SS 488 New Orleans, La, Port Everglades,
Fla, 3-11 June 1967
Navoceano
- 3078 NAVOCEANO
Gravity Data, USNS KEATHLEY, 22 Sep 68 - 9 Oct 68
Navoceano
- 3081 NAVOCEANO
Gravity Data, USNS KEATHLEY, 15 Aug 68 - 27 Aug 68
Navoceano
- 3082 NAVOCEANO
Gravity Data, USNS KEATHLEY, 23 Jul 68 - 9 Aug 68
Navoceano
- 3083 NAVOCEANO
Gravity Data (Evaluated), USNS KEATHLEY, 15 - 22 Jul 68
Navoceano
- 3084 NAVOCEANO
Gravity Data, USNS KEATHLEY, 15 Apr 68 - 10 May 68
Navoceano
- 3085 NAVOCEANO
Gravity Data, USNS KEATHLEY, 15 Jun 68 - 10 Jul 68
Navoceano
- 3088 NAVOCEANO
Gravity Data, USNS KEATHLEY, 21 May 68 - 10 Jun 68
Navoceano
- 3112 NAVOCEANO
Gravity Data for USNS KEATHLEY, Cruise No 3-69, Oct - Nov 68
Navoceano
- 3129 NAVOCEANO
Gravity Data in the Atlantic, USNS KEATHLEY, 18 Nov - 11 Dec 1968
Navoceano

- 3244 NAVOCEANO
Gravity Data in the Atlantic, USNS KEATHLEY, 18 Mar - 8 Apr 69.
Navoceano
- 3337 NAVOCEANO
Gravity Data, Gulf of Mexico, USNS KEATHLEY, 4 Jan - 24 Jan 70
Navoceano
- 3338 NAVOCEANO
USNS KEATHLEY Gravity Data, West Indies, 31 Jan - 10 Feb 1970
Navoceano
- 3339 NAVOCEANO
USNS KEATHLEY Gravity Data, Gulf of Mexico, 12 - 28 Feb 1970
Navoceano
- 3438 NAVOCEANO
USNS KEATHLEY Gravity Data, Gulf of Mexico, 18 Apr - 13 May 70
Navoceano
- 3439 NAVOCEANO
USNS KEATHLEY Gravity Data, Gulf of Mexico, 17 May - 12 Jun 70
Navoceano
- 3440 NAVOCEANO
USNS KEATHLEY Gravity Data, Gulf of Mexico, 11 Jan - 24 Jan 70

APPENDIX 2

DESCRIPTION OF COMPUTER PROGRAMS

Introduction

This appendix in addition to describing the computer programs used in this thesis also has examples of input data lists and output for the various user programs plus lists of control statements used to store and retrieve all the data and all programs, used by the author, and stored on a 9-track magnetic tape reel, #U362, which may be obtained from the Geology Department Office, University of Houston.

All programs are written in FORTRAN IV as accepted by the UNIVAC 1108 EXEC.8 time share system located at the University of Houston Computing Center. In the following description it is assumed that the user has a working knowledge of FORTRAN and is also familiar with the general structure of the UNIVAC 1108 file manipulation procedures and EXEC.8 control statements as explained in the Programmers Reference Manual (PRM) available at the Computing Center.

Explanation of File Terminology

It will be noted that liberal use is made of Programfiles, Datafiles, and Elementfiles. These are important concepts which require a brief explanation if one is to use an interactive system (i.e. Teletype ASR 33) for efficient data manipulation and program execution.

Any Programfile, Datafile, or Elementfile is simply any collection of images which may be stored on various mass-storage devices such as drum, disc, or magnetic tape.

A Programfile is broken down into elements (i.e. a main program with three subroutines could be listed as FILE3.MAIN, FILE3.SUB1, FILE3.SUB2,

and FILE3.SUB3). Note the use of the "." as a separator between the file name and the individual element names. The program elements exist in storage as Symbolic elements (FORTRAN source images), Relocatable elements (binary output of the FORTRAN compiler), or Absolute elements (the final collection of all Relocatable elements necessary for execution of a main program and its subroutines). Only Absolute elements may be executed or run.

A Datafile is any collection of images to be used as input or output by various Programfiles. Examples of Datafiles are GRAVITYDATA., HOUSE., or FILE13. Note that there are no elements of a Datafile.

An Elementfile is usually a collection of Executive control statements recognized by the master space "@" in column one of input is by teletype or by a " (7-8 punch) if input is by card image. Elementfiles are used in this thesis to add long lists of Executive control statements to the run stream. An example of an Elementfile is TAPEWRITE.MAIN, note the use of file name and element name and the use of the separator.

Input to Programfiles, Datafiles, or Elementfiles can be made through card images, magnetic tape, drum, disc, or by interactive devices (ASR33).

List of all Programfiles, Datafiles, and Elementfiles

The Programfiles and their elements used are:

- (1) DATACOUNTER.MAIN
- (2) DATALISTER.MAIN
- (3) DATAPROCESOR.MAIN
 DATAPROCESOR.GRAPH
 DATAPROCESOR.SORT
 DATAPROCESOR.TAPERD
 DATAPROCESOR.PUNWR
 DATAPROCESOR.RANGE
 DATAPROCESOR.ABSOLUTE

- (4) PROFILEPLOT.MAIN
PROFILEPLOT.READM
PROFILEPLOT.ABSOLUTE
- (5) MAPPLOT.MAIN
MAPPLOT.READM
MAPPLOT.ABSOLUTE
- (6) GRAVITYMODEL. COSINE
- (7) APPENDIX.MAIN
APPENDIX.READM
APPENDIX.OPERATION

The Datafiles used are:

- (1) ASHALEDIAPIR.
- (2) 3PARTLUMP.
- (3) REVISEDMODEL.
- (4) FISHBB.
- (5) FILEH1.
- (6) FILEH2.
- ⋮
- (26) FILEH22.
- (27) FILED1.
- ⋮
- (31) FILED5.

The Elementfiles and elements used are:

- (1) DATALISTFILE.ELEMENTS
- (2) TAPEWRITE.MAIN
- (3) FILERESTORE.MAIN

The Programfiles and Elementfiles PROFILEPLOT., MAPPLOT., APPENDIX., and DATALISTFILE. all reference Datafiles FILEH1. through FILED5. inclusive.

The Programfile GRAVITYMODEL. references Datafiles ASHALEDIAPIR., 3PARTLUMP., FINALMODEL., and FISHBB. The Elementfiles reference all

Programfiles and Datafiles.

It is suggested that the Documentation of Elementfile FILERESTORE.
MAIN be consulted before any use is made of the previously mentioned files.

Explanation of Documentation

The documentation of all Programfiles, Datafiles, and Elementfiles should allow the user to implement them directly on the UNIVAC 1108 EXEC.8 system. All Symbolic, Relocatable, and Absolute elements of the Programfiles are available on tape reel #U362. Consequently once these files have been restored to the system there will be no need to recompile the Program elements. It is assumed that the user will keep all files on permanent storage.

Unless otherwise noted all sample runs are in the batch mode (cards). Use of the @BRKPT and @BATCH statements can alter users time (i.e. faster turnaround time).

Listings of Files

All Programfiles and Elementfiles are listed directly after their respective documentation. The only Datafiles listed are REVISEDMODEL. and 3PARTLUMP.; both listings of the parameters for the gravity models shown in Figures 10 and 18 respectively.

DATACOUNTER

Purpose

This program allows the user to determine the density of gravity stations within ten minute squares of latitude and longitude of all data supplied by the DOD (Appendix L) on tape reels U3245 and U3478.

Input

NBLOKS(I4) - Number of blocks of data to be read from input tape (Appendix 1). There are ten records per block. Each record represents one gravity measurement and contains 23 words. NBLOKS cannot exceed 5,885 for U3478 or 984 for U3245.

Output

Each square degree is broken into 36 ten minute areas and a matrix is printed with densities within each ten minute block.

Special Instructions

The tape reel must be linked to the run by @ASG and @USE statements.

Sample Run

```
@RUN,A MIKE,3061GRAV,3061GRAV,2,1000
@ASG,T TAPE.,8C9,U3478
@USE2.,TAPE.
@ASG,AX TAPESEARCH.
@XQT TAPESEARCH.ABS
5885
@FIN
```

Explanation

This run will list the number of data points in ten minute areas for each degree of latitude and longitude within 26° - 36° N and 81° - 98° W inclusive, for tape reel U3478.

```

SOR LEVEL      4
000 C
000 C          DATACOUNTER   WRITTEN BY MIKE BURNAMAN SPRING,1973
000 C
000 C          THIS PROGRAM IS DESIGNED TO DETERMINE THE DENSITY OF GRAVITY
000 C          STATIONS IN 10 MINUTE BLOCKS
000 C          FOR EXCLUSIVE USE ON TAPE REEL U362   AS REFERENCED   00000400
000 C          IN THE AUTHORS THESIS
000 C
000 C          IMPLICIT INTEGER(A-Z)
000 C          DIMENSION R(230),B(18,20,6,6),SUMLAT(18,20,6),SUMLON(18,20,6),X(20
000 C          1),Y(20),Z(20)
000 C
000 C          NBLOCKS IS THE NUMBER OF BLOCKS OF DATA TO BE READ
000 C
000 C          READ(5,102)NBLOCKS
000 102      FORMAT(I4)
000 C          DO 10 M1=1,18
000 C          DO 10 M2=1,20
000 C
000 C          DO 10 N1 = 1,6
000 C          DO 10 N2 = 1,6
000 10      B(M1,M2,N1,N2) = 0
000 C          DO 20 L=1,NBLOCKS
000 C          UNIT 2 IS A TAPE DRIVE TO WHICH THE TAPE REEL HAS BEEN PREVIOUSLY
000 C          LINKED BY A SYSTEM ASC STATEMENT AND A SYSTEM USE STATEMENT
000 C          R IS A SINGLE BLOCK OF DATA
000 C
000 C          READ(2)R
000 C          DO 28 N=1,10
000 C
000 C          I1,I2,J1,J2 ARE WORDS OF EACH INDIVIDUAL LOGICAL RECORD
000 C          THERE ARE 23 WORDS IN EACH LOGICAL RECORD
000 C          THERE ARE 10 LOGICAL RECORDS IN ONE BLOCK OF DATA
000 C          I1 = DEGREES LATITUDE
000 C          I2 = MINUTES LATITUDE
000 C          J1 = DEGREES LONGITUDE
000 C          J2 = MINUTES LONGITUDE
000 C
000 C          I1 = ((N-1)*23)+7
000 C          I2 = ((N-1)*23)+8
000 C          J1 = ((N-1)*23)+9
000 C          J2 = ((N-1)*23)+10
000 C          DO 21 M1 = 1,18
000 C          LAT = 17+ M1
000 C          IF(R(I1)-LAT)21,100,21
000 100      DO 22 M2 = 1,20
000 C          LONG = 80 + M2
000 C          IF(R(J1)+LONG)22,200,22
000 200      DO 23 N1 = 1,6
000 C          ZAP = ( 8000 - ( 1000 * N1 ) )
000 C          IF(R(I2)-ZAP)23,300,300
000 300      DO 24 N2 = 1,6
000 C          ZIF = ( 8000 - ( 1000 * N2 ) )
000 C          IF(R(J2)-ZIF)24,400,400
000 400      B(M1,M2,N1,N2) = B(M1,M2,N1,N2) + 1
000 C          GO TO 23
000 24      CONTINUE
000 23      CONTINUE
000 22      CONTINUE
000 21      CONTINUE

```

```

000 28 CONTINUE
000 30 CONTINUE
000 C
000 C SUNLAT AND SUMLON ARE HORIZONTAL AND VERTICAL SUMS OF THE
000 C INDIVIDUAL 10 MINUTE AREAS IN ONE DEGREE
000 C IN THIS CONFIGURATION SUMLAT AND SUMLON ARE NOT PRINTED
000 C
000 DO 30 M1 = 1,13
000 DO 30 M2 = 1,20
000 DO 30 N1 = 1,3
000 30 SUMLAT(M1,M2,N1) = 0
000 DO 40 M1 = 1,13
000 DO 40 M2 = 1,20
000 DO 40 N2 = 1,3
000 40 SUMLON(M1,M2,N2) = 0
000 DO 50 M1 = 1,13
000 DO 50 M2 = 1,20
000 DO 50 N1 = 1,3
000 DO 50 N2 = 1,3
000 50 SUMLAT(M1,M2,N1) = SUMLAT(M1,M2,N1) + 2(M1,M2,N1,N2)
000 DO 54 M1 = 1,13
000 DO 54 M2 = 1,20
000 DO 52 N2 = 1,3
000 DO 52 N1 = 1,3
000 62 SUMLON(M1,M2,N2) = SUMLON(M1,M2,N2) + 8(M1,M2,N1,N2)
000 54 CONTINUE
000 DO 51 M2 = 1,20
000 51 X(M2) = 30 + M2
000 DO 52 N1 = 1,18
000 52 Y(N1) = 17 + N1
000 DO 53 M = 1,7
000 53 Z(M) = (M*10) - 10
000 C
000 C SUMS ARE OUTPUT IN THE FOLLOWING STATEMENTS
000 C
000 DO 61 M2 = 20,1
000 DO 61 M1 = 18,1
000 COUNT = 3
000 DO 65 M1 = 1,6
000 95 COUNT = SUMLAT(M1,M2,N1) + COUNT
000 C
000 C THIS IF CHECKS TO SEE IF THERE ARE ANY STATIONS IN THE DEGREE
000 C
000 IF(COUNT)61,61,500
000 500 WRITE(6,254)
000 254 FORMAT(1H1,15X,' GRAVITY STATION DENSITY GULF OF MEXICO'
000 1,' CONTINENTAL SHELF AND LAND DATA DOB')
000 WRITE(6,1001)Y(M1),Z(7),X(M2+1),Z(1),X(M2),Z(6),X(M2),
000 12(5),X(M2),Z(4),X(M2),Z(3),X(M2),Z(2),X(M2),Z(1),Y(M1),
000 1Z(7)
000 1001 FORMAT(///,I2,I3,'*',I5,I3,'*',6(3('-'),I2,I3,'*'),I7,I3,
000 1'****')
000 DO 75 M=1,4
000 75 WRITE(6,2001)
000 2001 FORMAT(1H ,11X,'*',5(13X,'*'),13X,'*')
000 WRITE (6,2002)(3(M1,M2,1,N2),N2 = 1,6)
000 2002 FORMAT(1H ,11X,'*',I8,5X,5('!',I8,5X),'*')
000 DO 76 N1 = 2,5
000 DO 77 M = 1,3
000 77 WRITE(6,2003)
000 2003 FORMAT(1H ,11X,'*',5(13X,'*'),13X,'*')
000 WRITE(6,2004)Y(M1),Z(3-N1),Y(M1),Z(3-N1)

```

```

12. LISTING FOR DATA CONVERTER
000      2004 FORMAT(1H ,I2,I3,'',5X,'+',C(13('-',),'+'), I7,I3,'')
000      DO 73 M = 1,4
000      73 WRITE(6,2005)
000      2005 FORMAT(1H ,11X,'',5(13X,''),13X,'')
000      WRITE (6,2006)(P(M1,M2,N1,M2),M2 = 1,6)
000      2006 FORMAT(1H ,11X,'',I3,5X,5('',I3,5X),'')
000      76 CONTINUE
000      DO 79 M = 1,3
000      79 WRITE(6,2007)
000      2007 FORMAT(1H ,11X,'',5(13X,''),13X,'')
000      WRITE(6,2008)Y(M1),Z(1),X(M2+1),Z(1),X(M2),Z(6),X(M2),
000      1Z(3),X(M2),Z(4),X(M2),Z(3),X(M2),Z(2),X(M2),Z(1),Y(M1),
000      1Z(1)
000      2008 FORMAT(1H ,I2,I3,'',I5,I3,'',6(3('-',),I2,I3,''),I7,I3,
000      1'')
000      81 CONTINUE
000      STOP
000      END

```

DATALISTER

Purpose

This program allows the user to obtain an unsorted general listing of all data contained on magnetic tapes U3245 and U3478 supplied by the DOD (Appendix 1).

Input

Line 1: NBLOKS(I4) - Number of blocks of data to be read from input tape (Appendix 1). This number cannot exceed 5,885 for reel U3478 or 984 for reel U3245.

Line 2: NUMB(I2) - Number of lat. - long. areas to list.

Line 3 to Line NUMB + 2: G1,G2(2I3) - Degrees of latitude and longitude for one area. Longitude is negative.

Output

The output consists of all data listed in "contents of a logical record" in Appendix 1.

Special Instructions

The input tape must be linked to the run by @ASG and @USE statements.

Sample Run

```
@RUN,A MIKE,3061GRAV,3061GRAV,2,2000
@ASG,T TAPE.,8C9,U3478
@ASG,AX DATALISTER.
@USE 2.,TAPE.
@XQT DATALISTER.ABS
5885
  2
028-96
028-97
```

Explanation

All the Marine gravity stations within 28° N lat., 96° W long. and 28° N lat., 97° W long. available through the DOD will be listed.

```

SOR LEVEL      4
000           DIMENSION R(230),G1(20),G2(20)
000           READ 57,NBLOCKS
000    57      FORMAT(I4)
000           IMPLICIT INTEGER (A-Z)
000           READ(5,101)NUM3
000           DO 19 MM=1,NUM3
000    19      READ(5,19)G1(MM),G2(MM)
000           DO 29 MM=1,NUM3
000           COUNT=C
000           COUNT2=1
000           WRITE(C,23)
000           DO 30 L=1,NBLOCKS
000           READ(2)R
000           DO 30 N=1,11
000           I=((N-1)*23)+1
000           J=I+22
000           L3=I+3
000           J1=((N-1)*23)+7
000           J2=((N-1)*23)+9
000           IF(R(J1).EQ.G1(MM))GO TO 1
000           GO TO 30
000    1       IF(R(J2).EQ.G2(MM))GO TO 215
000           GO TO 30
000    215     COUNT=COUNT+1
000           IF (COUNT.EQ.51)GO TO 25
000           GO TO 42
000    25      WRITE(6,205)COUNT2
000           COUNT2=COUNTC+1
000           WRITE(C,23)
000           WRITE(C,200)(R(K),K=L3,J)
000           COUNT=1
000           GO TO 30
000    42      WRITE(6,200)(R(K),K=L3,J)
000    30      CONTINUE
000           REWIND 2
000    39      CONTINUE
000    101     FORMAT(I2)
000    10      FORMAT(2I3)
000    20      FORMAT(1H1,2X,'ELTYPE REFBS SOURCE  LATITUDE  LONGITUDE  SONDEL  EL
000           LEVTN  CBGRAV FRARAY BCGAY TERCCR SEQNUM COUNT SIGMA SIGFAA SIGBAY
000    1  RC REFBSV')
000    200     FORMAT(1H ,I5,I9,I6,I5,I5,I6,I5,I8,I8,
000           1I8,I7,I7,I5,5X,A4,I5,I4,I6,I7,I5,4X,A1)
000    205     FORMAT(1H ,CCX,'PAGE  ',I3)
000           STOP
000           END
    
```

DATAPROCESOR

Purpose

This program along with tape reel U3478 allows the user to:

- (1) Select specific areas of interest within a grid of latitude and longitude coordinates.
- (2) Sort the data within these specific areas into their original sequential order.
- (3) Punch sorted data onto cards.
- (4) Graph the data a free-air anomaly vs. distance.

Input

Line 1: NI(I1) - This value is zero if no cards are to be punched, 1 - 9 otherwise.

NY(I1) - This value is zero if no graph of anomaly vs. distance is to be produced, 1 - 9 otherwise.

NSETS(I2) - Number of areas to search for data.

NBLOKS(I5) - Number of blocks of data to read from tape
(5,885 for reel U3478)

Line 2: X1(F8.4) - Minimum latitude to search (repeated for each data set).

X2(F8.4) - Maximum latitude to search (repeated for each data set).

Y1(F8.4) - Minimum longitude to search, west = negative (repeated for each data set).

Y2(F8.4) - Maximum longitude to search, west = negative (repeated for each data set).

Z1(I4) - Cruise number obtained from Appendix 1 (repeated

for each data set).

Lines 3 and 4 to line (2 + NSETS X 2): U1,U2,U3 (3A4) - An arbitrary track number assigned to this data set (repeated for each data set).

Output

The output for each set of areas may consist of:

- (1) A printout of unsorted gravity stations with the latitude, longitude, free-air anomaly, and cruise number for each gravity station.
- (2) A printout of the sequenced gravity stations listing latitude, longitude, free-air anomaly, and cruise number.
- (3) A line graph of free-air anomaly vs. distance.
- (4) Cards punched with each stations latitude, longitude, free-air anomaly, cruise number, and an arbitrary track number.

Special Instructions

The tape reel must be linked to the run via @ASG and @USE control statements.

Sample Run

```
@RUN,A MIKE,3061GRAV,3061GRAV,5,1000/5000
@ASG,T TAPE.,8C9,U3478
@USE 2.,TAPE.
@ASG,AX DATAPROCESOR.
@XQT DATAPROCESOR.ABSOLUTE
 5885
7703
027.0000027.3500-97.5000-94.00003339
TRACK H6
TRACK H6
028.0000028.6000-96.8000-94.00003337
TRACK H8
TRACK H8
027.0000027.3500-97.5000-94.00003438
TRACK H9
TRACK H9
@FIN
```

Explanation

This run will use reel #U3478 and search for data within three areas. Output will be an unsequenced listing, a sequenced listing, a line graph, and punched cards for each of the three areas.

```

COR LEVEL      4
000  C
000  C
000  C      DATAPROCESSOR  WRITTEN BY MIKE PURNAMAN SUMMER,1973
000  C
000  C
000  C      DATAPROCESSOR CONSISTS OF A MAIN PROGRAM WHICH CALLS
000  C      VARIOUS SUBROUTINES USED TO LOCATE DATA AND ORDER THEM BACK INTO
000  C      THE TRACKS IN WHICH THEY WERE ORIGINALLY ACQUIRED
000  C
000  C      DAT IS THE DATA MATRIX USED BY THE MAIN AND SUBROUTINES
000  C      N = STATION NUMBER ASSIGNED DURING THE DATA SEARCH
000  C      DAT(N,1) = LATITUDE
000  C      DAT(N,2) = LONGITUDE
000  C      DAT(N,3) = FREE-AIR ANOMALY
000  C      DAT(N,4) = CRUISE NUMBER
000  C
000  C      DIMENSION DAT(2000,4)
000  C      COMMON X1,X2,Y1,Y2,NZ1,DAT
000  C
000  C      NI = 0 IF NO CARDS ARE TO BE PUNCHED , 1-9 OTHERWISE
000  C      NY = 0 IF NO GRAPH OF ANOMALY VS DISTANCE IS TO BE MADE
000  C      1-9 OTHERWISE
000  C      NSETS = NUMBER OF AREAS TO SEARCH
000  C      NBLOKS = NUMBER OF DATA BLOCKS ON TAPE REEL TO SEARCH
000  C
000  C      READ 13,NI,NY,NSETS,NBLOKS
000  C      DC 999 MCO = 1,NSETS
000  C
000  C      X1 = MINIMUM LATITUDE
000  C      X2 = MAXIMUM LATITUDE
000  C      Y1 = MINIMUM LONGITUDE  WEST = NEGATIVE
000  C      Y2 = MAXIMUM LONGITUDE  WEST = NEGATIVE
000  C      NZ1 = CRUISE NUMBER
000  C
000  C      READ (5,10)X1,X2,Y1,Y2,NZ1
000  C
000  C      M1 = NUMBER OF GRAVITY STATIONS IN AREA OF SEARCH RETURNED BY
000  C      SUBROUTINE TAPERD
000  C
000  C      CALL TAPERD (M1,DAT,NBLOKS)
000  C      PRINT 43,MCO,NZ1,X2,X1,Y1,Y2
000  C      CALL PUNWR(1,M1)
000  C      CALL SORT (M1)
000  C      IF(NI.EQ.0)GO TO 41
000  C      CALL PUNWR(3,M1)
000  C
000  C      XMIN = MINIMUM FREE-AIR ANOMALY ON THE TRACK
000  C      XMAX = MAXIMUM FREE-AIR ANOMALY ON THE TRACK
000  C      DX = RANGE OF FREE-AIR ANOMALY ON THE TRACK
000  C
000  C      41      XMIN = 0.0
000  C      XMAX = 0.0
000  C      DX = 0.0
000  C      NUM = 0.0
000  C      CALL RANGE(XMIN,XMAX,DX,NUM,M1)
000  C      PRINT 12,XMIN,XMAX,DX,NUM
000  C      IF (NY.EQ.0)GO TO 999
000  C      CALL GRAPH(XMIN,XMAX,DX,NUM,M1)
000  C      999 CONTINUE
000  C      10 FORMAT(4F3.4,I4)

```

```

CCC      11  FORMAT (1H1,/////,4F9.4,14)
CCC      12  FORMAT (1H1,/////,3F10.1,110)
CCC     13  FORMAT(2I1,I2,I5)
CCC     43  FORMAT(1H1,////, ' DATA SET NO  ',I4,/,
CCC        1'THE FOLLOWING DATA, TAKEN ON CRUISE',F9.0, ' OF THE U S N S  ',
CCC        2'KEITHLY, ARE LOCATED WITHIN THESE COORDINATES',/,/,
CCC        3' LATITUDE ',F9.4, ' N',/,/,
CCC        4' LATITUDE ',F9.4, ' N',/,/,
CCC        5' LONGITUDE ',F10.4, ' W',/,/,
CCC        6' LONGITUDE ',F10.4, ' W')
CCC        STOP
CCC        END

```

```

FOR LEVEL      4
000          SUBROUTINE GRAPH(XMIN,XMAX,DX,NUM,N)
000          COMMON DAT(2000,4)
000          DIMENSION ICUT(121),XX(25)
000          DATA II,ISTAR,IBLNK,IZERO/'I','*',' ','*'/
000          IF(NUM.GT.0)GO TO 401
000          XXX=XMIN
000          DO 101 I=1,25
000             XX(I)=XXX
000          101   XXX=XXX*DY/D4.
000          GO TO 75
000          401   XXX=XMIN
000          DO 201 I=1,25
000             XX(I)=XXX
000          201   XXX=XXX*2.5
000          75   WRITE(6,20004)
000             WRITE(6,20000)(XX(I),I=2,24,2)
000             WRITE(6,20001)(XX(I),I=1,25,2)
000             WRITE(6,20002)
000             DO 102 I=1,N
000             DO 103 J=1,121
000          103   ICUT(J)=IBLNK
000             DO 104 J=1,121,10
000          104   ICUT(J)=II
000             XXX=DAT(I,3)
000             IF(NUM.LT.0)GO TO 30
000             IF(XMIN)40,40,33
000          40   IF(XXX)30,33,33
000          30   IX=IFIX(XXX*2.)*(2*NUM)*1
000             IRO=(2*NUM)*1
000             ICUT(IRO)=IZERO
000             ICUT(IX)=ISTAR
000             GO TO 102
000          33   IX=IFIX(ABS(XXX-XMIN)*2.)*1
000             ICUT(IX)=ISTAR
000             GO TO 102
000          30   IX=IFIX((XXX-XMIN)*120./DX)*1
000             ICUT(IX)=ISTAR
000          100   WRITE(6,20003)DAT(I,3),ICUT,IX
000             WRITE(6,20002)
000             WRITE(6,20001)(XX(I),I=1,25,2)
000             WRITE(6,20000)(XX(I),I=2,24,2)
000             RETURN
000          2000  FORMAT(6X,F5.1,11F10.1)
000          2001  FORMAT(3X,F5.1,12F10.1)
000          2002  FORMAT(6X,'*',24('----*'))
000          2003  FORMAT(1X,F5.1,121A1,10)
000          2004  FORMAT(1H1)
000          END
    
```

DATAPROCESSOR.SORT .

```
SCR LEVEL      4
 000          SUBROUTINE SORT(N)
 000          COMMON DAT(2000,4)
 000          DIMENSION SAVE(2000,4)
 000          INTEGER START
 000          LIM=N-1
 000          DO 3 I=1,LIM
 000             START=I-1
 000             DO 3 J=START,N
 000                IF(DAT(I,2)-DAT(J,2))3,2,2
 000                   2 DO 21 M=1,4
 000                      SAVE(I,M)=DAT(I,M)
 000                   21 DO 20 M=1,4
 000                      DAT(I,M)=DAT(J,M)
 000                   20 DO 22 M=1,4
 000                      DAT(J,M)=SAVE(I,M)
 000                   22
 000             3 CONTINUE
 000             RETURN
 000          END
```

DATAPROCESSOR.TAPERD .

```

ISOR LEVEL      4
000      SUBROUTINE TAPERD (M1,DAT,NBLOKS)
000      COMMON X1,Y2,Y1,Y2,Z1
000      DIMENSION DAT(2000,4),R(230)
000      INTEGER R,Z1
000      M1=0
000      DO 22 L= 1,NBLOKS
000      READ(2)R
000      DO 22 N=1,10
000      C
000      C      I1 = LATITUDE DEGREES
000      C      I2 = LATITUDE MINUTES
000      C      I3 = LONGITUDE DEGREES
000      C      I4 = LONGITUDE MINUTES
000      C      I5 = FREE-AIR ANOMALY
000      C      I6 = CRUISE NUMBER
000      C
000      I1=((N-1)*23)-7
000      I2=((N-1)*23)-8
000      I3=((N-1)*23)-9
000      I4=((N-1)*23)-10
000      I5=((N-1)*23)-14
000      I6=((N-1)*23)-6
000      G1=FLOAT(R(I1))-((FLOAT(R(I2))*0.01)/60.)
000      G2=FLOAT(R(I3))-((FLOAT(R(I4))*0.01/60.)
000      G3=FLOAT(R(I5))*0.1
000      IF(C1.GT.X1.AND.C1.LT.X2.AND.C2.GT.Y1.AND.C2.LT.Y2.AND.R(I6).EQ.Z
000      11)GO TO 5
000      GO TO 22
000      5      M1=M1-1
000      DAT(M1,1)=G1
000      DAT(M1,2)=G2
000      DAT(M1,3)=G3
000      DAT(M1,4)=FLOAT(R(I6))
000      22 CONTINUE
000      REWIND 2
000      RETURN
000      END

```

DATAPROCESSOR.PUNWR .

```
SCR LEVEL      4
000             SUBROUTINE PUNWR (JA,L)
000             COMMON DAT(2000,4)
000             READ (5,50) U1,U2,U3
000             WRITE (6,20) U1,U2,U3
000             DO 10 M=1,L
000             WRITE(6,20)M,(DAT(M,J),J=1,4),U1,U2,U3
000             IF (JA.EQ.1) GO TO 10
000             WRITE(1,30)M,(DAT(M,J),J=1,4),U1,U2,U3
000             10 CONTINUE
000             RETURN
000             20 FORMAT(1H1,/,30X,3A4,/,2X,'SEQ.NUM.',5X,'LATITUDE',5X,'LONGITUD
000             1E',2X,'GRAVITY',3X,'CRUISE NO. ')
000             30 FORMAT(1H ,I13,2F12.4,F8.1,F12.0,10X,3A4)
000             30 FORMAT(I4,2F12.4,F8.1,F12.0,5X,3A4)
000             50 FORMAT(3A4)
000             END
```

DATAPROCESSOR.RANGE .

```
ISCR LEVEL      4
000      SUBROUTINE RANGE(XMIN,XMAX,DX,NUM,M1)
000      COMMON DAT(2000,4)
000      NUM=0
000      DX=1.0
000      XMAX=DAT(1,3)
000      XMIN=DAT(1,3)
000      DO 10 L=2,M1
000          IF(DAT(L,3).LT.XMIN)GO TO 20
000      08 IF(DAT(L,3).GT.XMAX)GO TO 40
000          GO TO 10
000      20 XMIN=DAT(L,3)
000          GO TO 03
000      40 XMAX=DAT(L,3)
000      10 CONTINUE
000          RANGE=ABS(XMAX)+ABS(XMIN)
000          IF(RANGE.GT.60.)GO TO 20
000          DO 30 N=-60,50
000      30 IF(XMIN.GT.FLOAT(N).AND.XMIN.LT.FLOAT(N+1))GO TO 50
000      50 XMIN=FLOAT(N)
000          NUM=3
000          IF(XMIN.LE.0.0)NUM=ABS(XMIN)
000          GO TO 75
000      20 DX=XMAX-XMIN
000          NUM=0
000      75 RETURN
000          END
```

PROFILEPLOT

Purpose

This program allows the user to construct a line plot of the free-air anomaly vs. real distance of the sequenced ship tracks with annotations. This is accomplished by use of an off-line Benson Lehner 48 inch flat bed plotter operated by the Electrical Engineering Department of the University of Houston. The software necessary to write the individual plot commands on tape is kept on permanent file at the University of Houston Computing Center and may be easily accessed by the user. Once the plot tapes are generated at the Computer Center they are retrieved and mounted on the plotter tape drive by the user. An instruction manual explaining the use of the available software for the plotter is available from the Electrical Engineering Department.

Input

The input data are:

KENR(I2) - The number of tracks to plot (should be less than seven due to space limitation on the tape).

Output

The output consists of:

- (1) Plotting instructions written on the plot tape.
- (2) A listing of cumulative distance from the first data point of the ship track for every data point on the track (in feet).

Special Instructions

The plot tape and the ship track Datafiles must be linked to the program by use of @ASG and @USE control statements. A temporary file must

be assigned to receive the printout.

Sample Run

BATCH

```
@RUN,A MIKE,3061GRAV,3061GRAV,2,100
@ASG,LITE 4.,8C,PLOTTAPE
@ASG,AX PROFILEPLOT.
@MSG,W PLEASE RING IN PLOTTAPE
@ASG,AX FILEH1
@ASG,AX FILEH2
@ASG,AX FILED3
@USE 21.,FILEH1.
@USE 22.,FILEH2.
@USE 23.,FILED3.
@ASG,T TEMPFIL.
@USE 16.,TEMPFIL.
@XQT PROFILEPLOT.ABSOLUTE
3
@DATA,L TEMPFIL.
@END
@FIN
```

DEMAND

```
@RUN MIKE,3061GRAV,3061GRAV,10,1000
@ASG,AX FILEH1.
@ASG,AX FILEH2.
@ASG,AX FILED3.
@USE 21.,FILEH1.
@USE 22.,FILEH2.
@USE 23.,FILED3.
@ASG,AX PROFILEPLOT.
@ASG,T TEMPFIL.
@USE 16.,TEMPFIL.
@ASG,LITE 4.,8C,PLOTTAPE
@MSG,W PLEASE RING IN PLOTTAPE
@XQT PROFILEPLOT.AGS
3
@FIN
```

Explanation

BATCH

Profiles H1, H2, and D3 are plotted and the cumulative distances are written into a temporary file (TEMPFIL) which is then listed.

DEMAND

Profiles H1, H2, and D3 are plotted and the cumulative distances are

written into a temporary file (TEMPFILE.). The temporary file may be listed at the terminal by the user or selectively read by using the EDIT processor (see PRM).

PROFILEPLOT.MAIN .

DDR LEVEL 4

```

000 C
000 C PROFILEPLOT WRITTEN BY MIKE BURNAMAN FALL,1973
000 C
000 C MAPPLOT PRODUCES AN ANNOTATED LINE PLOT OF FREE-AIR
000 C GRAVITY VS. DISTANCE
000 C
000 C THIS PROGRAM USES SOFTWARE DEVELOPED FOR USE ON THE BENSON-
000 C LEHNER PLOTTER LOCATED IN THE ELECTRICAL ENG. DEPT.
000 C OF THE U. OF H.
000 C
000 C THE PLOTTING SOFTWARE IS AVAILABLE FROM THE ELECTRICAL
000 C ENG. DEPT.
000 C
000 C DAT IS THE DATA MATRIX
000 C
000 C COMMON DAT(1300,3)
000 C
000 C A AND D ARE MATRICES USED IN COORDINATE CONVERSION
000 C
000 C DIMENSION A(1300,3),D(1300,2)
000 C DIMENSION A1(3),W(3)
000 C
000 C THE 400 SPECIFIES 400 INCREMENTS PER INCH FOR THE PLOTTER
000 C
000 C CALL PLOTS(400.,400.,4)
000 C
000 C KENR IS THE NUMBER OF PROFILES TO DRAW
000 C
000 C READ(5,806)KENR
000 C 806 FORMAT(I2)
000 C AMILE=6200.
000 C AKILO=AMILE*1.003344
000 C EARTH=3983.34*AMILE
000 C RAD=174532925E-10
000 C PIG2=3.1415927/2.
000 C DO 123 KIKK=1,KENR
000 C
000 C READM IS THE SUBROUTINE THAT READS IN THE DATA FILE
000 C
000 C CALL READM(M1)
000 C
000 C DO 10 M=1,M1
000 C
000 C M1 IS THE NUMBER OF GRAVITY STATIONS
000 C
000 C BLAT AND BLON ARE THE LAT AND LON CONVERTED TO RADIANS
000 C
000 C BLAT=DAT(M,1)*RAD
000 C
000 C BLON=ADD(DAT(M,2))*RAD
000 C
000 C STATEMENTS TO 23 CONTINUE CONVERT FROM SPHERICAL
000 C TO RECTANGULAR COORDINATES
000 C
000 C A(M,1)=EARTH*SIN(PIG2-BLAT)*COS(PIG2-BLON)
000 C A(M,2)=EARTH*SIN(PIG2-BLAT)*SIN(PIG2-BLON)
000 C A(M,3)=EARTH*COS(PIG2-BLAT)
000 C 10 CONTINUE
000 C DO 20 N=2,M1
000 C C1=(A(N,1)-A(1,1))*2.

```

```

000      C2=(A(N,2)-A(1,2))*2.
000      C3=(A(N,3)-A(1,3))*2.
000      D(N,1)=(C1+C2+C3)**0.5
000      D(N,2)=DAT(N,3)
000  20 CONTINUE
000      I03=IFIX(M1/3)+1
000      DO 23 J=1,I03
000      N=(J-1)*3+1.
000      N3=(J*3).
000  C
000  C      THE NEXT STATEMENT PRINTS OUT THE CUMULATIVE DISTANCE
000  C      OF EACH GRAVITY STATION FROM THE FIRST STATION TO THE WEST
000  C
000      WRITE(16,87)((I,D(I,1)),I=N,N3)
000  87 FORMAT(1H0,8(I4,F12.0))
000  23 CONTINUE
000  C
000  C      ALL FOLLOWING STATEMENTS ARE EITHER LINE OR ANNOTATION
000  C      COMMANDS AND MAY BE CHANGED BY THE USER
000  C
000      D(1,1)=0.0
000      D(1,2)=DAT(1,3)
000      X=(D(1,1)*1./26400.+2.)
000      Y=(D(1,2)*.125+10.)
000      CALL PLOT(X,Y,1)
000      MIKE=M1-1
000      DO 31 J=2,MIKE
000      Z=((D(J,1)-D(J-1,1)))
000      IF(3.0T.3000.)GO TO 24
000      GO TO 64
000  24 X=(D(J,1)*1./26400.+2.)
000      Y=(D(J,2)*.125+10.)
000      CALL PLOT(X,Y,1)
000      GO TO 31
000  64 X=(D(J,1)*1./26400.+2.)
000      Y=(D(J,2)*.125+10.)
000      CALL PLOT(X,Y,2)
000  31 CONTINUE
000      X=(D(M1,1)*1./26400.+2.)
000      Y=(D(M1,2)*.125+10.)
000      DO 63 I=1,5
000  63 CALL PLOT(X,Y,2)
000      CALL PLOT(2.,3.75,1)
000      CALL AXIS(2.,3.75,12.5,50.,.15,90.)
000      X=(D(M1,1)*1./26400.+2.)
000      CALL AXIS(X,3.75,12.5,50.,.15,90.)
000      CALL PLOT(2.,10.,1)
000      X1=X-2.
000      CALL AXIS(2.,10.,X1,1.,.1,0.)
000      READ(15,101)(A1(I),I=1,3)
000  101 FORMAT(ZA4)
000      DO 28 I=1,3
000      ENCODE(4,18,W(I))A1(I)
000  13 FORMAT(A4)
000      ANX=(X/2.-1.)+FLOAT(I-1)+0.5
000      CALL SYMBOL(ANX,1.7,W(I),4.,3,0.)
000  28 CONTINUE
000      DO 202 I=1,11
000      N=-50+(I-1)*10
000      YY=3.35+1.25*FLOAT(I-1)
000      ENCODE(3,171,BLOCK)N
000  171 FORMAT(I3)

```

```

000 202 CALL SYMBOL(1.2,YY,BLOCK,3,.2,C.)
000      DO 203 I=1,11
000      N=-50+(I-1)*10
000      YY=3.65+1.25*FLOAT(I-1)
000      ENCODE(3,171,B)N
000      XX=X+.2
000 203 CALL SYMBOL(XX,YY,B,3,.2,C.)
000      CALL SYMBOL(.75,C.,'FREE-AIR GRAVITY IN MILLIGALS',29,.3,C.)
000      CALL SYMBOL(1.55,2.7,'WEST',4,.3,C.)
000      F17=X-.3
000      CALL SYMBOL(F17,2.7,'EAST',4,.3,C.)
000      CALL PLOT(2.,3.75,1)
000      CALL PLOT(X,3.75,2)
000      CALL PLOT(2.,3.75,1)
000      NUM=IFIX(D(N1,1))/32810
000      DO 31 I=1,NUM
000      F=FLOAT(I)*32810./26400.+2.
000      CALL SYMBOL(F,3.75,'-',1,.1,C.)
000      N7=I*10
000      ENCODE(3,272,H)N7
000 272 FORMAT(I3)
000      E1=F-.25
000 31 CALL SYMBOL(E1,3.25,H,3,.2,C.)
000      AOX=ANX-1.5
000      CALL SYMBOL(AOX,2.5,' KILOMETERS ',17,.3,C.)
000      XXX=XX-2.5
000      CALL SYMBOL(XXX,1.,'MIKE BURNAMAN',13,.2,C.)
000      CALL SYMBOL(XXX,.75,'SPRING,1974',11,.2,C.)
000      IF(MTKK.EQ.KENR)GO TO 31
000      CALL HALT(10)
000      GO TO 123
000 31 CALL HALT(999)
000 123 CONTINUE
000      STOP
000      END

```

PROFILEPLOT.READM .

```
ISOR LEVEL      4
000             SUBROUTINE READM(NIN)
000   C
000   C       THIS SUBROUTINE READS IN THE DATA FILE
000   C       THE LAST STATION SHOULD HAVE A FREE-AIR ANOMALY OF
000   C       99.9 TO END DATA ENTRY
000   C
000   C       THE LAST IMAGE OF THE DATA FILE SHOULD BE THE TRACK NUM.
000   C
000             COMMON DAT(1300,3)
000             NIN=0
000   43  NIN=NIN+1
000             READ(15,25)(DAT(NIN,J),J=1,3)
000             IF(DAT(NIN,7).GT.99.9)GO TO 36
000             GO TO 43
000   38  NIN=NIN-1
000             RETURN
000   25  FORMAT(8X,F8.4,F12.4,F8.1)
000             END
```

MAPPLOT

Purpose

This program allows the user to post the individual shiptracks and free-air anomaly profiles on a base map. The plotting technique is that described in PROFILEPLOT.

Input

Line 1: KENR(I2) - This is the number of Datafiles (in this case ship tracks) to be plotted. This number should be less than seven due to tape length limitations.

Output

The output consists of:

- (1) Plotting instructions written directly on the tape.
- (2) A printed list of the track numbers plotted.

Special Instructions

The plot tape should be assigned and the ship track Datafiles should be assigned and linked to the run via @ASG and @USE statements. The Datafile @USE statements should start at 21 and continue consecutively to 27. For a complete plot of all 27 tracks it is only necessary to execute the program four times consecutively, relinking the new Datafiles via @USE statements. All scale factors of the chosen base map must be changed if another base is used. The interior unit numbers are the same as in PROFILEPLOT.

Sample Run

DEMAND

@RUN MIKE,3061GRAV,3061GRAV,5,250

```
@ASG,LITE TAPE.,8C,PLOT56
@MSG,W PLEASE RING IN PLOT56
@USE 4.,TAPE.
@ASG,AX FILEH16.
@ASG,AX FILEH17.
@ASG,AX FILEH18.
@ASG,AX FILEH19.
@USE 21.,FILEH16.
@USE 22.,FILEH17.
@USE 23.,FILEH18.
@USE 24.,FILEH19.
@ASG,AX MAPPLOT.
@XQT MAPPLOT.ABS
4
@FIN
```

Explanation

This run will post the gravity stations on tracks H16-H19 along with their free-air anomalies.

MAPPLOT.MAIN

```

550R LEVEL      4
000 C
000 C      MAPPLOT WRITTEN BY MIKE BURNAMAN FALL,1973
000 C      THIS PROGRAM PLOTS SHIPTRACKS AND IS SIMILAR TO PROFILEPLOT
000 C
000 C      DAT IS THE INPUT DATA MATRIX FOR EACH SHIPTRACK
000 C
000 C      DIMENSION DAT(1300,3)
000 C      COMMON DAT
000 C
000 C      SET THE PLOTTER TO 400 COUNTS/INCH
000 C
000 C      CALL PLOTS(400.,400.,4)
000 C
000 C      FUDGE IS A SCALE FACTOR TO SET ONE PLOTTER INCH
000 C      EQUAL TO ONE INCH IN THE PROGRAM, IT MAY VARY DEP-
000 C      ENDING ON THE CALIDRATION OF THE PLOTTER
000 C
000 C      FUDGE=1.25
000 C      RAD=2.*3.14159265/360.
000 C
000 C      NUM IS THE NUMBER OF TRACKS TO PLOT
000 C
000 C      READ(5,12)NUM
000 C      DO 103 K=1,NUM
000 C
000 C      ANGLE IS THE ANGLE WHICH THE TRACK SUBTENDS FROM THE
000 C      HORIZONTAL, CLOCKWISE IS POSITIVE
000 C
000 C      READ(5,27)ANGLE
000 C      M1 IS THE NUMBER OF GRAVITY STATIONS
000 C
000 C      CALL READM(M1)
000 C      DEGRE=ANGLE*RAD
000 C
000 C      THE NEXT TWO STATEMENTS CONVERT THE SPHERICAL COORDINATES
000 C      TO SCALED MAP COORDINATES FOR THE FIRST GRAVITY STATION
000 C
000 C      X=(38.+DAT(1,2))*3.33*FUDGE
000 C      Y=(DAT(1,1)-26.)*9.37*FUDGE
000 C      CALL PLOT(X,Y,1)
000 C      LOOP 275 PLOTS THE POSITIONS OF THE GRAVITY STATIONS AS
000 C      AS A CONTINUOUS LINE UNLESS ANY TWO CONSECUTIVE
000 C      STATIONS ARE SEPERATED BY MORE THAN 0.01 DEGREES
000 C
000 C      DO 275 L=2,M1
000 C      X=(38.+DAT(L,2))*3.33*FUDGE
000 C      Y=(DAT(L,1)-26.)*9.37*FUDGE
000 C      DIF1=DAT(L-1,1)-DAT(L,1)
000 C      DIF2=DAT(L-1,2)-DAT(L,2)
000 C      IF(DIF1.GR.DIF2.GT.C.C100)GO TO 111
000 C      CALL PLOT(X,Y,2)
000 C      GO TO 275
000 C 111 CALL PLOT(X,Y,1)
000 C 275 CONTINUE
000 C
000 C      MOVE THE PEN BACK TO THE ORIGIN
000 C
000 C      CALL HALT(0)
000 C
000 C      LOOP 300 PLOTS THE MAGNITUDE OF THE GRAVITY ANOMALY

```

```

CCC C AS A FUNCTION OF THE ORIENTATION OF THE TRACK
CCC C
CCC X=(35.+DAT(1,2))*3.38*FUDGE
CCC Y=(DAT(1,1)-20.)*3.37*FUDGE
CCC B=DAT(1,3)*.02*SIN(DEGRE)*FUDGE+X
CCC C=DAT(1,3)*.02*COS(DEGRE)*FUDGE+Y
CCC CALL PLOT(B,C,1)
CCC GO 380 L=2,M1
CCC X=(93.+DAT(L,2))*3.33*FUDGE
CCC Y=(DAT(L,1)-20.)*3.37*FUDGE
CCC B=DAT(L,3)*.02*SIN(DEGRE)*FUDGE+X
CCC C=DAT(L,3)*.02*COS(DEGRE)*FUDGE+Y
CCC DIF1=DAT(L-1,1)-DAT(L,1)
CCC DIF2=DAT(L-1,2)-DAT(L,2)
CCC IF(DIF1.OR.DIF2.GT.C.C100)GO TO 210
CCC CALL PLOT(B,C,2)
CCC GO TO 380
CCC 210 CALL PLOT(B,C,1)
CCC 300 CONTINUE
CCC C
CCC C THE TRACK NUMBER IS READ AS THE LAST DATA IMAGE
CCC C IS PRINTED TO SIGNIFY THAT THE PLOTTER COMMANDS HAVE
CCC C HAVE BEEN WRITTEN ON TAPE
CCC C
CCC READ(5,121)AB,AC,AD
CCC 121 FORMAT(3A4)
CCC WRITE(6,222)AB,AC,AD
CCC 222 FORMAT(1HD,3A4)
CCC 100 CONTINUE
CCC CALL HALT(0)
CCC 12 FORMAT(I3)
CCC 27 FORMAT(F4.0)
CCC CALL HALT(999)
CCC STOP
CCC END

```

MAPPLOT,READM .

```
SSOR LEVEL      4
   CCC      C
   CCC      C      READM IS IDENTICAL TO READM IN PPROFILEPLOT
   CCC      C
   CCC      SUBROUTINE READM(NIN)
   CCC      COMMON DAT(1300,3)
   CCC      NIN=C
   CCC      43 NIN=NIN+1
   CCC      READ(5,25)(DAT(NIN,J),J=1,3)
   CCC      IF(DAT(NIN,3).GT.20.3)GO TO 36
   CCC      GO TO 48
   CCC      30 NIN=NIN-1
   CCC      RETURN
   CCC      25 FORMAT(3X,FS.4,F12.4,FS.1)
   CCC      END
```

GRAVITYMODEL

Purpose

This program allows the user to calculate the gravitational attraction of any two-dimensional body whose cross section can be represented as an N-sided polygon. The computed attraction of this polygon (or polygons for a more complicated model) is then compared to the observed gravity attraction along the line of calculation.

Method

The theoretical derivation of this procedure was first developed by Hubbert (1948). He showed that the vertical component of the gravitational attraction (g_v) caused by a two-dimensional body could be represented as,

$$g_v = 2 G \rho \oint z d\theta$$

where G is the gravitational constant, ρ is the density, and $\oint z d\theta$ is the line integral around the polygon at the origin. This procedure is powerful yet cumbersome since the computation of the line integral for anything but the simplest geometrical form is a difficult task. With the advent of modern digital computers, however, it remained only necessary to develop the general form of the analytical expression to solve the integrals for a two-dimensional body of arbitrary shape. That logic was developed by Talwani and others (1959, p. 50-57).

Their method consists of describing a Cartesian coordinate system for the polygon and the points of computation which may be anywhere within the plane. Next the vertical and horizontal attraction at a point (field point) are described as functions of subtended angles between the field points and the polygon vertices (body points) in a clockwise direction (described as the line integral), the gravitational constant, and the density. The specific

line integrals involved are evaluated for the general case and seven special cases.

The program GRAVITYMODEL. was supplied by Manik Talwani of the Lamont Geological Observatory, Columbia University. Several modifications have been made by this author but the method used in calculating the integrals remains the same.

Input

IGRAV(I3) - This represents the number of observed gravity stations (corresponding to the field points). This value is read from unit 27. The origin is the first station.

GRAV(F5.1) - Observed gravity anomaly at the computation station.

M(I4) - Number of field (computation) stations.

FACTOR(F5.2) - Length of a graph unit of model in kilofeet; also the station spacing and the field point (computation station) spacing.

L(I5) - Number of polygons to compute.

NO(I5) - Always zero.

CONS(F7.3) - Always zero.

LNO(I5) - Number of first, second, third, etc. polygons, in sequence.

N(I5) - Number of vertices of the polygon, plus one.

RHO(F7.3) - Density or density contrast.

X(F7.2) - Horizontal coordinate of polygon vertex in graph units with respect to the origin (first computation station).

Z(F6.3) - Vertical coordinate of polygon vertex in kms. (+ below sea level).

Sample Input Datafiles for GRAVITYMODEL

File name FISHBB.

line 1	IGRAV (I3)
line 2	GRAV(1) (F5.1)

```

line 3          GRAV(2)

line (1 + IGRAV - 1)  GRAV(IGRAV -1)
line (1 + IGRAV)      GRAV(IGRAV)

File name REVISEDMODEL.

line 1          M
line 2          FACTOR
line 3          L,NO,CONS
line 4          LNO,N,RHO
line 5          X,Z
line 6          X,Z
{
line (4 + N1 - 1)  X,Z
line (4 + N1)    X,Z
line (5 + N1)    LNO,N,RHO      (note new LNO,N, and RHO)
line (5 + N1 + 1) X,Z
line (5 + N1 + 2) X,Z
{
line (5 + N1 + N2 - 1) X,Z
line (5 + NN1 + N2) X,Z

```

This form continues for L(number of polygons) loops.

The actual contents of Datafile REVISEDMODEL is given later in this Appendix.

Output

For each polygon the raw data and the attraction for each computation station are listed. The total attraction of all polygons at each station is listed as is the difference between the observed and computed gravity.

Special Instructions

The Datafile containing observed gravity should be linked by @ASG and @USE statements. Since it is advantageous to run this program from a demand terminal it is necessary to assign a special print file to receive the lengthy output. This technique is given in the Sample Run.

.....
Sample Run
.....

DEMAND

@RUN MIKE,3061GRAV,3061GRAV,10,1000
@ASG,AX GRAVITYMODEL
@ASG,AX FISHBB.
@ASG,AX REVISEDMODEL.
@USE 27.,FISHBB.
Make any necessary changes in REVISEDMODEL. via EDIT
@ASG,T TEMP.
@BRKPT PRINT\$/TEMP
@XQT GRAVITYMODEL.COSINE
@ADD REVISEDMODEL.
@BKRPT PRINT\$
Go into EDIT and look at output

BATCH

Same as Demand except delete @BRKPT and @ADD control statements and
use cards for the REVISEDMODEL. Datafile.

```

SSOR LEVEL      4
000  C
000  C          GRAVITYMODEL
000  C
000  C  THIS PROGRAM COMPUTES THE ATTRACTION OF A SET
000  C  TWO-DIMENSIONAL BODYS TO A SET OF FIELD POINTS
000  C  THE METHOD USED IS THAT OF MANIK TALWANI OF GAMONT
000  C  GEOLOGICAL OBSERVATORY, REVISED BY MIKE BURNAMAN
000  C          DIMENSION FX(500),FZ(500),POELZ(500),SSELZ(500),X(500),Z(700)
000  C          DIMENSION GRAV(500)
000  C
000  C  READ IN THE NUMBER OF COMPUTATION(FIELD) POINTS
000  C
000  C          READ(27,38)IGRAV
000  C
000  C  READ IN THE OBSERVED GRAVITY ANOMALY AT THE FIELD POINT
000  C
000  C          READ(27,39)(GRAV(I),I=1,IGRAV)
000  C
000  C  READ IN THE NUMBER OF FIELD POINTS AGAIN.
000  C
000  C  READ 13,M
000  C 13  FORMAT(I4)
000  C
000  C  READ IN THE HORIZONTAL SCALE FACTOR IN
000  C  UNITS OF KILOFEET/HORIZONTAL GRAPH UNIT,
000  C  THIS NUMBER SHOULD BE EQUAL TO THE FIELD POINT SPACING
000  C
000  C          READ 36,FACTOR
000  C 36  FORMAT(F5.2)
000  C
000  C  COMPUTE THE HORIZONTAL DISTANCES BETWEEN THE FIELD POINTS
000  C
000  C          DO 451 K=1,M
000  C          FX(K)= (FACTOR/3.28)*FLOAT(K-1)
000  C          FZ(K)=0.0
000  C 451  CONTINUE
000  C          PRINT 73
000  C
000  C  READ IN THE NUMBER OF POLYGONS(L),DISREGARD THE
000  C  NEXT VARIABLE, AND READ IN A CONSTANT TO BE ADDED TO
000  C  THE TOTAL ATTRACTION AT EACH FIELD POINT(IF APPLICABLE)
000  C
000  C 520  READ 3,L,NO,CONS
000  C
000  C  ADD THE CONSTANT (IF APPLICABLE)
000  C
000  C          DO 93 K=1,M
000  C 93  SSELZ(K)=CONS
000  C
000  C  READ IN THE POLYGON NUMBER(LNO), THE NUMBER OF VERTICES
000  C  OF THE POLYGON PLUS ONE(N), AND THE DENSITY OF THE
000  C  POLYGON(RHO).
000  C
000  C 60  READ 3,LNO,N,RHO
000  C
000  C  PRINT THE POLYGON NUMBER.
000  C
000  C          PRINT 103,LNO
000  C
000  C  READ IN THE VERTICES OF THE POLYGON AS X AND Z

```

```

000 C WITH THE X VALUES IN GRAPH UNITS AND THE Z
000 C VALUES IN KILOMETERS.
000 C
000 C DO 301 I=1,N
000 C READ 2,X(I),Z(I)
000 C
000 C PRINT OUT THE RAW X AND Z VALUES
000 C
000 C PRINT 37,X(I),Z(I)
000 C
000 C CONVERT THE X VALUES IN GRAPH UNITS TO KILOMETERS.
000 C
000 C X(I)=X(I)*FACTOR/3.28
000 C 301 CONTINUE
000 C
000 C PRINT A HEADING.
000 C
000 C PRINT 52
000 C
000 C PRINT THE NUMBER OF FIELD POINTS, NUMBER OF VERTICES, AND
000 C DENSITY CONTRAST OF THE POLYGON.
000 C
000 C PRINT 53,K,N,RHO
000 C PRINT 33
000 C
000 C PRINT A HEADING.
000 C
000 C PRINT 99
000 C
000 C COMPUTE THE ATTRACTION OF THE POLYGON AT EACH FIELD POINT.
000 C
000 C DO 420 K=1,M
000 C
000 C SET THE LINE INTEGRAL OF THE POLYGON TO ZERO.
000 C
000 C SDCLZ=C.0
000 C
000 C SET THE BODY POINT COUNTER TO ONE
000 C
000 C I=1
000 C
000 C COMPUTE THE DISTANCE(RR) FROM THE FIELD POINT TO
000 C THE BODY POINT .
000 C
000 C 205 EXXX=X(I)-FX(K)
000 C ZEEE=Z(I)-FZ(K)
000 C RR=EXXX**2+ZEEE**2
000 C
000 C CHECK TO SEE IF THE BODY POINT IS TO THE RIGHT OR
000 C LEFT OF THE FIELD POINT OR DIRECTLY UNDER IT
000 C AND THEN CHECK TO SEE IF THE BODY POINT IS ABOVE
000 C OR BELOW THE FIELD POINT IF NECESSARY.
000 C THIS PROCESS DETERMINES THE SPECIAL CASES USED
000 C TO DETERMINE THE ANGLE FROM THE FIELD POINT
000 C TO THE BODY POINT FROM THE HORIZONTAL.
000 C
000 C
000 C IF (EXXX)210,240,260
000 C 210 IF(ZEEE)220,230,230
000 C 220 THETA=ATAN(ZEEE/EXXX)-3.1415927
000 C GO TO 300

```

```

000 230 THETA=ATAN(ZEEE/EXXX)+3.1415927
000      GO TO 300
000 240 IF(ZEEE)250,200,270
000 250 THETA=-1.5707963
000      GO TO 300
000 260 THETA=0.0
000      GO TO 300
000 270 THETA=1.5707963
000      GO TO 300
000 230 THETA=ATAN(ZEEE/EXXX)
000 C
000 C CHECK TO SEE IF THIS IS FIRST ANGLE.
000 C
000 300 IF(I-1)3001,3002,3001
000 C
000 C SET FIRST ANGLE (THETA) EQUAL TO THETA AND KEEP
000 C THETA AS REFERENCE ANGLE.
000 C
000 3002 EXX=EXXX
000      ZEE=ZEEE
000      R=RR
000      THETA=THETA
000 C
000 C CHECK TO SEE IF FIRST ANGLE AGAIN.
000 C
000 IF (I-1)205,200,205
000 200 I=2
000 C
000 C RETURN TO STATEMENT 205 (IF FIRST POINT) AND
000 C GET NEXT BODY POINT.
000 C
000      GO TO 205
000 C
000 C DETERMINE IF THE DISTANCE FROM THE FIRST BODY POINT
000 C TO THE PRESENT ONE IS ZERO AND
000 C IF SO SET THE ADDITION TO THE LINE INTEGRAL EQUAL ZERO
000 C IF NOT EQUAL ZERO THEN DETERMINE THE PROPER
000 C ANGLE, DEPENDING ON QUADRANT, TO USE TO COMPUTE
000 C THIS PORTION OF THE LINE INTEGRAL AT STATEMENT 370
000 C
000 3001 CHECK=EXX*ZEEE-ZEE*EXXX
000      IF(CHECK)320,310,320
000 310 DELZ=0.0
000      GO TO 400
000 320 OMEGA=THETA-THETA
000      IF(OMEGA)3201,3202,3202
000 3201 IF(OMEGA-3.1415927)330,330,340
000 3202 IF(OMEGA+3.1415927)340,330,330
000 330 DTHET=OMEGA
000      GO TO 370
000 340 IF(OMEGA)350,300,360
000 350 DTHET=OMEGA+6.2831853
000      GO TO 370
000 360 DTHET=OMEGA-6.2831853
000 C
000 C COMPUTE THE ADDITION TO THE LINE INTEGRAL.
000 C
000 370 A=CHECK/((EXXX-EXX)**2+(ZEEE-ZEE)**2)
000      B=(EXXX-EXX)*DTHET
000      C=.5*(ZEEE-ZEE)*ALOG(RR/R)
000      DELZ=A*(B+C)
000 C

```

```

000 C ADD THIS PORTION TO THE SUM OF THE LINE INTEGRAL.
000 C
000 400 SDELZ=SDELZ+DELZ
000 C
000 C IF THIS IS NOT THE LAST BODY POINT REPEAT THE STEPS
000 C FOR THE NEXT, IF IT IS THE LAST GO TO
000 C STATEMENT 3005 AND COMPUTE THE GRAVITY.
000 C IF(I-N) 3002,3005,3005
000 3002 I=I+1
000 C GO TO 3002
000 C
000 C COMPUTE THE ATTRACTION OF THE POLYGON AT THE PRESENT
000 C FIELD POINT AS THE PRODUCT OF 13.34(GAMMA IN UNITS
000 C CONVERTED TO KMS), RHO( THE DENSITY), AND SDELZ
000 C (THE LINE INTEGRAL).
000 C
000 3005 PDELZ(K)=13.34*RHO*SDELZ
000 C
000 C ADD THE ATTRACTION OF THIS POLYGON(PDELZ) AT
000 C THE PRESENT FIELD POINT TO THE SUM OF THE
000 C ATTRACTION OF ALL POLYGONS AT THIS POINT.
000 C
000 C SSELZ(K)=SSELZ(K)+PDELZ(K)
000 C
000 C PRINT THE FIELD POINT(K), POLYGON NUMBER(LNO),
000 C AND THE ATTRACTION OF THAT POLYGON AT THE POINT(PDELZ).
000 C
000 C PRINT 56,K,LNO,PDELZ(K)
000 C
000 C START ON THE NEXT FIELD POINT.
000 C
000 420 CONTINUE
000 C PRINT 73
000 C
000 C CHECK TO SEE IF ALL POLYGONS HAVE BEEN COMPUTED.
000 C
000 C IF(L-LNO)430,430,60
000 C
000 C PRINT HEADING
000 C
000 430 PRINT 59
000 C
000 C COMPUTE THE DIFFERENCE BETWEEN THE COMPUTED GRAVITY
000 C AND THE OBSERVED GRAVITY AT EACH FIELD POINT
000 C PRINT IT OUT.
000 C DO 4301 K=1,M
000 C DIFF=SSELZ(K)-GRAV(K)
000 C PRINT 31,K,SSELZ(K),GRAV(K),DIFF
000 4301 CONTINUE
000 1 FORMAT(' M=',I6)
000 2 FORMAT(F7.2,F8.3)
000 3 FORMAT(I5,I5,F7.3)
000 4 FORMAT(I5,3F10.3)
000 5 FORMAT(//,3X,'LNO=',I4,4X,'N=',I5,4X,'RHO=',F3.3,/)
000 6 FORMAT(/,6X,'L=',I2,3X,'NO=',I8,3X,'CONS=',F8.2)
000 7 FORMAT(/,35X,' K FX(K) FZ(K) ANOMALY')
000 73 FORMAT(72('='))
000 109 FORMAT(1H1,'!', ' POLYGON NUMBER',I3,' RAW DATA',6X,1X'!',/,
000 12X,'!',1X,'HORIZONTAL VERTICAL',13X,'!')
000 33 FORMAT(1X,37('='))
000 87 FORMAT(1X,'!',F10.1,F10.4,13X,'!')
000 52 FORMAT(1H1,'!', ' NUMBER OF NUMBER OF DENSITY',3X,'!',/,

```

```
CCC      1,1X,'!',',', STATIONS',', POLY SIDES CONTRAST',1X,'!',',204
CCC      55      FORMAT(1X,'!',',',I7,I13,F12.3,3X,'!')
CCC      59      FORMAT(/,,' STATION POLYGON TOTAL',/,
CCC      1' NUMBER NUMBER GRAVITY')
CCC      56      FORMAT(I3,I7,F12.1)
CCC      33      FORMAT(I3)
CCC      39      FORMAT(F5.1)
CCC      53      FORMAT(1H1,' STATION FREE AIR OBSERVED DIFFERENCE',
CCC      1/,', NUMBER ANOMALY ANOMALY')
CCC      81      FORMAT(I7,F11.1,F10.1,F10.1)
CCC      700     STOP
CCC      END
```

APPENDIX

Purpose

This program allows the user to obtain a listing of the final data of each ship track to use as a reference.

Input

NFILES(I2) - This is the number of ship tracks to include in the appendix. A maximum of 9 is allowed due to input file limitations.

Output

A listing of all gravity stations for each track. Each gravity station includes the latitude, longitude, absolute gravity, free-air anomaly, and cruise number.

Special Instructions

The input files (FILEH1., Etc.) must be assigned and linked to the run via @ASG and @USE control statements. The interior unit names in the @USE statements must start with 21 and be consecutive and no larger than 29 (i.e. @USE 26., FILEH6.). A temporary file must be assigned to the run and must contain only a zero in I6 format. If a complete list of all 27 ship tracks used in this thesis is necessary consult DATALISTFILE.ELEMENTS.

Sample Run

```
@RUN,A MIKE,3061GRAV,3061GRAV,2,1000
@STDPAG,YES
@ASG,T TEMP.
@ASG,AX FILEH7.
@USE 9.,TEMP.
Enter zero in TEMP via EDIT
@ASG,AX FILEH8.
@ASG,AX FILEH9.
```

@USE 21.,FILEH7.
@USE 22.,FILEH8.
@USE 23.,FILEH9.
@ASG,AX APPENDIX.
@XQT APPENDIX.OPERATION
3
@FIN

Explanation

This run will produce a listing of the data for tracks H7, H8, and H9. The pages within each track will be listed as well as the cumulative number of pages for the entire appendix.

A listing of the complete Appendix (all 27 tracks) is available from the Geology Department, University of Houston.

APPENDIX.MAIN .

```

COMMON LEVEL 4
000 COMMON DAT(2000,4)
000 RAD = 3.1415927/180.
000 READ(9,69) NPAGE
000 REWIND 9
000 READ 10, NFILES
000 10 FORMAT(I2)
000 DO 100 M=1, NFILES
000 MFILE = 20 + M
000 READ (MFILE,97) B
000 97 FORMAT(A1)
000 CALL READM( MFILE, M1 )
000 READ( MFILE , 20) TRACK1,TRACK2
000 20 FORMAT( 2A6)
000 RM1 = M1
000 R20 = 28.
000 RQUO = RM1 / R20
000 NQUO = M1 / 28
000 RNQUO = NQUO
000 IF ( RQUO .GT. RNQUO ) NQUO = NQUO + 1
000 DO 200 I = 1, NQUO
000 PRINT 30
000 30 FORMAT ( 1H1,3X,'SEQ-',3X,'LATITUDE',4X,'LONGITUDE',3X,'ABSOLUTE',
000 11X,'FREE-AIF',1X,'CRUISE',1X,'TRACK',/,4X,'UENCE',2X,
000 2'DEG MIN',4X,'DEG MIN',4X,'GRAVITY',2X,'ANOMALY',1X,
000 3'NUMBER',/, 4X, 5('-' ),2X,8('-' ),4X,9('-' ),3X,8('-' ),1X,8('-' ),1X,
000 36('-' ),1X,5('-' ))
000 I3 = (( I - 1 ) * 28 ) + 1
000 I17 = (( I - 1 ) * 28 ) + 28
000 DO 300 N = I3, I17
000 ALAT = DAT(N,1)
000 ALON = DAT(N,2)
000 FAANOM = DAT(N,3)
000 CRUISE = DAT(N,4)
000 NCRUISE = CRUISE
000 DEG = ALAT * RAD
000 THGRAV = 973043. * ( 1. + 0.0052334 * ( SIN( DEG ) ** 2. )
000 1 - 0.0000050 * ( SIN ( 2. * DEG ) ** 2. ))
000 ABGRAV = THGRAV + FAANOM
000 NLATD = ALAT
000 ANLATD = NLATD
000 FLATM = ALAT - ANLATD
000 FLATMS = FLATM * 60.
000 NLOND = ALON
000 ALOND = NLOND
000 FLONM = ALON - ALOND
000 FLONMS = ABS(FLONM * 60.)
000 PRINT 40, N, NLATD, FLATM6, NLOND, FLONMS, ABGRAV, FAANOM,
000 1 NCRUISE, TRACK2
000 40 FORMAT (/,4X, I4, I5, F6.2,I6, F7.2, F11.1, F8.1, I7, A6 )
000 300 CONTINUE
000 NPAGE = NPAGE + 1
000 PRINT 50, TRACK1,TRACK2, I,NQUO, NPAGE
000 50 FORMAT(/, 5X, 2A6,2X, ', PAGE',I5,' OF',I5,
000 12X,', PAGE', I5,' OF APPENDIX')
000 200 CONTINUE
000 100 CONTINUE
000 WRITE(9,69) NPAGE
000 69 FORMAT(I6)
000 END FILE 9
000 REWIND 9

```

000
000

STOP
END

```
DSOR LEVEL      4
000             SUBROUTINE READM(MFILE,NIN)
000             COMMON DAT(2000,4)
000             NIN=C
000             40 NIN=NIN+1
000             READ(MFILE,25)(DAT(NIN,J),J=1,4)
000             IF(DAT(NIN,3).GT.99.9)GO TO 36
000             GO TO 48
000             30 NIN=NIN-1
000             RETURN
000             25 FORMAT(8X,F8.4,F12.4,F8.1,F12.C)
000             END
```

DATALISTFILE

Purpose

This Elementfile, when added to the runstream, will produce a listing of all the data for the 27 ship tracks used in this thesis. The output is described in the documentation of APPENDIX.

Input

No special input is used, other than the single @ADD statement.

Output

An appendix of all the thesis data.

Special Instructions

All the ship track Datafiles must be catalogued, along with the Programfile APPENDIX and the Elementfile DATALISTFILE. A single control statement, adding DATALISTFILE.ELEMENTS, is all that is necessary for execution.

Note: Check with the computer center before running this program to ascertain the line-printers are set to leave a two line margine at the top and bottom of each page and print six lines/inch; also check to make sure that the page control command is not being suppressed.

Listing

A listing of the contents of DATALISTFILE.ELEMENTS is shown immediately following this documentation.

Sample Run

BATCH

@RUN,A MIKE,3061GRAV,3061GRAV,3,100
@ASG,AX DATALISTFILE.

@ADD DATALISTFILE.ELEMENTS
@FIN

DATALISTFILE.ELEMENTS .

SSOR LEVEL

4

```

000 @ASC,AX FILEH1.
000 @ASC,AX FILEH2.
000 @ASC,AX FILEH3.
000 @ASC,AX FILEH4.
000 @ASC,AX FILEH5.
000 @ASC,AX FILEH6.
000 @ASC,AX FILEH7.
000 @ASC,AX FILEH8.
000 @ASC,AX FILEH9.
000 @ASC,AX FILEH10.
000 @ASC,AX FILEH11.
000 @ASC,AX FILEH12.
000 @ASC,AX FILEH13.
000 @ASC,AX FILEH14.
000 @ASC,AX FILEH15.
000 @ASC,AX FILEH16.
000 @ASC,AX FILEH17.
000 @ASC,AX FILEH20.
000 @ASC,AX FILEH21.
000 @ASC,AX FILEH22.
000 @ASC,AX FILED1.
000 @ASC,AX FILED2.
000 @ASC,AX FILED3.
000 @ASC,AX FILED4.
000 @ASC,AX FILED5.
000 @ASC,AX APPENDIX.
000 @ASC,T TEMP.
000 @USE 9.,TEMP.
000 @ED,I TEMP.
000 C
000 @EOF
000 @USE 21.,FILEH1.
000 @USE 22.,FILEH2.
000 @USE 23.,FILEH3.
000 @USE 24.,FILEH4.
000 @USE 25.,FILEH5.
000 @USE 26.,FILEH6.
000 @USE 27.,FILEH7.
000 @USE 28.,FILEH8.
000 @USE 29.,FILEH9.
000 @XQT APPENDIX.OPERATION
000 9
000 @USE 21.,FILEH10.
000 @USE 22.,FILEH11.
000 @USE 23.,FILEH12.
000 @USE 24.,FILEH13.
000 @USE 25.,FILEH14.
000 @USE 26.,FILEH15.
000 @USE 27.,FILEH16.
000 @USE 28.,FILEH17.
000 @USE 29.,FILEH18.
000 @XQT APPENDIX.OPERATION
000 9
000 @USE 21.,FILEH19.
000 @USE 22.,FILEH20.
000 @USE 23.,FILEH21.
000 @USE 24.,FILEH22.
000 @USE 25.,FILED1.
000 @USE 26.,FILED2.
000 @USE 27.,FILED3.

```

CCC @USE 22.,FILED4.
CCC @USE 23.,FILED5.
CCC @XGT APPENDTX.OPERATION
CCC 3

TAPEWRITE

Purpose

TAPEWRITE is an Elementfile which contains all the Executive control statements necessary to transfer all files used in this thesis (as described in Appendix 2) onto tape reel #U362.

Input

None

Output

None

Special Instructions

This Elementfile is included only to show the instructions used to store all files used in the thesis on tape for later reference. The listing of the commands is shown immediately following this documentation.

TAPEWRITE.MAIN .

SSOR LEVEL

4

```
000 @ASS,T TAPE.,809,U362R
000 @MSS,W RING IN U362R, PLEASE
000 @ASS,AX FILESTORE.
000 @COPCUT,C FILESTORE.MAIN,TAPE.RESTORE
000 @ASS,AX FILEH1.
000 @ASS,AX FILEH2.
000 @ASS,AX FILEH3.
000 @ASS,AX FILEH4.
000 @ASS,AX FILEH5.
000 @ASS,AX FILEH6.
000 @ASS,AX FILEH7.
000 @ASS,AX FILEH8.
000 @ASS,AX FILEH9.
000 @ASS,AX FILEH10.
000 @ASS,AX FILEH11.
000 @ASS,AX FILEH12.
000 @ASS,AX FILEH13.
000 @ASS,AX FILEH14.
000 @ASS,AX FILEH15.
000 @ASS,AX FILEH16.
000 @ASS,AX FILEH17.
000 @ASS,AX FILEH18.
000 @ASS,AX FILEH19.
000 @ASS,AX FILEH20.
000 @ASS,AX FILEH21.
000 @ASS,AX FILEH22.
000 @ASS,AX FILED1.
000 @ASS,AX FILED2.
000 @ASS,AX FILED3.
000 @ASS,AX FILED4.
000 @ASS,AX FILED5.
000 @COPY,CM FILEH1.,TAPE.
000 @COPY,CM FILEH2.,TAPE.
000 @COPY,CM FILEH3.,TAPE.
000 @COPY,CM FILEH4.,TAPE.
000 @COPY,CM FILEH5.,TAPE.
000 @COPY,CM FILEH6.,TAPE.
000 @COPY,CM FILEH7.,TAPE.
000 @COPY,CM FILEH8.,TAPE.
000 @COPY,CM FILEH9.,TAPE.
000 @COPY,CM FILEH10.,TAPE.
000 @COPY,CM FILEH11.,TAPE.
000 @COPY,CM FILEH12.,TAPE.
000 @COPY,CM FILEH13.,TAPE.
000 @COPY,CM FILEH14.,TAPE.
000 @COPY,CM FILEH15.,TAPE.
000 @COPY,CM FILEH16.,TAPE.
000 @COPY,CM FILEH17.,TAPE.
000 @COPY,CM FILEH18.,TAPE.
000 @COPY,CM FILEH19.,TAPE.
000 @COPY,CM FILEH20.,TAPE.
000 @COPY,CM FILEH21.,TAPE.
000 @COPY,CM FILEH22.,TAPE.
000 @COPY,CM FILED1.,TAPE.
000 @COPY,CM FILED2.,TAPE.
000 @COPY,CM FILED3.,TAPE.
000 @COPY,CM FILED4.,TAPE.
000 @COPY,CM FILED5.,TAPE.
000 @ASS,AX DATACOUNTER.
000 @COPCUT,C DATACOUNTER.MAIN,TAPE.P1M
```

```

000 @COPCUT,A DATACOUNTER.MAIN,TAPE.P1A
000 @ASC,AX DATALISTER.
000 @COPCUT,S DATALISTER.MAIN,TAPE.P2M
000 @COPCUT,A DATALISTER.MAIN,TAPE.P2A
000 @ASC,AX DATAPROCESSOR.
000 @COPCUT,S DATAPROCESSOR.MAIN,TAPE.P3M
000 @COPCUT,S DATAPROCESSOR.GRAPH,TAPE.P3S1
000 @COPCUT,S DATAPROCESSOR.SORT,TAPE.P3S2
000 @COPCUT,S DATAPROCESSOR.TAPERD,TAPE.P3S3
000 @COPCUT,S DATAPROCESSOR.PUNWR,TAPE.P3S4
000 @COPCUT,S DATAPROCESSOR.RANGE,TAPE.P3S5
000 @COPCUT,A DATAPROCESSOR.ABSOLUTE,TAPE.P3A
000 @ASC,AX PROFILEPLOT.
000 @COPCUT,S PROFILEPLOT.MAIN,TAPE.P4M
000 @COPCUT,S PROFILEPLOT.READM,TAPE.P4S1
000 @COPCUT,A PROFILEPLOT.ABSOLUTE,TAPE.P4A
000 @ASC,AX MAPPLOT.
000 @COPCUT,S MAPPLOT.MAIN,TAPE.P5M
000 @COPCUT,S MAPPLOT.READM,TAPE.P5S1
000 @COPCUT,A MAPPLOT.ABSOLUTE,TAPE.P5A
000 @ASC,AX GRAVITYMODEL.
000 @COPCUT,S GRAVITYMODEL.COSINE,TAPE.P6M
000 @COPCUT,A GRAVITYMODEL.COSINE,TAPE.P6A
000 @ASC,AX APPENDIX.
000 @COPCUT,S APPENDIX.MAIN,TAPE.P7M
000 @COPCUT,S APPENDIX.READM,TAPE.P7S1
000 @COPCUT,A APPENDIX.OPERATION,TAPE.P7A
000 @ASC,AX TAPEWRITE.
000 @COPCUT,S TAPEWRITE.MAIN,TAPE.E1
000 @ASC,AX DATALISTFILE.
000 @COPCUT,S DATALISTFILE.ELEMENTS,TAPE.E2
000 @ASC,AX 3PARTLUMP.
000 @COPY,GM 3PARTLUMP.,TAPE.
000 @ASC,AX REVISEDMODEL.
000 @COPY,GM REVISEDMODEL.,TAPE.

```

FILERESTORE

Purpose

This Elementfile restores all Programfiles, Datafiles, and Elementfiles used in this thesis back into the operating system from tape #U362.

Input

None

Output

None

Special Instructions

Check the listing of TAPEWRITE.MAIN to ascertain that no files with the same names as those listed are presently catalogued under the users password.

Sample RunBATCH

```
@RUN,A MIKE,3061GRAV,3061GRAV,2,100
@ASG,T TAPE.,8C9,U362
@ASG,T TEMP.
@COPY TAPE.RESTORE, TEMP.RESTORE
@ADD TEMP.RESTORE
@FIN
```

SSOR LEVEL

4

```

000 @ASC,U FILEH1.
000 @ASC,U FILEH2.
000 @ASC,U FILEH3.
000 @ASC,U FILEH4.
000 @ASC,U FILEH5.
000 @ASC,U FILEH6.
000 @ASC,U FILEH7.
000 @ASC,U FILEH8.
000 @ASC,U FILEH9.
000 @ASC,U FILEH10.
000 @ASC,U FILEH11.
000 @ASC,U FILEH12.
000 @ASC,U FILEH13.
000 @ASC,U FILEH14.
000 @ASC,U FILEH15.
000 @ASC,U FILEH16.
000 @ASC,U FILEH17.
000 @ASC,U FILEH18.
000 @ASC,U FILEH19.
000 @ASC,U FILEH20.
000 @ASC,U FILEH21.
000 @ASC,U FILEH22.
000 @ASC,U FILED1.
000 @ASC,U FILED2.
000 @ASC,U FILED3.
000 @ASC,U FILED4.
000 @ASC,U FILED5.
000 @COPY,G TAPE.,FILEH1.
000 @DATA,L FILEH1.
000 @END
000 @COPY,G TAPE.,FILEH2.
000 @DATA,L FILEH2.
000 @END
000 @COPY,G TAPE.,FILEH3.
000 @DATA,L FILEH3.
000 @END
000 @COPY,G TAPE.,FILEH4.
000 @DATA,L FILEH4.
000 @END
000 @COPY,G TAPE.,FILEH5.
000 @DATA,L FILEH5.
000 @END
000 @COPY,G TAPE.,FILEH6.
000 @DATA,L FILEH6.
000 @END
000 @COPY,G TAPE.,FILEH7.
000 @DATA,L FILEH7.
000 @END
000 @COPY,G TAPE.,FILEH8.
000 @DATA,L FILEH8.
000 @END
000 @COPY,G TAPE.,FILEH9.
000 @DATA,L FILEH9.
000 @END
000 @COPY,G TAPE.,FILEH10.
000 @DATA,L FILEH10.
000 @END
000 @COPY,G TAPE.,FILEH11.
000 @DATA,L FILEH11.
000 @END
    
```

```

000 @COPY,S TAPE.,FILEH12.
000 @DATA,L FILEH12.
000 @END
000 @COPY,S TAPE.,FILEH13.
000 @DATA,L FILEH13.
000 @END
000 @COPY,S TAPE.,FILEH14.
000 @DATA,L FILEH14.
000 @END
000 @COPY,S TAPE.,FILEH15.
000 @DATA,L FILEH15.
000 @END
000 @COPY,S TAPE.,FILEH16.
000 @DATA,L FILEH16.
000 @END
000 @COPY,S TAPE.,FILEH17.
000 @DATA,L FILEH17.
000 @END
000 @COPY,S TAPE.,FILEH18.
000 @DATA,L FILEH18.
000 @END
000 @COPY,S TAPE.,FILEH19.
000 @DATA,L FILEH19.
000 @END
000 @COPY,S TAPE.,FILEH20.
000 @DATA,L FILEH20.
000 @END
000 @COPY,S TAPE.,FILEH21.
000 @DATA,L FILEH21.
000 @END
000 @COPY,S TAPE.,FILEH22.
000 @DATA,L FILEH22.
000 @END
000 @COPY,S TAPE.,FILED1.
000 @DATA,L FILED1.
000 @END
000 @COPY,S TAPE.,FILED2.
000 @DATA,L FILED2.
000 @END
000 @COPY,S TAPE.,FILED3.
000 @DATA,L FILED3.
000 @END
000 @COPY,S TAPE.,FILED4.
000 @DATA,L FILED4.
000 @END
000 @COPY,S TAPE.,FILED5.
000 @DATA,L FILED5.
000 @END
000 @ASS,U DATACOUNTER.
000 @ASS,U DATALISTER.
000 @ASS,U DATAPROCESSOR.
000 @ASS,U PROFILEPLOT.
000 @ASS,U MAPFLOT.
000 @ASS,U GRAVITYMODEL.
000 @ASS,U APPENDIX.
000 @ASS,U TAPEWRITE.
000 @ASS,U REVISEDMODEL.
000 @ASS,U SPARTLUMP.
000 @FIND TAPE.P1M
000 @COPIN,S TAPE.P1M,DATACOUNTER.MAIN
000 @FIND TAPE.P1A
000 @COPIN,A TAPE.P1A,DATACOUNTER.MAIN

```

```
000 @PRT DATACOUNTER.MAIN
000 @FIND TAPE.P2M
000 @CCPIN,S TAPE.P2M,DATALISTER.MAIN
000 @FIND TAPE.P2A
000 @CCPIN,A TAPE.P2A,DATALISTER.MAIN
000 @PRT DATALISTER.MAIN
000 @FIND TAPE.P3M
000 @CCPIN,S TAPE.P3M,DATAPROCESSOR.MAIN
000 @FIND TAPE.P3S1
000 @CCPIN,S TAPE.P3S1,DATAPROCESSOR.GRAPH
000 @FIND TAPE.P3S2
000 @CCPIN,S TAPE.P3S2,DATAPROCESSOR.SORT
000 @FIND TAPE.P3S3
000 @CCPIN,S TAPE.P3S3,DATAPROCESSOR.TAPERD
000 @FIND TAPE.P3S4
000 @CCPIN,S TAPE.P3S4,DATAPROCESSOR.PUNWP
000 @FIND TAPE.P3S5
000 @CCPIN,S TAPE.P3S5,DATAPROCESSOR.RANGE
000 @FIND TAPE.P3A
000 @CCPIN,A TAPE.P3A,DATAPROCESSOR.ABSOLUTE
000 @PRT DATAPROCESSOR.MAIN
000 @PRT DATAPROCESSOR.GRAPH
000 @PRT DATAPROCESSOR.SOFT
000 @PRT DATAPROCESSOR.TAPERD
000 @PRT DATAPROCESSOR.PUNWR
000 @PRT DATAPROCESSOR.RANGE
000 @FIND TAPE.P4M
000 @CCPIN,S TAPE.P4M,PROFILEPLOT.MAIN
000 @FIND TAPE.P4S1
000 @CCPIN,S TAPE.P4S1,PROFILEPLOT.READM
000 @FIND TAPE.P4A
000 @CCPIN,A TAPE.P4A,PROFILEPLOT.ABSOLUTE
000 @PRT PROFILEPLOT.MAIN
000 @PRT PROFILEPLOT.READM
000 @FIND TAPE.P5M
000 @CCPIN,S TAPE.P5M,MAPPLOT.MAIN
000 @FIND TAPE.P5S1
000 @CCPIN,S TAPE.P5S1,MAPPLOT.READM
000 @FIND TAPE.P5A
000 @CCPIN,A TAPE.P5A,MAPPLOT.ABSOLUTE
000 @PRT MAPPLOT.MAIN
000 @PRT MAPPLOT.READM
000 @FIND TAPE.P6M
000 @CCPIN,S TAPE.P6M,GRAVITYMODEL.COSINE
000 @FIND TAPE.P6A
000 @CCPIN,A TAPE.P6A,GRAVITYMODEL.COSINE
000 @PRT GRAVITYMODEL.COSINE
000 @FIND TAPE.P7M
000 @CCPIN,S TAPE.P7M,APPENDIX.MAIN
000 @FIND TAPE.P7S1
000 @CCPIN,S TAPE.P7S1,APPENDIX.READM
000 @FIND TAPE.P7A
000 @CCPIN,A TAPE.P7A,APPENDIX.OPERATION
000 @PRT APPENDIX.MAIN
000 @PRT APPENDIX.READM
000 @CCPIN,S TAPE.E1,TAPEWRITE.MAIN
000 @PRT TAPEWRITE.MAIN
000 @CCPIN,S TAPE.E1,TAPEWRITE.MAIN
000 @PRT TAPEWRITE.MAIN
000 @CCPIN,S TAPE.E2,DATALISTFILE.ELEMENTS
000 @PRT DATALISTFILE.ELEMENTS
000 @COPY,C TAPE.,3PARTLUMP.
```

000 @DATA,L 3PARTLUMP.
000 @END
000 @COPY,C TAPE.,REVISEDMODEL.
000 @DATA,L REVISEDMODEL.
000 @END
000 @REWIND TAPE.

000 - IN CONTROL MODE

REVISEDMODEL

This Datafile contains the parameters used by GRAVITYMODEL to compute the gravitational attraction of the crustal section of Figure 10.

TA, L REVISED MODEL.

A PROCESSOR LEVEL 4

001	0070
002	15.03
003	00013000000000.
004	00001000000 0.01
005	-2.0014.4
006	0.0015.3
007	-7.0020.0
008	-9.0021.1
009	-460.0001.7
010	-460.00 .
011	-55.00 .
012	-6.0012.
013	-2.0014.4
014	00002000050 -0.34
015	19.00 .001
016	40.00 0.182
017	41.00 0.333
018	42.00 0.475
019	43.00 0.595
020	44.00 0.740
021	45.00 0.790
022	45.00 0.820
023	47.00 0.920
024	48.00 1.040
025	49.00 1.100
026	50.00 1.200
027	51.00 1.250
028	52.00 1.26
029	53.00 1.22
030	54.00 1.29
031	55.00 1.28
032	56.00 1.34
033	57.00 1.38
034	58.00 1.43
035	460.00 3.5
036	460.0014.7
037	59.0014.1
038	48.0014.00
039	39.0014.2
040	38.0014.10
041	37.0014.20
042	36.0014.28
043	35.5014.27
044	35.0014.27
045	34.0014.77
046	33.5 14.3
047	34.0015.0
048	32.0015.4
049	31.0016.3
050	30.0016.2
051	29.0016.2
052	28.0016.1
053	27.2515.7
054	27.2515.7
055	25.0015.4
056	24.0015.1
057	23.6015.1
058	21.0014.3
059	19.0013.7
060	15.0011.1

061	10.00	9.84
062	5.00	8.1
063	-7.00	7.
064	-21.00	5.
065	-55.00	.
066	19.00	.001
067	00003000010000.	10
068	6.35	15.6
069	6.85	30.4
070	0.00	30.2
071	-4.00	32.0
072	-450.00	32.
073	-460.00	21.7
074	-21.00	21.7
075	-7.00	20.0
076	1.00	15.40
077	6.85	15.0
078	0000400010	-0.07
079	-55.00	.
080	-21.00	5.
081	-7.00	7.
082	5.00	3.1
083	6.85	9.1
084	6.85	15.6
085	-2.00	14.4
086	-6.00	12.
087	-21.00	8.
088	-55.00	.
089	0000500023000.	53
090	-400.00	32.
091	-4.00	32.0
092	0.00	30.2
093	8.00	29.6
094	10.00	29.34
095	13.00	27.8
096	19.00	27.0
097	27.25	26.6
098	27.25	27.5
099	31.00	27.2
100	34.00	25.9
101	34.50	25.5
102	35.00	25.3
103	37.00	25.2
104	40.00	24.9
105	45.00	23.50
106	51.00	23.35
107	55.00	24.00
108	59.00	22.25
109	74.00	20.0
110	400.00	19.3
111	400.00	32.
112	-460.00	32.
113	0000600024	-1.04
114	400.00	.00
115	400.00	3.5
116	58.00	1.43
117	57.00	1.38
118	56.00	1.34
119	55.00	1.28
120	54.00	1.29
121	53.00	1.22
122	52.00	1.26

123 51.00 1.25
 124 50.00 1.20
 125 49.00 1.10
 126 48.00 1.04
 127 47.00 0.92
 128 46.00 0.82
 129 45.00 0.79
 130 44.00 0.74
 131 43.00 0.585
 132 42.00 0.475
 133 41.00 0.333
 134 40.00 0.132
 135 37.00 .012
 136 19.00 .01
 137 450.00 .00
 138 0000700010000.00
 139 34.0015.0
 140 33.5 14.9
 141 34.0014.77
 142 35.0014.27
 143 35.5014.27
 144 37.0014.20
 145 37.0025.3
 146 34.5025.5
 147 34.0025.9
 148 34.0015.0
 149 0000000015000.10
 150 37.0014.20
 151 38.0014.1
 152 48.0014.00
 153 59.0014.1
 154 460.0014.7
 155 460.0019.30
 156 74.0020.00
 157 59.0022.25
 158 55.0024.00
 159 51.0023.350
 160 45.0023.500
 161 40.0024.9
 162 37.0025.3
 163 37.0025.3
 164 37.0014.20
 165 0000900000000.50
 166 23.6015.1
 167 25.0015.4
 168 27.2515.7
 169 27.2526.6
 170 23.0026.5
 171 23.6015.1
 172 0001000013 0.13
 173 7.0015.5
 174 10.0016.62
 175 13.0015.80
 176 19.0013.70
 177 21.0014.8
 178 23.6015.1
 179 23.0026.70
 180 19.0027.0
 181 13.0027.9
 182 10.0029.34
 183 9.0029.60
 184 7.0023.60

185	7.0015.50
186	0001100012 0.10
187	27.2515.7
188	23.0016.1
189	29.0016.3
190	30.0015.3
191	31.0010.3
192	32.0015.4
193	34.0015.0
194	34.0025.9
195	31.0027.2
196	27.2527.5
197	27.2520.00
198	27.2515.7
199	0001200000 -0.07
200	7.00 9.2
201	10.00 9.84
202	15.0011.1
203	19.0013.7
204	13.0015.3
205	10.0010.62
206	7.0015.5
207	7.00 9.2
208	0001300005 0.50
209	6.85 9.1
210	7.00 9.2
211	7.0029.1
212	6.8530.4
213	6.85 9.1

3PARTLUMP

This Datafile contains the parameters used by GRAVITYMODEL to compute the gravitational attraction of the model shown in Figure 18.

ZPARTLUMP.

FLOOR LEVEL 4

-GC35

0002	00003000000000.
0003	0001000005 -0.06
0004	19.00 2.5
0005	21.00 2.5
0006	23.00 3.5
0007	18.00 3.5
0008	19.00 2.5
0009	0000200007 -0.16
0010	18.00 3.5
0011	23.00 3.5
0012	24.00 4.2
0013	24.50 4.9
0014	14.50 4.9
0015	17.00 3.7
0016	18.00 3.5
0017	0000300005 -0.25
0018	14.50 4.9
0019	24.50 4.5
0020	27.00 6.5
0021	13.00 6.5
0022	14.50 5.0